CODED COOPERATION: A NEW FRAMEWORK FOR USER COOPERATION IN WIRELESS NETWORKS

APPROVED BY SUPERVISORY COMMITTEE:

Dr. Aria Nosratinia, Chair

Dr. Naofal Al-Dhahir

Dr. John Fonseka

Dr. Hlaing Minn

CODED COOPERATION: A NEW FRAMEWORK FOR USER COOPERATION IN WIRELESS NETWORKS

by

TODD EDWARD HUNTER, B.S.E.E, M.S.E.E

DISSERTATION

Presented to the Faculty of the Graduate School of

The University of Texas at Dallas

in Partial Fulfillment

of the Requirements

for the Degree of

DOCTOR OF PHILOSOPHY IN ELECTRICAL ENGINEERING

THE UNIVERSITY OF TEXAS AT DALLAS

May 2004

ACKNOWLEDGMENTS

First, I would like to gratefully acknowledge Dr. Aria Nosratinia, my advisor and committee chair. Dr. Nosratinia has supported me and collaborated with me in my research, has supported me financially, and has gone to considerable effort to create an environment for myself and his other graduate students that is conducive to conducting high-quality research. For all of these things I am extremely thankful. I would also like the thank the other members of my Ph.D. supervisory committee, Dr. Naofal Al-Dhahir, Dr. John Fonseka, and Dr. Hlaing Minn, for their time and effort in evaluating my work and helping me bring it to a level worthy of a Ph.D.

Secondly, I would like to thank my current and former graduate student colleagues, Ahmadreza Hedayat, Mohammad Janani, Shahab Sanayei, Harsh Shah, Ramakrishna Vedantham, Vijay Suryavanshi, Vimal Thilak, and Hong Bo, for their support of my work and for their friendship over the past several years.

Thirdly, I would like to thank my family, my parents Ed and Diane, my brother Jeff, his wife Gail, and their family, my grandparents, and all of my extended family, for all of the love, support, and encouragement they have given me throughout this process. I would also like to thank my wife's parents, Mario and Rosario Zuluaga, for treating me like their own son and supporting me in the completion of this work. I have been truly blessed and am extremely grateful to have the family that I have.

Finally, and most importantly, I would like to thank my wife, María Argeny. Her undying love, companionship, friendship, and belief in me has meant more to me than I can adequately express with words. No one could ask for more than she gives me everyday; she is truly God's miracle in my life.

CODED COOPERATION: A NEW FRAMEWORK FOR USER COOPERATION IN WIRELESS NETWORKS

Publication No. _____

Todd Edward Hunter, Ph.D.
The University of Texas at Dallas, 2004

Supervising Professor: Aria Nosratinia

Whenever size, power, or other constraints preclude the use of multiple transmit antennas, wireless systems cannot benefit from the well-known advantages of space-time coding methods. Cooperation between wireless users has been proposed as a means to provide transmit diversity in the face of this limitation. Cooperation involves two single-antenna users forming a partnership, in which each achieves diversity by using their partner's antenna as a relay. Previously proposed user cooperation methods involve a user *repeating* in some form the symbols transmitted by its partner. In this dissertation, we present a new paradigm for cooperative communication: *coded cooperation*. A significant departure from previous methods, coded cooperation integrates user cooperation with channel coding. Instead of repeating some form of the received information, the user decodes the partner's transmission and transmits additional parity symbols (e.g. incremental redundancy) according to some overall coding scheme. This framework maintains the same information rate, code rate, bandwidth, and transmit power as a comparable non-cooperative system. To characterize performance, we develop analytical bounds for bit and block error rates, which are

confirmed by simulations. In addition, we develop outage probability expressions for non-ergodic fading, which show that coded cooperation achieves full diversity (i.e., diversity order two for two cooperating users). Finally, we extend the coded cooperation framework to a multi-user (i.e., ad hoc) network, and consider both distributed and centralized protocols for partner assignment and cooperation.

TABLE OF CONTENTS

LIST OF FIGURES

LIST OF TABLES

CHAPTER 1
INTRODUCTION

The mobile wireless channel suffers from *multi-path fading*, which causes the signal attenuation to vary significantly over the course of a given transmission (see for example [48, 58]). The concept of mitigating the detrimental effects of fading through *diversity*, e.g., providing the receiver with multiple versions of an information-bearing signal that are subject to independent fading realizations, goes back at least to 1927 [35] and remains today a key element in the design of powerful coding and signal processing methods for the wireless channel. In particular, *transmit diversity* is generated by transmitting different versions of the signal from different locations using multiple antennas. These multiple transmissions can be processed at the destination such that accurate detection of the signal of interest is significantly improved. The conventional view of transmit diversity is that a single wireless terminal transmits using an array of multiple antennas which are spatially located so that the paths from each antenna to the destination experience independent fading. Among the noteworthy recent discoveries in this area are the numerous space-time coding techniques that have been developed for multi-element antenna arrays (see for example [2, 60, 59]).

Unfortunately, transmit diversity methods are not applicable to many wireless systems because size, complexity, or other constraints preclude the use of multiple transmit antennas. One example is the uplink of cellular systems, where the size of the mobile unit is the limiting factor. Other important examples are ad-hoc networks and sensor networks, where size, complexity, and power are all limiting issues. Cooperation between wireless terminals (which we shall call *users* in the remainder of this dissertation) has been recently proposed as a means to provide transmit diversity

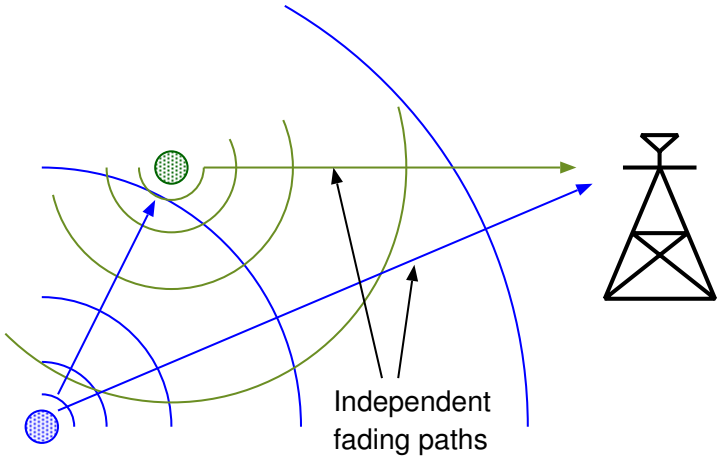

Figure 1.1. Cooperative communication.

in the face of this limitation. Transmit diversity is achieved by a signaling scheme that allows two single-antenna users to send their information using both of their antennas.

For an explanation of the ideas behind cooperative communication, we refer the reader to Figure 1.1, which shows two mobile users communicating with a destination. Each user has only one antenna and thus cannot individually generate transmit diversity. However, due to the inherently broadcast nature of wireless communication, it may be possible for one user to receive the other, in which case it can forward some version of the received information, along with its own data. Because the fading paths from the two users are statistically independent, this generates transmit diversity.

In previously proposed methods for user cooperation, a user *repeats* the symbols received from the partner. This repetition generally assumes one of two forms. The user may simply forward the analog signal received from its partner, a technique known as *amplify-and-forward*. Alternatively, the user may retransmit estimates of the received symbols, obtained via hard detection. This technique is generally referred to as *detect-and-forward*.

In this dissertation, we present a new paradigm for cooperative communication, which we term *coded cooperation*. A significant departure from previous methods, coded cooperation integrates user cooperation with channel coding. Instead of repeating some form of the received information, the user decodes the partner's transmission and transmits additional parity symbols (e.g., incremental redundancy) according to some overall coding scheme. This framework maintains the same information rate, code rate, bandwidth, and transmit power as a comparable non-cooperative system. The users employ error checking (i.e., via cyclic redundancy check (CRC) code) to avoid transmitting erroneous data for their partner. As a result of this, coded cooperation exhibits a graceful degradation behavior such that in the worst case it always performs at least as well as a comparable non-cooperative system. This is a significant improvement over the previous methods. In the following chapters, we describe in detail the coded cooperation framework for two wireless users, and present both error rate analysis and outage probability analysis. Through these analyses we characterize the performance of coded cooperation, and demonstrate the impressive gains it provides relative to a comparable non-cooperative system. We then extend the framework to a network consisting of multiple users; i.e., an ad hoc network. We propose protocols for implementing coded cooperation, and demonstrate the performance improvement that it provides in such an environment.

1.1 Outline of the Dissertation

In Chapter 2, we present some background material and a review of previous work in cooperative communication.

In Chapter 3 we formally introduce the coded cooperation framework and describe in detail its operation and associated practical details of implementation. We develop error rate analysis via the derivation of pairwise error probability expressions

and the corresponding union bounds for bit and block error rate. This analysis is confirmed through simulations. Numerical results, obtained using a simple but effective implementation of coded cooperation with rate-compatible punctured convolutional (RCPC) codes, demonstrate the performance of coded cooperation under a variety of conditions.

Chapter 4 considers two extensions to the coded cooperation framework. The first borrows ideas from space-time coding and MIMO systems in order to improve the performance of coded cooperation in fast fading. We refer to this extension as *space-time cooperation*. The second extension involves implementing coded cooperation using turbo codes. We extend the error rate analysis from Chapter 3 to incorporate these extensions, and also provide numerical results to demonstrate performance.

In Chapter 5 we develop information-theoretic bounds for coded cooperation. Specifically, we consider the case of quasi-static Rayleigh fading and derive outage probability expressions for coded cooperation and space-time cooperation. A key result of this analysis is that we demonstrate definitively that coded cooperation achieves full diversity (order two in the case of two cooperating users). We present numerical outage probability results which demonstrate the gains of coded cooperation, and illustrate its advantages over previously proposed repetition-based methods.

The objective of Chapter 6 is to extend the coded cooperation framework to a network with multiple wireless users. We propose both distributed and centralized protocols for partner assignment and cooperation. We characterize performance in terms of outage probability, and present results that compare the various protocols and demonstrate the significant gains that coded cooperation can provide in the network environment.

Finally, Chapter 7 presents conclusions and discusses possible avenues for future work in this area.

CHAPTER 2
BACKGROUND AND RELATED WORK

This chapter presents a brief review of prior work in the area of cooperative communication. In particular, we first review key results for the classical relay channel. This in turn leads us to the idea of cooperative communication, and a discussion of several two-user cooperative signaling schemes that have been proposed to date. We conclude this chapter with a brief discussion of recent works on wireless ad hoc networks and their relationship to cooperative communication.

2.1 The Relay Channel

The genesis of cooperative communication can be traced back to the work of Cover and El Gamal [16] on the relay channel. The relay channel model is shown in Figure 2.1. In this model, transmitter A sends a signal X, whose noisy, attenuated version is received by both the destination C and a relay B. The relay then transmits another signal X_1 to the destination, based on what it has received. This model can be decomposed into a broadcast channel (A transmitting, B and C receiving), and a multiple access channel (A and B transmitting, C receiving). Cover and El Gamal calculated the information theoretic capacity of this channel and found that it is bounded by the minimum of the rates of transmission of the constituent broadcast and multiple access channels. In many instances, the overall capacity is better than the individual capacity between A and C.

Interestingly, the recent work in user cooperation seems to have sparked renewed interest in the relay channel. The original work by Cover and El Gamal [16] assumes that the relay can simultaneously transmit and receive in the same frequency

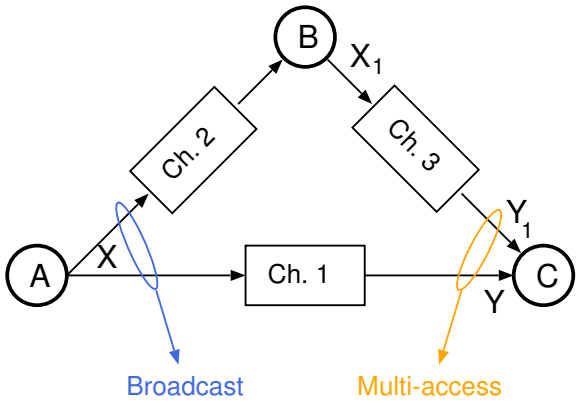

Figure 2.1. The relay channel.

channel. Realizing that this may be impractical with current RF technology, Høst-Madsen [31] has developed alternative capacity results for the relay channel. Using ideas from [16, 15], ergodic capacity bounds for the relay channel are derived with the constraint that the relay receives the source transmission in one time or frequency slot, and then transmits in a different time or frequency slot. These results are extended to the case of user cooperation in [30]. However, in [31] and [30], as in [16], it is assumed that the source and the relay can transmit coherently and achieve a beamforming effect. Valenti and Zhao [64, 71] give capacity and outage probability results for various protocols for the relay channel. Valenti and Zhao impose an additional constraint, again motivated by practical considerations, that the source and relay transmit on orthogonal (i.e., in time or frequency) channels.

2.2 Cooperative Communication

Cooperative communication, while similar to the relay channel model in some respects, differs significantly in that each wireless user is assumed to both transmit data *as well as* act as a cooperative agent for another user. In other words, cooperative signaling protocols should be designed so that users can assist other users while still being able to send their own data. This reciprocal arrangement is illustrated in

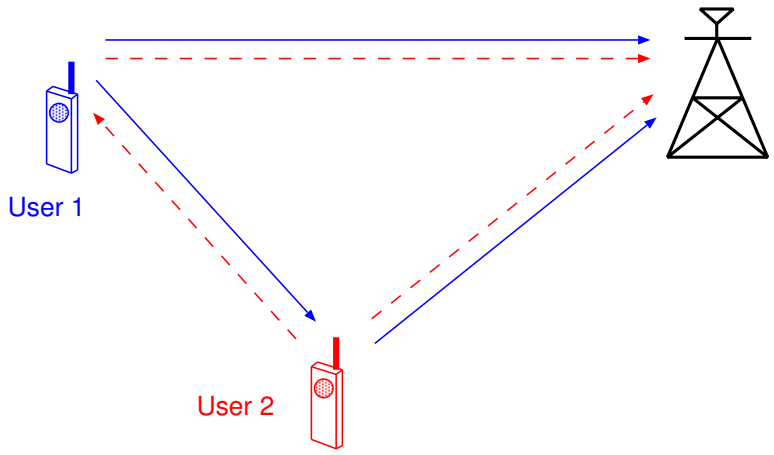

Figure 2.2. In cooperative communication each user is both a source and a relay.

Figure 2.2. Although this may not be true at every given point in time for each user, it is considered to be valid in a statistical sense.

Cooperation leads to interesting tradeoffs in code rates and transmit power. In the case of power, it may seem that more power is required because each user, when in cooperative mode, is transmitting for both itself and a partner. However, the point to be made is that the gain in diversity from cooperation allows the users to reduce their transmit powers and maintain the same performance. In the face of this tradeoff, one hopes for a net reduction of transmit power, given everything else being constant.

Similar questions arise for the rate of the system. In cooperative communication, each user transmits both its own bits as well as some information for its partner, so it may appear that each user requires more bandwidth. On the other hand the spectral efficiency of each user improves because, due to cooperation diversity, the channel code rates can be increased. Again a tradeoff is observed. The key question, whether cooperation is worth the incurred cost, has been answered in the positive by several prior studies.

We now review several of the main cooperative signaling methods that have

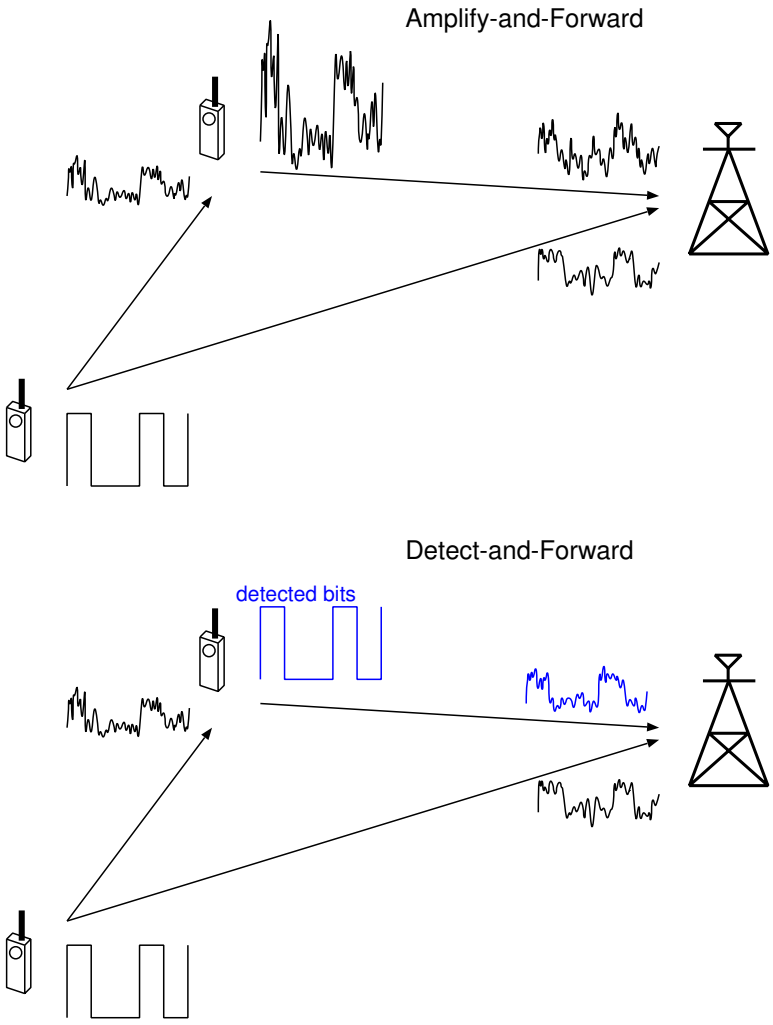

Figure 2.3. Comparison of amplify-and-forward and detect-and-forward cooperative methods. For clarity only one user's cooperation is shown via baseband equivalent signals.

been proposed previously. As indicated in the previous chapter, these methods are generally grouped into two classes: amplify-and-forward, and detect-and-forward methods. A simplified demonstration and comparison of these two classes appears in Figure 2.3.

2.2.1 Amplify-and-Forward Methods

Amplify-and-forward is conceptually the most simple of the cooperative signaling methods. Each user in this method receives a noisy version of the signal transmitted by its partner. As the name implies, the user then amplifies and retransmits this noisy signal (see Figure 2.3). The destination will combine the information sent by the user and partner and will make a final decision on the transmitted symbol. Although the noise of the partner is amplified in this scheme, the destination still receives two independently-faded versions of the signal and is thus able to make better decisions for the transmitted symbols. A potential challenge in this scheme is that sampling, amplifying, and retransmitting analog values may be technologically non-trivial. Nevertheless, amplify-and-forward is a simple method that lends itself to analysis, and therefore has been very useful in furthering the understanding of cooperative communication systems.

Laneman and Wornell first proposed amplify-and-forward as a cooperative signaling scheme in [41]. In this work, they compute the bit error rate (BER) for uncoded symbol-wise amplify-and-forward, and show that, despite the noise propagation from the partner, amplify-and-forward performs significantly better than non-cooperative transmission. Laneman, Wornell, and Tse [43, 40] (see also [39]) extend this work by deriving the outage probability for amplify-and-forward in quasi-static Rayleigh fading. They demonstrate that amplify-and-forward signaling achieves diversity order two for two cooperating users.

2.2.2 Detect-and-Forward Methods

Under detect-and-forward, a user attempts to detect the partner's symbols, and then retransmits an estimate of the detected symbols (see Figure 2.3). The first work proposing a detect-and-forward protocol for user cooperation was by Sendonaris,

Erkip, and Aazhang [51, 52, 53] (see also [50]). This was actually the first work in the area of cooperative communication and has inspired much of the current activity in this area.

Sendonaris, Erkip, and Aazhang [51, 52, 53] first present a general information-theoretic model for cooperation between a pair of users, for which achievable rate regions and outage probabilities are examined. They then propose a CDMA-based implementation of detect-and-forward cooperative signaling, and examine achievable rate regions and outage capacity for this particular scheme. The following is an example of the proposed CDMA implementation. The two user's data bits are denoted $b_i^{(n)}$, where $i = 1, 2$ are the user indices and n denotes the time index of information bits. Each user has its own spreading code, denoted by $c_i(t)$. The term $\hat{b}_i^{(n)}$ denotes the partner's hard-detected estimate of User i's bit. Factors $a_{i,j}$ denote signal amplitudes, and hence represent power allocation to various parts of the signaling. Each signaling period consists of three bit intervals. Denoting the signal of User 1 by $X_1(t)$ and the signal of User 2 by $X_2(t)$,

$$\begin{aligned} X_1(t) &= a_{11}b_1^{(1)}c_1(t) \quad , \quad a_{12}b_1^{(2)}c_1(t) \quad , \quad a_{13}b_1^{(2)}c_1(t) + a_{14}\hat{b}_2^{(2)}c_2(t) \\ X_2(t) &= a_{21}b_2^{(1)}c_2(t) \quad , \quad a_{22}b_2^{(2)}c_2(t) \quad , \quad a_{23}\hat{b}_1^{(2)}c_1(t) + a_{24}b_2^{(2)}c_2(t). \end{aligned}$$

In other words, in the first and second intervals, each user transmits its own bits. Each user then detects the other user's second bit, and in the third interval, both users transmit *a linear combination* of their own second bit and their estimate of the partner's second bit, each multiplied by the appropriate spreading code. The transmit powers for the first, second, and third intervals are variable, and by optimizing the relative transmit powers according to the conditions of the uplink channel and the inter-user channel, this method provides adaptability to channel conditions. The powers are allocated through the factors $a_{i,j}$ such that an average power constraint

is maintained. Roughly speaking, whenever the inter-user channel is favorable, more power will be allocated to cooperation, whereas whenever the inter-user channel is not favorable, cooperation is reduced.

With this signaling scheme, it is possible that the partner forwards an erroneous estimate $\hat{b}_i^{(n)}$ of the user's bit, in which case cooperation can be detrimental to the eventual detection of the bits at the destination. In order to mitigate this, [53] shows that the optimal (e.g. maximum likelihood) combiner/detector weights $\hat{b}_i^{(n)}$ proportional to the bit error probability of the channel between the cooperating users. Laneman and Wornell obtain a similar result for their version of an uncoded symbol-wise detect-and-forward protocol proposed in [41]. The key issue here is that the destination must somehow know the bit error probability of the channel between the users in order to perform optimal detection.

In [43, 40], Laneman, Wornell, and Tse consider the outage probability of a basic detect-and-forward protocol, for which an outage event occurs if the channel between the user and partner is in outage. In other words, an outage is assumed if a user does not successfully detect the partners symbols. It is shown that this protocol achieves diversity order one, the same as non-cooperative transmission, and actually performs worse than non-cooperative transmission for a wide range of conditions. This is due to the fact that a user may often relay erroneous estimates of the partner's symbols.

To avoid the problem of error propagation by the partner, Laneman, Wornell, and Tse [43, 40] propose a hybrid detect-and-forward method where, at times when the channel between the users has high instantaneous SNR, users detect and forward their partner's data, but when the channel has low SNR, the users revert to a non-cooperative mode. In particular, if the channel between the users is in outage (which the users can determine through SNR measurements), each user chooses not to coop-

erate, but simply to repeat its own symbols for that period. We note that his method is a variation of adapting the coefficients $a_{i,j}$ in the method of [53]. Laneman, Wornell, and Tse [43, 40] show that this hybrid detect-and-forward protocol does achieve diversity two, and provides gains over non-cooperative transmission similar to those of their amplify-and-forward scheme discussed above.

As mentioned in Chapter 1, these previous cooperative methods have one key similarity: cooperative diversity is achieved by having a user *repeat* in some form the symbols received from the partner. Beginning with the following chapter, we introduce coded cooperation, a new paradigm for user cooperation in which cooperative signaling is combined with channel coding to produce a framework that maintains the same information rate *and* code rate, as well as the same bandwidth and transmit power, as a comparable non-cooperative system.

2.3 Wireless Ad Hoc Networks

In cellular networks, mobile users communicate solely with a common central destination, typically referred to as a base station, which also serves as organizer and controller of the network, or cell. In contrast, ad hoc networks are primarily characterized by their lack of centralized control. Users are distributed randomly within some finite area, and in general each user may communicate with any other user in the network at any given time. The users must be able to function independently, as well as dynamically interact to enable operation of the network. Due to the random nature of the links between users, scheduling and random access, routing, and network organization are all challenging problems for ad hoc networks that are under investigation by numerous researchers.

A popular area of study for ad hoc networks is multihop transmission. In this scenario, a data packet from a source user reaches the destination via a path that

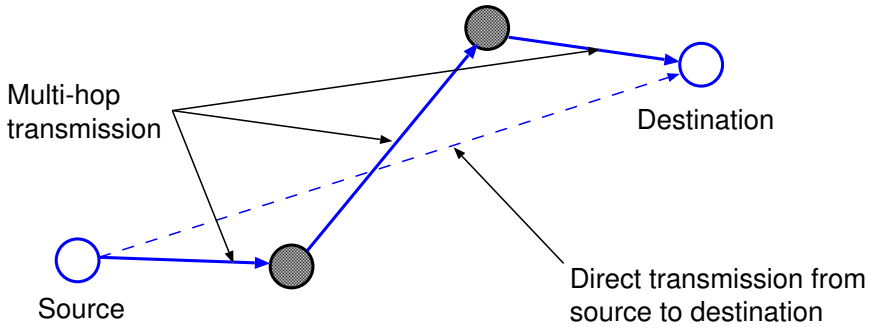

Figure 2.4. Multihop transmission compared with direct transmission between source and destination for a wireless ad hoc network.

consists of one or more intermediate users. Each intermediate user receives a version of the packet from the previous user in the path, and in turn relays or forwards the packet to the next user in the path. Multihop transmission is illustrated in Figure 2.4. Prior works typically consider that a packet is relayed using detect-and-forward signaling, with the packet being repeated during each hop; see [61] and references therein for examples of performance comparisons between various multihop schemes and direct transmission from source to destination. The multihop transmission model differs from user cooperation in that the destination receives the packet only from the last intermediate user in the path. Thus, multihop transmission in general does not seek to create spatial diversity, as does user cooperation. The gains result from the fact that the SNR of each hop is relatively high, such that the multihop path is more reliable overall than the direct path from source to destination.

Recently, some interesting information-theoretic results have appeared for ad hoc networks with multihop transmission. Gupta and Kumar [24] consider ad hoc networks consisting of M stationary terminals within a finite area, and prove that the total throughput per terminal goes to zero as M increases. Specifically, they show that the capacity per terminal decreases as $1/\sqrt{M}$. In addition, they show that the multihop transmission scheme that maximizes the transport capacity (bit-meters/second) has terminals transmit only to their nearest neighbors. Thus, as the

number of terminals M increases, so does the number of hops between each user and its destination, thus leading to the decay in total throughput as M increases.

Grossglauser and Tse [23] consider an ad hoc network in which the nodes are mobile and move independently around the network. They propose a multihop transmission scheme for which the average long-term throughput per user remains constant even as the number of nodes increases. The basic idea of the scheme is that, when a source user has a packet to send, it transmits it to its nearest neighbor at that moment. This relay node subsequently moves around the network carrying the source packet and forwards it only once, when it becomes the nearest neighbor of the intended destination. Thus, like [24], terminals transmit or relay packets only to their nearest neighbors; however, due to the mobility of the terminals each packet need only traverse two hops, and the overall throughput per terminal remains $O(1)$ regardless of the number of terminals. A limitation of this scheme is that, while the throughput remains relatively high, a given packet may incur large delays waiting for the terminal that is carrying it to move close to the destination.

Toumpis and Goldsmith [62] formulate capacity regions for ad hoc networks consisting of a finite number of terminals. In this analysis they consider various transmission protocols and scenarios; for example, single-hop routing, multihop routing, power control for transmitting nodes, receiving nodes using successive interference cancellation, and mobile vs. fixed nodes. Among other results, they show that the capacity region with multihop routing is larger than the capacity region when only direct transmission from source to destination is permitted.

In terms of applying cooperative communication to multi-user networks, Laneman and Wornell [42] extend the repetition-based cooperative protocols developed in [40] for the multi-user case. In their scenario, each user attempts to cooperate simultaneously with all the other users through a detect-and-forward signaling scheme.

The diversity order achieved is shown to be equal to the number of users in the network, a significant improvement over non-cooperative transmission. In Chapter 6, we extend the coded cooperation framework developed in Chapters 3 through 5 for a network of multiple users, and develop protocols for partner selection, in which users may attempt to cooperate with one or more other users. These results demonstrate that coded cooperation is suitable for ad hoc network applications.

CHAPTER 3
CODED COOPERATION

In this chapter, we introduce a new user cooperation framework, called *coded cooperation*, in which cooperative signaling is integrated with channel coding. The basic idea behind coded cooperation is that each user tries to transmit incremental redundancy for its partner. Whenever that is not possible, the users automatically revert back to a non-cooperative mode. The key to the efficiency of coded cooperation is that all this is managed automatically through code design and there is no need for feedback between users. This method has two key characteristics. First, cooperation occurs through partitioning a user's code word such that part of the code word is transmitted by the user itself, while the remainder is transmitted by the partner through partial or complete decoding. In previous methods cooperation occurs via repetition, which may not be the best use of available bandwidth. Second, we employ error detection at the partner to avoid error propagation. Many of the previous methods either admit forwarding of erroneous estimates of the partner's symbols, or include propagation of the partner's noise. Error propagation diminishes the performance, particularly when the channel between partners is poor.

It is possible to implement these characteristics in a natural and simple manner by a method that uses common error control codes, as explained in the sequel. Furthermore, the incorporation of cooperation with channel coding allows a great degree of flexibility, since by varying the associated code rate, the coupling between the cooperating users can be controlled and adapted to channel conditions.

After reviewing the system model in Section 3.1, we present the coded cooperation protocol in Section 3.2. In Sections 3.3 and 3.4 we develop tight upper bounds

for bit and block error probability, using tools and techniques from Craig [18], Simon and Alouini [54], and Malkamäki and Leib [45]. This analysis is validated through simulations in Section 3.5. Performance results show that coded cooperation achieves impressive gains for a variety of channel conditions. In Section 3.6 we discuss several practical issues, including modeling of the inter-user channels and aspects of system implementation.

3.1 System Model

For the purposes of exposition, we consider two users both transmitting to a single destination. It is in the context of this multiuser communication that cooperation takes place. The channels between users (inter-user channels) and from each user to the destination (uplink channels) are mutually independent and subject to flat Rayleigh fading. We consider flat fading in order to isolate the benefits of spatial diversity provided by coded cooperation, however the technique easily extends to systems that experience frequency selective fading.

The users transmit on orthogonal channels (e.g., TDMA, CDMA, or FDMA), which allows the destination, and other users in the cooperative case, to separately detect each user. However, the basic idea and operation of our technique does not depend on the specifics of the channel access protocol. In our analysis and simulations for this chapter, we assume that the receivers maintain channel state information and employ coherent detection, so that we need only consider the magnitudes of the fading coefficients in the system model and analysis that follow. To simplify the presentation, we assume BPSK modulation, for which the baseband-equivalent discrete-time signal transmitted by User $i \in \{1, 2\}$ and received by User $j \in \{0, 1, 2\}$ ($j \neq i$, and $j = 0$ denotes the destination) is given by

$$r_{i,j}(n) = \alpha_{i,j}(n)\sqrt{E_{b,i}} \cdot b_i(n) + z_j(n) \tag{3.1}$$

where $E_{b,i}$ is the transmitted energy per bit for user i, $b_i(n) \in \{-1, +1\}$ is the BPSK-modulated code bit at time n, $\alpha_{i,j}(n)$ is the fading coefficient magnitude between Users i and j, and $z_j(n)$ accounts for noise and other additive interference at the receiver. We model $\alpha_{i,j}(n)$ as independent samples of a Rayleigh-distributed random variable characterized by mean-square value

$$\Omega_{i,j} = E_{\alpha_{i,j}} \left[\alpha_{i,j}^2(n) \right], \tag{3.2}$$

where $E_x[\cdot]$ denotes the expectation operator with respect to random variable x. The value of $\Omega_{i,j}$ accounts for large-scale path loss and shadowing effects. For slow (quasi-static) fading, the fading coefficients remain constant ($\alpha_{i,j}(n) = \alpha_{i,j}$) over the transmission of each source block, while for fast fading, they are i.i.d. for each transmitted symbol. The noise term $z_j(n)$ is modeled as independent, zero-mean additive white Gaussian noise with variance N_j (i.e., samples of a bandpass white noise process with two-sided power spectral density $N_j/2$).

We define the instantaneous received SNR for the channel between users i and j as

$$\gamma_{i,j}(n) = \frac{\alpha_{i,j}^2(n) E_{b,i}}{N_j}. \tag{3.3}$$

For $\alpha_{i,j}(n)$ Rayleigh distributed, $\gamma_{i,j}(n)$ has an exponential distribution with mean

$$\Gamma_{i,j} = E_{\alpha_{i,j}} \left[\gamma_{i,j}(n) \right] = E_{\alpha_{i,j}} \left[\frac{\alpha_{i,j}^2(n) E_{b,i}}{N_j} \right] = \Omega_{i,j} \frac{E_{b,i}}{N_j}. \tag{3.4}$$

Note that for our purposes we are assuming that $\Omega_{i,j}$ and $\Gamma_{i,j}$ are constant over n for a given channel, i.e., the channel statistics are not changing with time. We quantify the quality of each channel by its corresponding average received SNR as given by (3.4). We consider cases in which the average received SNR for the two uplink channels, $\Gamma_{1,0}$ and $\Gamma_{2,0}$, are equal (statistically similar channels) and unequal (statistically dissimilar channels). This symmetry or asymmetry results from, for

example, the relative proximity of the cooperating users to each other and to the destination.

In [52, 53, 41, 43], the channels between Users i and j are assumed to be reciprocal, e.g., $\alpha_{i,j}(n) = \alpha_{j,i}(n)$, for the case of slow fading. The applicability of this assumption depends on the multiple access scheme and the nature of the fading experienced by the inter-user channels. In this chapter we present slow fading results for two extremes: reciprocal inter-user channels, and those with a complete lack of reciprocity; i.e., the channels from User i to User j and User j to User i are mutually independent. We refer to these as independent inter-user channels. For the case of fast fading, we assume that the inter-user channels are always independent. We discuss further the issue of inter-user channel reciprocity in Section 3.6.1.

3.2 Coded Cooperation

The users segment their source data into blocks which are augmented with a cyclic redundancy check (CRC) code [70], for a total of K bits per source block (including the CRC bits). Each block is then encoded with a forward error-correcting code, so that, for an overall rate R code, we have $N = K/R$ total code bits per block. We emphasize that since most current and future wireless systems already employ CRC codes, this does not represent additional overhead required by coded cooperation.

The two users cooperate by dividing the transmission of their N-bit code words into two successive time segments, or frames. In the first frame, each user transmits a rate $R_1 > R$ code word with $N_1 = K/R_1$ bits. This itself is a valid (albeit weaker) code word which can be decoded to obtain the original information. Each user also receives and decodes the partner's transmission. If the user successfully decodes the partner's rate R_1 code word, determined by checking the CRC bits, the user computes and transmits N_2 additional parity bits for the partner's data in the second frame,

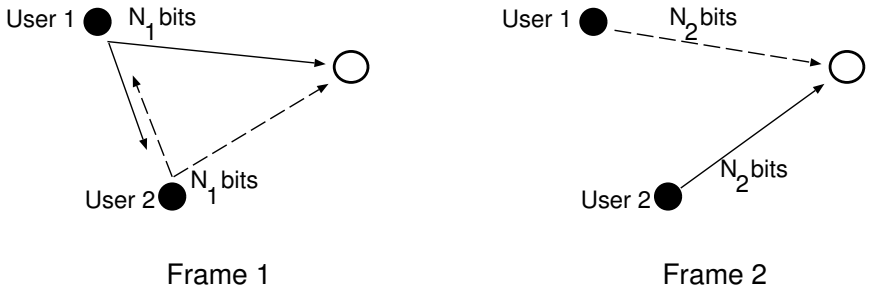

Figure 3.1. Cooperative transmission scheme.

where $N_1 + N_2 = N$. These additional parity bits are selected such that they can be combined with the first frame code word to produce a more powerful rate R code word. If the user does not successfully decode the partner, N_2 additional parity bits for the user's own data are transmitted. Each user always transmits a total of N bits per source block over the two frames, and the users only transmit in their own multiple access channels. Figure 3.1 illustrates the general coded cooperation framework, and Figure 3.2 shows an implementation for a TDMA system. The analogous FDMA and CDMA implementations are straightforward.

We define the level of cooperation as N_2/N, the percentage of the total bits per each source block that the user transmits for its partner. A smaller percentage implies a more powerful code for the first frame and increased probability that a user successfully decodes the parter. However, this also means a smaller N_2, thus reducing gain from diversity. We examine this tradeoff as part of our evaluation of the scheme in Section 3.5.

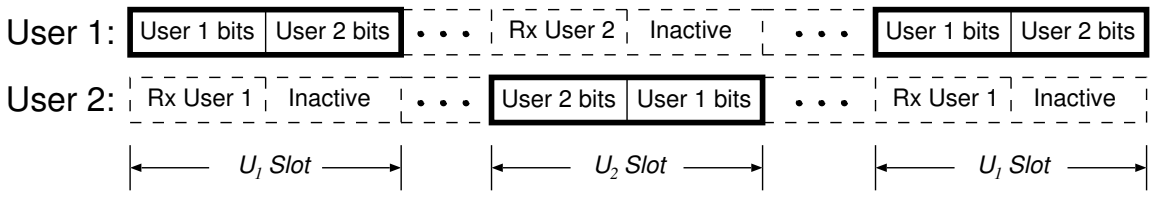

Figure 3.2. Coded cooperation implementation for a system using TDMA.

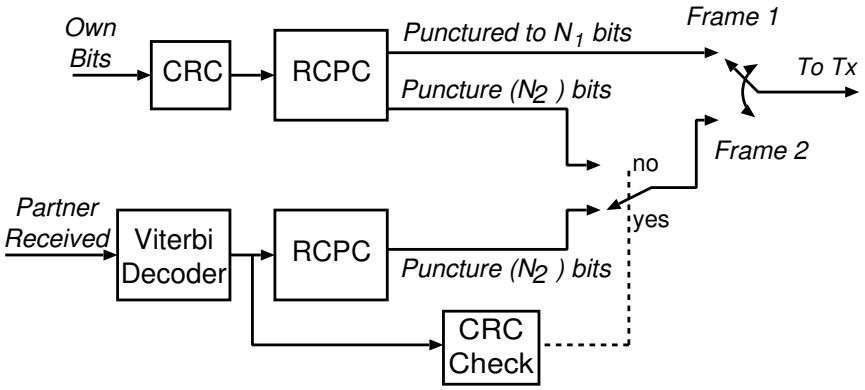

Figure 3.3. A user's implementation of coded cooperation with RCPC codes.

In general, various channel coding methods can be used within this coded cooperation framework. For example, the overall code may be a block or convolutional code, or a combination of both. The code bits for the two frames may be partitioned through puncturing, product codes, or other forms of concatenation. To obtain the performance results given in this chapter, we employ a simple but very effective implementation using rate-compatible punctured convolutional (RCPC) codes [25]. In this implementation, the overall rate R code is selected from a given RCPC code family (e.g., the mother code). The code word for the first frame is obtained by applying the puncturing matrix corresponding to rate R_1, and the additional parity bits transmitted in the second frame are those punctured from the first frame. Figure 3.3 illustrates a user's implementation of coded cooperation using RCPC codes.

The users act independently in the second frame, with no knowledge of whether their own first frame was correctly decoded. As a result, there are four possible cooperative cases for the transmission of the second frame, illustrated in Figure 3.4. In Case 1, both users successfully decode each other, so that they each transmit for their partner in the second frame, resulting in the fully cooperative scenario depicted in Figure 3.1. In Case 2, neither user successfully decodes their partner's first frame,

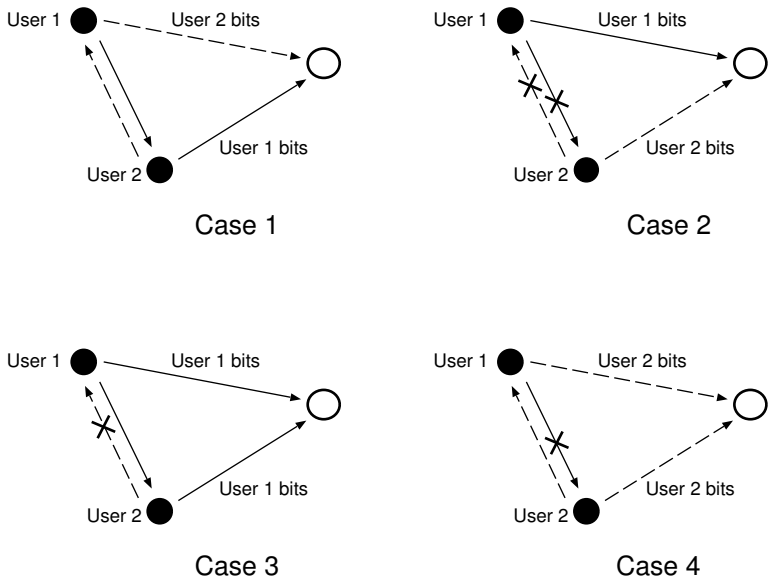

Figure 3.4. Four cooperative cases for second frame transmission based on the first frame decoding results.

and the system reverts to the non-cooperative case for that pair of source blocks. In Case 3, User 2 successfully decodes User 1, but User 1 does not successfully decode User 2. Consequently, neither user transmits the second set of code bits for User 2 in the second frame, but instead both transmit the second set for User 1. These two independent copies of User 1's bits are optimally combined at the destination prior to decoding. Case 4 is identical to Case 3 with the roles of User 1 and User 2 reversed. Clearly the destination must know which of these four cases has occurred in order to correctly decode the received bits. We discuss this issue in Section 3.6.3, and demonstrate that this does not significantly impact the performance or complexity of the cooperative system.

3.3 Pairwise Error Probability

The pairwise error probability (PEP) for a coded system is defined as selecting code word $\boldsymbol{e} = [e(1), e(2), \ldots, e(N)]$ when code word $\boldsymbol{c} = [c(1), c(2), \ldots, c(N)]$ is transmit-

ted. For a binary code with BPSK modulation, coherent detection, and maximum-likelihood decoding, the PEP conditioned on the set of instantaneous received SNR values $\boldsymbol{\gamma} = [\gamma(1), \gamma(2), \ldots, \gamma(N)]$ can be written as [54, (12.13)]

$$P(\boldsymbol{c} \to \boldsymbol{e}|\boldsymbol{\gamma}) = Q\left(\sqrt{2\sum_{n\in\eta}\gamma(n)}\right) \tag{3.5}$$

where $Q(x)$ denotes the Gaussian Q-function [47, (2-1-97)], and $\gamma(n)$ is the instantaneous received SNR for code bit n as defined in (3.3). The set η is the set of all n for which $c(n) \neq e(n)$, and the cardinality of η is equal to the Hamming distance d between code words $\boldsymbol{c}$ and $\boldsymbol{e}$. The selection of $\boldsymbol{e}$ over $\boldsymbol{c}$ is known as an error event, and thus d is typically referred to as the corresponding error event Hamming weight.

For the remainder of this analysis, we restrict ourselves to the class of linear codes, where, without loss of generality, the transmitted code word $\boldsymbol{c}$ can always be chosen as the all-zero code word for the purposes of error analysis. Consequently, the PEP depends only on d and not the particular code words $\boldsymbol{c}$ and $\boldsymbol{e}$, so that the conditional PEP will be denoted simply by $P(d|\boldsymbol{\gamma})$.

3.3.1 Coded Cooperation with Slow Fading

For slow fading, the fading coefficients for each uplink channel are constant over the code word; e.g., $\alpha_{i,0}(n) = \alpha_{i,0}$ and $\gamma_{i,0}(n) = \gamma_{i,0}$ constant for $n = 1, \ldots, N$ for User i's uplink channel. For Case 1 (Figure 3.4), when both users successfully decode each other's first frame, each user's coded bits are divided between the two user channels. Considering User 1's code word we can thus write (3.5) as

$$P(d|\gamma_{1,0}, \gamma_{2,0}) = Q\left(\sqrt{2d_1\gamma_{1,0} + 2d_2\gamma_{2,0}}\right) \tag{3.6}$$

where d_1 and d_2 are the portions of the error event bits transmitted through User 1's and User 2's channel respectively, such that $d_1 + d_2 = d$. Note that d_1 and d_2 are independent of $\gamma_{1,0}$ and $\gamma_{2,0}$.

To obtain the unconditional PEP we must average (3.6) over the fading distributions, as

$$P(d) = \int_0^\infty \int_0^\infty P(d|\gamma_{1,0}, \gamma_{2,0}) p(\gamma_{1,0}) p(\gamma_{2,0}) d\gamma_{1,0} d\gamma_{2,0} \tag{3.7}$$

where $p(x)$ is the probability density function of random variable x. We can obtain an exact solution to (3.7) using the techniques of Simon and Alouini [54]. The first step is to use the following alternative representation for the Gaussian Q-function, originally derived by Craig [18], and then applied to performance analysis in fading channels in [54]:

$$Q(x) = \frac{1}{\pi} \int_0^{\pi/2} \exp\left(-\frac{x^2}{2\sin^2\theta}\right) d\theta, \qquad x \geq 0. \tag{3.8}$$

Using (3.8) in (3.6) and (3.7) gives

$$\begin{aligned} P(d) &= \frac{1}{\pi} \int_0^{\pi/2} \left[\int_0^\infty \exp\left(-\frac{d_1 \gamma_{1,0}}{\sin^2\theta}\right) p(\gamma_{1,0}) d\gamma_{1,0} \right] \\ &\times \left[\int_0^\infty \exp\left(-\frac{d_2 \gamma_{2,0}}{\sin^2\theta}\right) p(\gamma_{2,0}) d\gamma_{2,0} \right] d\theta. \end{aligned} \tag{3.9}$$

The two inner integrals in (3.9) have the form of moment-generating functions for the two densities $p(\gamma_{1,0})$ and $p(\gamma_{2,0})$ [55, (3.5-1)–(3.5-3)],

$$M_x(s) = \int_0^\infty e^{sx} p(x) dx, \tag{3.10}$$

where $M_x(s)$ is the moment-generating function of random variable x. Thus we can write (3.9) as

$$P(d) = \frac{1}{\pi} \int_0^{\pi/2} M_{\gamma_{1,0}}\left(-\frac{d_1}{\sin^2\theta}\right) M_{\gamma_{2,0}}\left(-\frac{d_2}{\sin^2\theta}\right) d\theta. \tag{3.11}$$

Recall also that the moment-generating function is equivalent to the Laplace transform with a change of sign in the exponent. Thus, we can employ all the well-known techniques for evaluating moment-generating functions and Laplace transforms to

solve integrals of this form. In the case of Rayleigh fading, the moment-generating function for the instantaneous SNR γ is [22, (17)]

$$M_\gamma(-s) = \frac{1}{1+s\Gamma}, \quad s > 0. \tag{3.12}$$

Using (3.12) in (3.11) results in

$$P(d) = \frac{1}{\pi}\int_0^{\pi/2} \left(1 + \frac{d_1\Gamma_{1,0}}{\sin^2\theta}\right)^{-1} \left(1 + \frac{d_2\Gamma_{2,0}}{\sin^2\theta}\right)^{-1} d\theta. \tag{3.13}$$

Equation (3.13) is an exact expression for the unconditional PEP and is easily evaluated using numerical integration techniques. In addition, using [54, (5A.58)-(5A.60)], we can obtain a closed-form expression for (3.13), but since it does not give additional insight into coded cooperation we do not provide it here.

We can obtain the following upper bound from (3.13) by noting that the integrand is maximized for $\sin^2\theta = 1$, so that

$$P(d) \le \frac{1}{2}\left(\frac{1}{1+d_1\Gamma_{1,0}}\right)\left(\frac{1}{1+d_2\Gamma_{2,0}}\right). \tag{3.14}$$

For large SNR, the PEP is inversely proportional to the product of the average SNR of the uplink channels. Thus, if d_1 and d_2 are both non-zero, full diversity order of two is achieved when both partners successfully receive each other and cooperate. This is a significant improvement over no cooperation, which is fundamentally limited to diversity order one (see (3.24)).

For Case 3, where User 1 does not successfully decode User 2, but User 2 successfully decodes User 1, both users send the same additional parity bits for User 1 in the second frame. These bits are optimally combined at the destination, so that the conditional PEP (3.6) for User 1 becomes

$$\begin{aligned} P(d|\gamma_{1,0},\gamma_{2,0}) &= Q\left(\sqrt{2d_1\gamma_{1,0} + 2d_2(\gamma_{1,0}+\gamma_{2,0})}\right) \\ &= Q\left(\sqrt{2d\gamma_{1,0} + 2d_2\gamma_{2,0}}\right) \end{aligned} \tag{3.15}$$

and the unconditional PEP becomes

$$\begin{aligned} P(d) &= \frac{1}{\pi}\int_0^{\pi/2}\left(1+\frac{d\Gamma_{1,0}}{\sin^2\theta}\right)^{-1}\left(1+\frac{d_2\Gamma_{2,0}}{\sin^2\theta}\right)^{-1}d\theta \\ &\leq \frac{1}{2}\left(\frac{1}{1+d\Gamma_{1,0}}\right)\left(\frac{1}{1+d_2\Gamma_{2,0}}\right). \end{aligned} \tag{3.16}$$

Thus, (3.16) illustrates that User 1 again achieves full diversity order two for Case 3.

3.3.2 Coded Cooperation with Fast Fading

For fast fading, the fading coefficients are no longer constant over the code word, but are i.i.d. across the coded bits. Thus, for Case 1, we generalize (3.5) as

$$P(d|\boldsymbol{\gamma}_{1,0},\boldsymbol{\gamma}_{2,0}) = Q\left(\sqrt{2\sum_{n\in\eta_1}\gamma_{1,0}(n)+2\sum_{n\in\eta_2}\gamma_{2,0}(n)}\right) \tag{3.17}$$

where the set η_i is the portion of the d error event bits transmitted through User i's channel. The cardinalities of η_1 and η_2 are d_1 and d_2 respectively, where again $d_1+d_2 = d$, and d_1 and d_2 are independent of $\gamma_{1,0}(n)$ and $\gamma_{2,0}(n)$ for all n.

Averaging over the fading to obtain the unconditional PEP now involves a d-fold integration, for which the techniques of [54] again provide a tractable solution. Applying (3.8) gives the following integral expression for unconditional PEP

$$\begin{aligned} P(d) &= \frac{1}{\pi}\int_0^{\pi/2}\prod_{n\in\eta_1}\left[\int_0^{\infty}\exp\left(-\frac{\gamma_{1,0}(n)}{\sin^2\theta}\right)p\left(\gamma_{1,0}(n)\right)d\gamma_{1,0}(n)\right] \\ &\times \prod_{n\in\eta_2}\left[\int_0^{\infty}\exp\left(-\frac{\gamma_{2,0}(n)}{\sin^2\theta}\right)p\left(\gamma_{2,0}(n)\right)d\gamma_{2,0}(n)\right]d\theta. \end{aligned} \tag{3.18}$$

Each inner integral in (3.18) has the same form as in (3.9), so that for Rayleigh fading we obtain

$$P(d) = \frac{1}{\pi}\int_0^{\pi/2}\left[\prod_{n\in\eta_1}\left(1+\frac{\Gamma_{1,0}}{\sin^2\theta}\right)^{-1}\right]\left[\prod_{n\in\eta_2}\left(1+\frac{\Gamma_{2,0}}{\sin^2\theta}\right)^{-1}\right]d\theta. \tag{3.19}$$

Applying our assumption that $\Gamma_{1,0}$ and $\Gamma_{2,0}$ are constant over n results in

$$\begin{aligned} P(d) &= \frac{1}{\pi}\int_0^{\pi/2}\left(1+\frac{\Gamma_{1,0}}{\sin^2\theta}\right)^{-d_1}\left(1+\frac{\Gamma_{2,0}}{\sin^2\theta}\right)^{-d_2}d\theta \\ &\leq \frac{1}{2}\left(\frac{1}{1+\Gamma_{1,0}}\right)^{d_1}\left(\frac{1}{1+\Gamma_{2,0}}\right)^{d_2}. \end{aligned} \tag{3.20}$$

Again we have in (3.20) an exact expression for the unconditional PEP that is easily evaluated via numerical techniques (we can obtain a closed-form expression for the integral in (3.20) from [54, (5A.58)-(5A.60)], but again it gives no further insight to coded cooperation).

Equation (3.20) shows that the diversity order for fast fading is equal to the total Hamming weight $d = d_1 + d_2$. This is also true for no cooperation (see (3.25)). For statistically dissimilar uplink channels ($\Gamma_{1,0} \neq \Gamma_{2,0}$), (3.20) indicates definite improvement for the user with the lower uplink average SNR, which is an important practical result. For statistically similar uplink channels, (3.20) becomes equal to (3.25). Intuitively we see that coded cooperation does not provide additional diversity in fast fading when the average uplink SNR are equal.

For Case 3, the conditional PEP (3.17) for User 1 becomes

$$\begin{aligned} P(d|\boldsymbol{\gamma}_{1,0},\boldsymbol{\gamma}_{1,0}) &= Q\left(\sqrt{2\sum_{n\in\eta_1}\gamma_{1,0}(n)+2\sum_{n\in\eta_2}\gamma_{1,0}(n)+2\sum_{n\in\eta_2}\gamma_{2,0}(n)}\right) \\ &= Q\left(\sqrt{2\sum_{n\in\eta}\gamma_{1,0}(n)+2\sum_{n\in\eta_2}\gamma_{2,0}(n)}\right) \end{aligned} \tag{3.21}$$

and unconditional PEP becomes

$$\begin{aligned} P(d) &= \frac{1}{\pi}\int_0^{\pi/2}\left(1+\frac{\Gamma_{1,0}}{\sin^2\theta}\right)^{-d}\left(1+\frac{\Gamma_{2,0}}{\sin^2\theta}\right)^{-d_2}d\theta \\ &\leq \frac{1}{2}\left(\frac{1}{1+\Gamma_{1,0}}\right)^{d}\left(\frac{1}{1+\Gamma_{2,0}}\right)^{d_2}. \end{aligned} \tag{3.22}$$

Equation (3.22) shows that User 1 does achieve improved diversity compared with no cooperation ($d + d_2$ vs. d) for Case 3.

3.3.3 No Cooperation

For non-cooperative transmission in slow fading, all the code bits for a user are transmitted through the same channel (e.g., $d_1 = d$ and $d_2 = 0$). Thus for slow fading we have conditional and unconditional PEP

$$P(d|\gamma) = Q\left(\sqrt{2d\gamma}\right) \tag{3.23}$$

$$\begin{aligned} P(d) &= \frac{1}{\pi}\int_0^{\pi/2}\left(1+\frac{d\Gamma}{\sin^2\theta}\right)^{-1} d\theta \\ &\leq \frac{1}{2}\left(\frac{1}{1+d\Gamma}\right). \end{aligned} \tag{3.24}$$

For fast fading, the conditional PEP is given by (3.5), and the unconditional PEP is

$$\begin{aligned} P(d) &= \frac{1}{\pi}\int_0^{\pi/2}\left(1+\frac{\Gamma}{\sin^2\theta}\right)^{-d} d\theta \\ &\leq \frac{1}{2}\left(\frac{1}{1+\Gamma}\right)^{d}. \end{aligned} \tag{3.25}$$

These are similar to the results reported in, for example, [25, (13)], [47, (14-3-7)]. They are included here for reference because they are used in Section 3.4.2 to compute the end-to-end performance of coded cooperation. Specifically, for Case 2, the PEP for both users corresponds to non-cooperative transmission with the overall rate R code word. For Cases 3 and 4, the PEP for the user that is not decoded correctly by the partner corresponds to non-cooperative transmission with the rate R_1 code word used for transmission of the first frame.

3.4 Bit and Block Error Rate Analysis

We now use the above PEP results to determine the end-to-end bit and block error probabilities for coded cooperation. The first step is calculating the probabilities of the cooperative cases.

3.4.1 Cooperative Case Probabilities

The cooperative case probabilities are determined by the BLER of the first frame transmission. The BLER for a terminated convolutional code is bounded by [45, (12)], [36, (11)]

$$P_{block}(\boldsymbol{\gamma}) \leq 1 - (1 - P_E(\boldsymbol{\gamma}))^B \leq B \cdot P_E(\boldsymbol{\gamma}) \tag{3.26}$$

where B is the number of trellis branches in the code word, and $P_E(\boldsymbol{\gamma})$ is the error event probability conditioned on $\boldsymbol{\gamma}$, the vector state of the channel. P_E is bounded as [67, (4.4.5)]

$$P_E(\boldsymbol{\gamma}) \leq \sum_{d=d_f}^{\infty} a(d)\, P(d|\boldsymbol{\gamma}), \tag{3.27}$$

where d_f is the code free distance and $a(d)$ is the number of error events of Hamming weight d.

We parameterize the four cases by $\Theta \in \{1, 2, 3, 4\}$ and we can express the conditional probability for Case 1 ($\Theta = 1$) as follows:

$$\begin{aligned} P(\Theta = 1|\boldsymbol{\gamma}_{1,2}, \boldsymbol{\gamma}_{2,1}) &= (1 - P_{block,1}(\boldsymbol{\gamma}_{1,2}))(1 - P_{block,2}(\boldsymbol{\gamma}_{2,1})) \\ &\geq (1 - P_{E,1}(\boldsymbol{\gamma}_{1,2}))^B (1 - P_{E,2}(\boldsymbol{\gamma}_{2,1}))^B \\ &\geq (1 - B\, P_{E,1}(\boldsymbol{\gamma}_{1,2}))(1 - B\, P_{E,1}(\boldsymbol{\gamma}_{2,1})). \end{aligned} \tag{3.28}$$

Bounds for the other cases are developed similarly.

To calculate end-to-end error probabilities, we need the unconditional probability of Case Θ, $P(\Theta)$:

$$P(\Theta) = \int_{\boldsymbol{\gamma}_{1,2}} \int_{\boldsymbol{\gamma}_{2,1}} P(\Theta|\boldsymbol{\gamma}_{1,2}, \boldsymbol{\gamma}_{2,1}) p(\boldsymbol{\gamma}_{1,2}) p(\boldsymbol{\gamma}_{2,1})\, d\boldsymbol{\gamma}_{1,2} d\boldsymbol{\gamma}_{2,1}. \tag{3.29}$$

For slow fading, vectors $\boldsymbol{\gamma}_{1,2}$ and $\boldsymbol{\gamma}_{2,1}$ reduce to scalars $\gamma_{1,2}$ and $\gamma_{2,1}$. In addition, for reciprocal inter-user channels, $\gamma_{1,2} = \gamma_{2,1}$, and $P(\Theta|\gamma_{1,2})$ is conditioned on a single

variable, reducing (3.29) to a single integral

$$P(\Theta) = \int_0^\infty P(\Theta|\gamma_{1,2}) p(\gamma_{1,2})\, d\gamma_{1,2}. \tag{3.30}$$

For independent inter-user channels, the first-frame BLER of the two users are independent, and $P(\Theta)$ has form analogous to the first line of (3.28); i.e., for Case 1,

$$P(\Theta = 1) = (1 - P_{block,1}) \cdot (1 - P_{block,2}). \tag{3.31}$$

To obtain tight bounds for the case of slow fading, we use the limit-before-average technique from Malkamäki and Leib [45], with the appropriate conditional (on fading) PEP, to evaluate (3.29) and (3.31). For example, for Case 1 with reciprocal inter-user channels we have

$$\begin{aligned} P(\Theta = 1) \;\; &\geq \;\; \int_0^\infty \left(1 - \min\left[1, \sum_{d=d_f}^{\infty} a(d) P(d|\gamma_{1,2})\right]\right)^B \\ &\times \;\; \left(1 - \min\left[1, \sum_{d=d_f}^{\infty} a(d) P(d|\gamma_{1,2})\right]\right)^B p(\gamma_{1,2})\, d\gamma_{1,2}. \end{aligned} \tag{3.32}$$

With independent inter-user channels, we compute the unconditional BLER for User i as

$$P_{block,i} \leq 1 - \int_0^\infty \left(1 - \min\left[1, \sum_{d=d_f}^{\infty} a(d)\, P(d|\gamma_{i,j})\right]\right)^B p(\gamma_{i,j}) d\gamma_{i,j} \tag{3.33}$$

and apply the results to (3.31). The unconditional probabilities for the other cases are evaluated similarly. Note that these expressions involve the conditional (on fading) PEP, not the unconditional one. Specifically, since the first frame transmission is non-cooperative in nature, $P(d|\gamma_{1,2})$ in (3.32) and (3.33) corresponds to (3.23) in Section 3.3.3. Furthermore, because of the minimization operation, (3.32) and (3.33) must be computed numerically.

For fast fading, a tight bound for the unconditional BLER is obtained simply by using the unconditional PEP, $P(d)$ from (3.25), in (3.27), and then using the

resulting unconditional error event probability, P_E, in (3.26) [45]. Since we assume that the inter-user channels are always independent for fast fading, we can again apply these results to (3.31) for Case 1, and the corresponding expressions for the other cases. Finally, we note that for both slow and fast fading, $a(d)$ in (3.27), (3.32), and (3.33) corresponds to the rate R_1 code used for first-frame transmission.

3.4.2 End-to-End Error Analysis

The overall end-to-end unconditional BER is equal to the average of the unconditional BER over the four possible transmission scenarios discussed in Section 3.4.1 as

$$P_b = \sum_{i=1}^{4} P_b(\Theta) P(\Theta = i). \tag{3.34}$$

The end-to-end BLER has a similar expression.

The conditional BLER is given by (3.26)–(3.27), and the conditional BER is bounded by [67, (4.4.8)]

$$P_b(\boldsymbol{\gamma}, \Theta) \leq \frac{1}{k_c} \sum_{d=d_f}^{\infty} c(d) P(d|\boldsymbol{\gamma}, \Theta) \tag{3.35}$$

where $c(d)$ is the number of information bit errors for code words or error events with Hamming weight d, and k_c is the number of input bits for each branch of the code trellis.

We again use the limit-before-average technique [45] with the appropriate conditional PEP expressions to obtain tight bounds for slow fading. The unconditional

BER and BLER are

$$\begin{aligned} P_b(\Theta) &\leq \int_0^\infty \int_0^\infty \min\left[\frac{1}{2}, \frac{1}{k_c}\sum_{d=d_f}^{\infty} c(d)P(d|\gamma_{1,0},\gamma_{2,0},\Theta)\right] \\ &\times\ p(\gamma_{1,0})p(\gamma_{2,0})d\gamma_{1,0}d\gamma_{2,0} \qquad (3.36) \\ P_{block}(\Theta) &\leq 1 - \int_0^\infty \int_0^\infty \left(1 - \min\left[1, \sum_{d=d_f}^{\infty} a(d)\,P(d|\gamma_{1,0},\gamma_{2,0},\Theta)\right]\right)^B \\ &\times\ p(\gamma_{1,0})p(\gamma_{2,0})d\gamma_{1,0}d\gamma_{2,0}. \qquad (3.37) \end{aligned}$$

For fast fading, tight bounds are obtained using the unconditional (on fading) $P(d|\Theta)$ expression directly in the summation (3.27) or (3.35), in lieu of computing (3.36) and (3.37) [45]. Applying these results and the results for the case probabilities to (3.34) gives upper bounds for the end-to-end bit and block error probabilities. (Although the case probabilities from Section 3.4.1 are not all strictly upper bounds, i.e. (3.28) and (3.32), the net effect is that the cases with lower error rate are weighted less than their actual probabilities, and those with higher error rate are weighted more, resulting in an overall upper bound for (3.34).)

Whenever both users cooperate (Case 1) each user's message sees two independent fading paths and a diversity order of two is achieved. When a user's message does not benefit from cooperation the diversity is one. Therefore, the overall diversity order, interpreted as the slope of the error rate, is the average of the diversities in the four cases, weighted by the probabilities of the four cases. These probabilities are determined by the inter-user channel conditions. At high inter-user SNR, Case 1 is dominant and coded cooperation achieves full diversity order of two.[1] We note that,

[1]For any fixed set of probabilities, the errors of diversity order one will eventually dominate at high enough uplink SNR (even though such SNR's may be unrealistic in practice). Strictly speaking, to achieve diversity order of two, the ratio of the case probabilities in the asymptote must keep up with the increased uplink SNR. Therefore to make the above statement more precise, one more condition must be added. For example, one might say: "diversity of two is achieved if a fixed uplink to inter-user SNR ratio is maintained in the asymptote."

in order to highlight certain characteristics, we generally choose to fix the inter-user SNR. Thus, some of our simulations are not in this dominant mode, and for that reason show diversity less than two.

3.5 Performance Evaluation

In order to evaluate the performance of coded cooperation, we employ the implementation using RCPC codes as described in Section 3.2. Specifically, we use the family of RCPC codes with memory $M = 4$, puncturing period $P = 8$, and rate $1/4$ mother code given by Hagenauer [25]. For slow fading, we choose overall code rate $R = 1/4$, while for fast fading we use $R = 2/5$. In all cases, the source block size is $K = 128$ bits. We computed via computer enumeration the distance spectra $a(d)$ and $c(d)$, including the partitioning of the Hamming weight d into d_1 and d_2. For the simulations, we use a 16-bit CRC code with generator polynomial given by coefficients 15935 (hexadecimal notation). For our analysis we assume perfect error detection. Our results indicate that suboptimal error detection of the CRC code has a negligible effect on the overall performance, and we refer the reader to Section 3.6.4 for further discussion on this issue. Figures 3.5 through 3.10 present analytical and simulation results for various scenarios described in more detail below. Due to space considerations, we only show results for BER. Curves for BLER appear virtually identical, save for a shift in the y-axis values (for slow fading, the BLER is about one order of magnitude more than BER, while for fast fading it is about two orders of magnitude more). Since all comparisons are between systems with equal information rate K bits per source block, and equal code rate R, we plot the BER versus the channel SNR. Plotting BER versus the information bit SNR yields identical results, with the x-axis values shifted by $10 \log R$ dB.

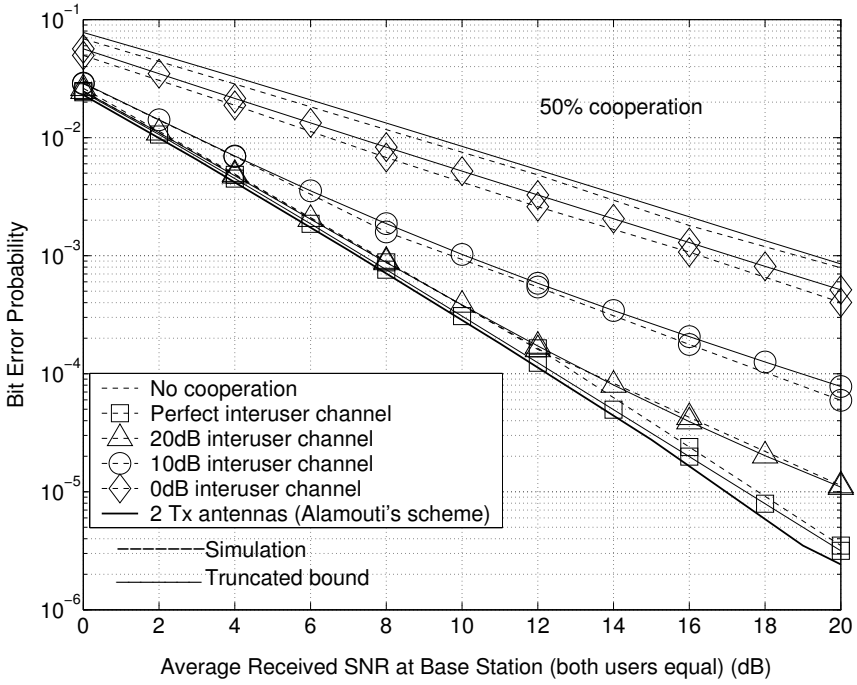

Figure 3.5. Performance in slow Rayleigh fading with 50% cooperation, equal uplink SNR, and reciprocal inter-user channels.

3.5.1 Slow Fading

Figure 3.5 shows the BER for slow fading with reciprocal inter-user channels of various qualities. The users have statistically similar uplink channels ($\Gamma_{1,0} = \Gamma_{2,0}$), and the level of cooperation is 50%. We see that coded cooperation with a perfect inter-user channel performs virtually identically to a comparable two-antenna transmit diversity system. In this system, we use as an outer code the same rate 1/4 RCPC code that we use for coded cooperation, concatenated with the space-time block code proposed by Alamouti [2]. Since the Alamouti code is known to provide full diversity order two [2], this result confirms the PEP analysis from Section 3.3.1 and demonstrates that coded cooperation does achieve full diversity for Case 1. The improvement over no cooperation remains dramatic for good inter-user channels. For example, when the inter-user channel has 10dB average SNR, the gain is about 9dB for BER 10^{-3}. The gain decreases as the inter-user channel worsens, as well as the curve slope

as discussed at the end of Section 3.4.2. However, coded cooperation still achieves significant improvement even when the inter-user channel is much worse that the uplink channels. For example, we see a 2–3dB gain for an inter-user channel with average SNR 0dB over the range of 0–20dB average uplink SNR.

Figure 3.6 compares the performance of coded cooperation at 50% and 25%, for both a perfect inter-user channel and one with average SNR of 10dB. The user uplink channels again have equal average SNR. When the inter-user channel is perfect, both users always cooperate (e.g., we have Case 1 exclusively), and consequently 50% cooperation yields better performance. This is predicted by the PEP of (3.14), since we expect the product $d_1 \cdot d_2$ to be maximized for 50% cooperation (d_1 and d_2 should be approximately equal). However, as the inter-user channel becomes worse, the situation changes. Figure 3.6 shows that 25% cooperation becomes better than 50% cooperation for the 10dB inter-user channel, by as much as 2dB for higher uplink SNR. For poor inter-user channels, a stronger code in the first frame is more important to the overall performance than maximizing the product $d_1 \cdot d_2$. This is again a result of averaging over the four cooperative cases.

In Figure 3.7, we examine the performance of coded cooperation when the users have statistically dissimilar uplink channels. We fix the average uplink SNR for User 1 at 20dB, while varying User 2's average uplink SNR from 0dB to 20dB. The inter-user channel has average SNR 10dB. Figure 3.7 shows that User 2, with the worse uplink channel, improves dramatically with coded cooperation, exhibiting a gain of 11–13dB relative to no cooperation. More interestingly however, User 1, with the better uplink channel, also achieves a marked improvement in performance by cooperating, a result that is not necessarily intuitive. Specifically, the results show that User 1, with an uplink SNR of 20dB, has significant improvement (a factor of two reduction in BER) even when the partner's uplink channel is 20dB worse. Thus,

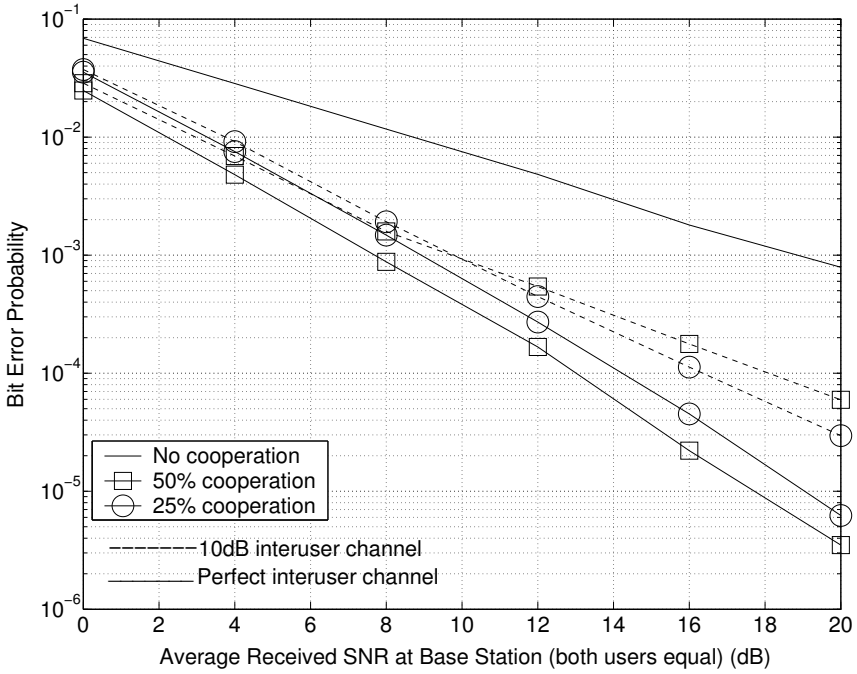

Figure 3.6. Comparison of 50% and 25% cooperation in slow Rayleigh fading, equal uplink SNR.

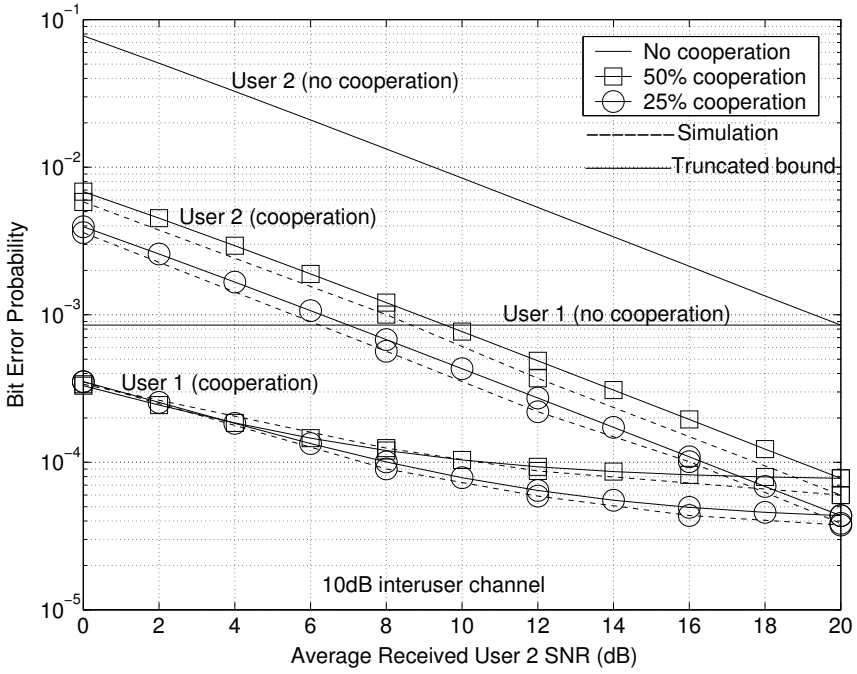

Figure 3.7. Performance under asymmetric uplink conditions in slow Rayleigh fading.

even a user with a very good uplink channel has a strong motivation to cooperation in a slow-fading environment.

In order to simplify the plots, we show in Figures 3.5 and 3.7 the analytical bounds truncated using only the first few terms of the distance spectrum, which is sufficient for our purposes. Because of this approximation, these bounds appear slightly tighter than that of [45]. Using all of the terms gives tight upper bounds with convergence behavior similar to [45].

3.5.2 Destination with Receive Diversity

In many current and proposed wireless systems, the destinations have multiple antennas in order to take advantage of the various transmit and receive diversity methods that have been developed in recent years. It is natural, therefore, to investigate the performance of coded cooperation when the destination has multiple antennas. Figure 3.8 shows simulation results for coded cooperation when the destination has two receive antennas. We consider slow Rayleigh fading, equal average SNR uplink channels, 50% cooperation, and reciprocal inter-user channels with various average SNR. We see that again coded cooperation provides substantial gains.

Bauch and Hagenauer [5] have shown that, for transmit diversity using orthogonal space-time block codes [2, 59], the equivalent single-input single-output channel between the transmitter and receiver asymptotically becomes an additive white Gaussian noise (AWGN) channel as the number of transmit antennas increases. Clearly, receive diversity with maximal-ratio combining has an identical result as the number of receive antennas increases. Since the AWGN channel has no fading, cooperation will not provide any additional diversity gain. This is illustrated by the fact that the PEP (3.6) and (3.23) are equal for equal uplink SNR. Consequently, we would expect the gain from coded cooperation to decrease as the number of receive antennas

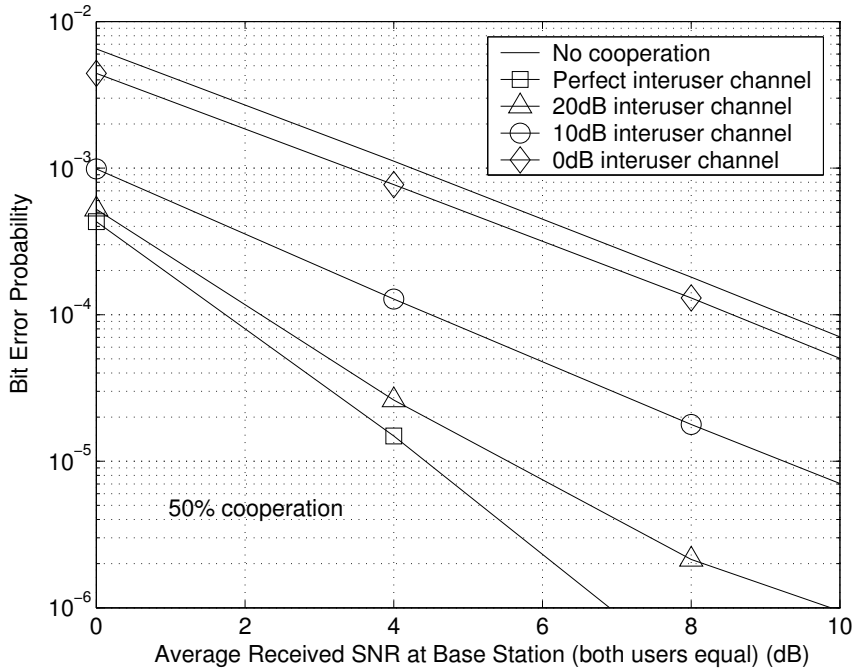

Figure 3.8. User cooperation combined with two receive antennas (receive diversity).

increases. This is shown in Figure 3.8. For example, at BER 10^{-3} and 10dB inter-user channel, coded cooperation has a gain of about 9dB for a single receive antenna (Figure 3.5). This gain reduces to about 4dB for two receive antennas (Figure 3.8). Qualitatively we can say that the gain from cooperation becomes less significant in an environment that provides other sources of diversity. This is true in general for diversity techniques; that is, applying further diversity methods in an environment that already provides other forms of diversity yields diminishing returns (see for example [2, 5]). However, in this case, for a relatively small number of receive antennas, the gains from coded cooperation remain substantial.

3.5.3 Comparison with Amplify-and-Forward

In this section we compare coded cooperation with a coded version of the amplify-and-forward protocol proposed in [41, 43]. In this scheme, the coded bits of each user are amplified and forwarded in the analog domain by the partner. This comparison

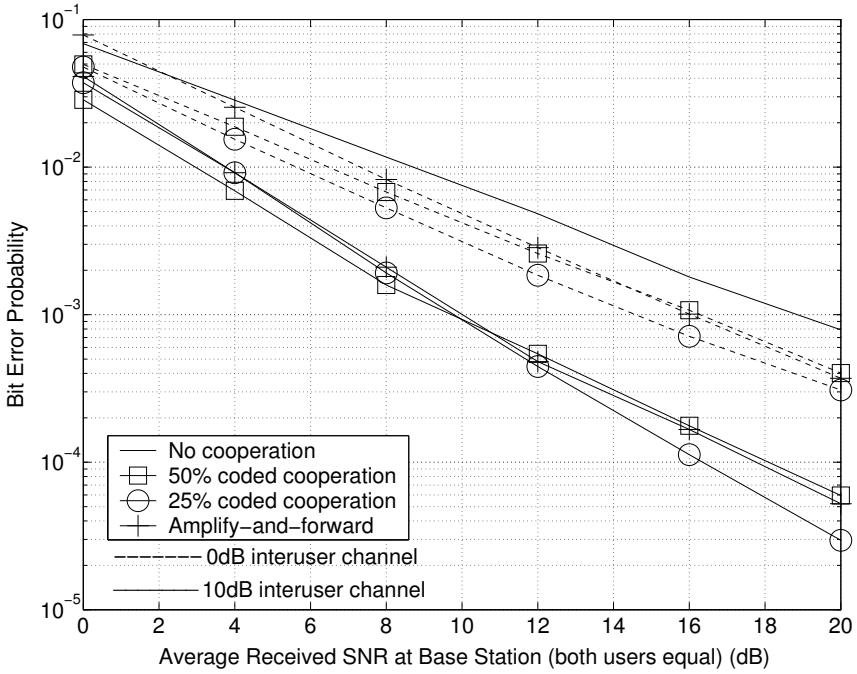

Figure 3.9. Comparison of coded cooperation with amplify-and-forward under slow Rayleigh fading.

serves to illustrate the advantages of coded cooperation over previously proposed repetition-based schemes.

We implement the amplify-and-forward protocol with a rate-1/2 convolutional code, resulting in an overall rate of 1/4. The overall code rate for coded cooperation is also $R = 1/4$. Figure 3.9 shows the comparison of simulated BER for slow Rayleigh fading, equal uplink average SNR, and inter-user channels with 10dB and 0dB average SNR. Coded cooperation maintains an edge of up to 1–2dB over amplify-and-forward, depending on the uplink SNR. The level of cooperation that achieves the best performance for coded cooperation varies between 50% and 25%, depending on the channel conditions. The level of cooperation for amplify-and-forward, of course, is inflexible (set at 50%) since repetition is a core part of that protocol. In addition, analog replication may be difficult to implement in practice.

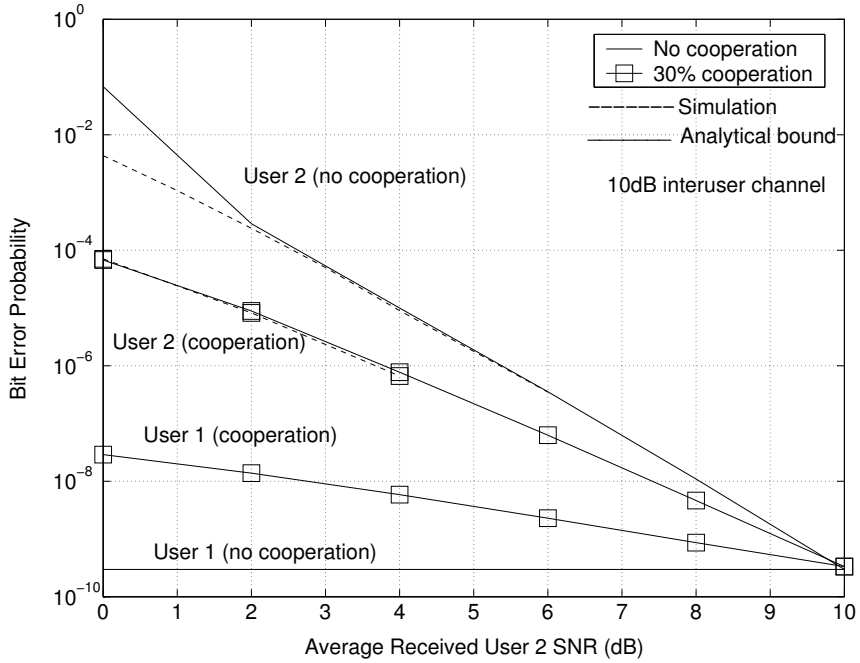

Figure 3.10. Fast i.i.d. Rayleigh fading, unequal uplink average SNR, and independent inter-user channels.

3.5.4 Fast Fading

Based on the results of Section 3.3.2, we focus our attention for fast fading on the case when the two users have statistically dissimilar uplink channels. In Figure 3.10, the average uplink SNR for User 1 is fixed at 10dB, while User 2's varies from 0dB to 10dB. The inter-user channels are independent and have average SNR of 10dB. Under these conditions, 30% cooperation provides the best performance. Figure 3.10 shows that the bounds developed in Sections 3.3 and 3.4 are quite tight. In terms of performance, User 2, with the worse uplink channel, experiences significant improvement, gaining up to 3–3.5dB at low uplink SNR. User 1, with the better uplink channel, sacrifices some performance by cooperating. Nevertheless, even in fast fading coded cooperation can help a user with a poor uplink channel, provided that the partner's performance remains acceptable. This is an important practical result with respect to maintaining a minimum system-wide quality of service.

3.6 Implementation Issues

3.6.1 Inter-user Channel Reciprocity and Multiple Access Protocol

As discussed in Section 3.1, previous works on user cooperation ([52, 53, 41, 43]) generally assume that the channels between the users are reciprocal for slow fading. In other words, for two Users i and j, the fading coefficients between them are equal ($\alpha_{i,j} = \alpha_{j,i}$), or equivalently the instantaneous SNR between them are equal ($\gamma_{i,j} = \gamma_{j,i}$). This is justifiable for TDMA systems and CDMA systems with slow fading, but less so for FDMA systems. In FDMA, adjacent frequency channels generally may not have identical fading. However, it is likely that they are correlated to some degree, and are not fully independent. The following results show that even if we assume the extreme condition of fully independent inter-user channels, the gains of coded cooperation can be maintained via judicious choice of cooperation level.

Figure 3.11 shows the difference in analytical BER bounds for reciprocal versus independent inter-user channels of various qualities. All channels are subject to slow Rayleigh fading, and the user uplink channels are statistically similar. For 50% cooperation, having independent inter-user channels reduces the gains by 1–3dB, depending on the inter-user channel quality. However, for 25% cooperation, the results for reciprocal and independent inter-user channels are well within 1dB of each other for all inter-user channel qualities.

Tables 3.1 and 3.2 list the inter-user BLER and cooperative case probabilities corresponding to Figure 3.11, and illustrate the reason for the difference in performance between reciprocal and independent inter-user channels. For reciprocal channels, it is more likely that both users will act similarly; e.g., both will either decode each other successfully or unsuccessfully. This symmetric behavior leads to (slightly) better performance. The stronger first-frame code employed with 25% cooperation reduces the effect of the more asymmetric behavior caused by independent inter-user

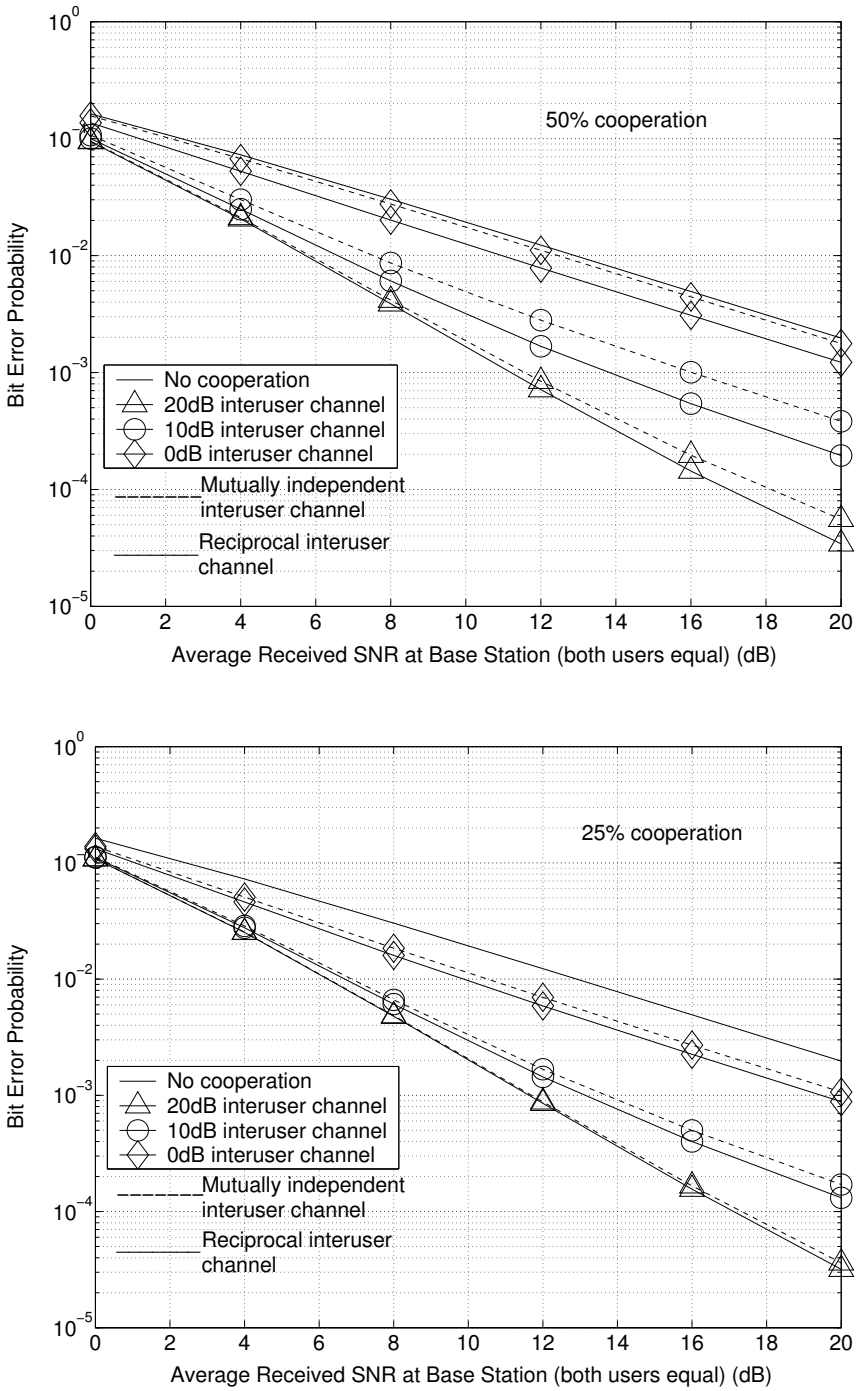

Figure 3.11. Comparison (analytical bound) of coded cooperation for reciprocal and mutually independent inter-user channels of various qualities.

Table 3.1. 50% Cooperation, Inter-user BLER and Cooperative Case Probabilities Corresponding to Figure 3.11.

Inter-user Average SNR	Reciprocal inter-user channel Case Probability				Independent inter-user channel Case Probability				Inter-user BLER
	$\Theta = 1$	$\Theta = 2$	$\Theta = 3$	$\Theta = 4$	$\Theta = 1$	$\Theta = 2$	$\Theta = 3$	$\Theta = 4$	
20dB	0.99	0.01	$\sim$0	$\sim$0	0.982	$\sim$0	0.009	0.009	0.009
10dB	0.91	0.084	0.003	0.003	0.83	0.008	0.081	0.081	0.089
0dB	0.385	0.59	0.011	0.011	0.16	0.36	0.24	0.24	0.6

Table 3.2. 25% Cooperation, Inter-user BLER and Cooperative Case Probabilities Corresponding to Figure 3.11.

Inter-user Average SNR	Reciprocal inter-user channel Case Probability				Independent inter-user channel Case Probability				Inter-user BLER
	$\Theta = 1$	$\Theta = 2$	$\Theta = 3$	$\Theta = 4$	$\Theta = 1$	$\Theta = 2$	$\Theta = 3$	$\Theta = 4$	
20dB	0.994	0.006	$\sim$0	$\sim$0	0.988	$\sim$0	0.006	0.006	0.006
10dB	0.942	0.054	0.002	0.002	0.89	0.003	0.053	0.053	0.056
0dB	0.55	0.43	0.01	0.01	0.32	0.19	0.25	0.25	0.44

channels. This again points to a key benefit of the flexibility available in the framework of coded cooperation: the ability to vary the code rates between the first and second frames provides a degree of robustness to unfavorable conditions.

For fast fading, the inter-user channels will clearly be independent unless the first frame transmissions of the users are exactly synchronized. Therefore, for all the fast fading experiments, we assume independent inter-user channels. We also note that for fast fading, empirical results (not included in here) show no significant difference in performance for reciprocal versus independent inter-user channels.

3.6.2 Coded Cooperation with CDMA

For CDMA systems, cooperation in general implies that a user is simultaneously transmitting and receiving in the same frequency band, which is generally considered infeasible with current radio technology. Sendonaris, Erkip, and Aazhang [52] allude to the possibility for a user to cancel its own echo in the received signal. Indeed it may be possible to do this using, for example, adaptive filtering methods for echo cancellation [28]. However, the real practicality of this remains unclear. Since many current CDMA wireless systems are actually hybrid CDMA/FDMA systems that use several uplink frequencies (see for example [33],[1]), we can avoid the difficulties of simultaneous transmission and reception, yet still preserve the advantages of CDMA, by having the partners use different frequency channels.

3.6.3 Cooperative Overhead

Section 3.2 notes that the destination must know which of the four cooperative cases has occurred in order to correctly decode the received frames. One approach is that each user sends one additional bit in the second frame to indicate the first-frame decision. This bit would have to be strongly protected via, for example, repetition

Table 3.3. Complexity Factors For End-to-End BLER 10^{-2}, 50% Cooperation, And Reciprocal Inter-user Channel

Inter-user Average SNR	Case Probability $\Theta = 1$	$\Theta = 2$	$\Theta = 3$	$\Theta = 4$	Complexity Factor k
20dB	0.992	0.0069	0.0007	0.0007	1.04
10dB	0.92	0.067	0.0066	0.0066	1.13
0dB	0.44	0.50	0.03	0.03	1.61

coding, which introduces a tradeoff between the additional overhead imposed and the probability of error for this bit.

An alternative approach is to have the destination simply decode according to each of the four cases in succession, according to their relative probabilities of occurrence, until the CRC code indicates correct decoding. This strategy maintains the overall system performance and rate at the cost of some added complexity at the destination. We can express this complexity in terms of the expected number of decoding attempts k required by the destination to process the received frames for a given code word. The complexity factor k can be expressed as

$$k = 4 \cdot P_{block} + (1 - P_{block}) \sum_{\Theta=1}^{4} \Theta \cdot P(\Theta), \tag{3.38}$$

where P_{block} denotes the end-to-end BLER for the code word, and $P(\Theta)$ denotes the probability of Case Θ, with index Θ ordered such that $\Theta = 1$ corresponds to the most probable case. For end-to-end BLER 10^{-2}, Table 3.3 gives k values for 50% cooperation with reciprocal inter-user channels, which show that the increase in complexity at the destination is minimal.

3.6.4 CRC Code

Since the CRC code is a key element of coded cooperation, for the sake of completeness we briefly discuss the error-detecting capabilities of CRC codes. For further details,

Table 3.4. CRC Code Error Detection Coverage

Number of CRC code bits p	Error detection coverage λ
4	0.9375
7	0.992188
12	0.999756
16	0.99998
24	0.9999999
32	0.9999999997

see [70, Section 5.3] and references therein. The fraction λ of all error patterns that are detectable by a binary CRC code with p bits is given by $\lambda = 1 - 2^{-p}$ [70, (5-16)], which is solely a function of the number of redundant bits. Table 3.4 gives λ for several common values of p. Comparing these results with the inter-user channel probabilities in Tables 3.1, and 3.2, we see that, for example, twelve CRC bits gives $1-\lambda$ an order of magnitude less than the inter-user BLER, and the effect of non-ideal error detection by the partner will not significantly affect the overall performance.

We emphasize that the CRC code does not represent additional overhead bits required by coded cooperation. Most current and future wireless systems already incorporate CRC codes into their channel coding schemes. For coded cooperation we are simply employing the CRC code that is already part of the comparable non-cooperative system.

3.7 Chapter Summary

In this chapter, we present a new technique for wireless user cooperation, called coded cooperation, in which cooperation is integrated with channel coding. Diversity is achieved by partitioning a user's code word into two parts. Each user receives the first partition from the partner, and upon successful decoding (determined via

a concatenated CRC code), generates and transmits the second partition. The two partitions are thus received at the destination through independent fading channels. This coded cooperation framework may be implemented using block or convolutional codes, and many different methods of partitioning the code words (puncturing, product codes, parallel and serial concatenation, etc). Our examples in this chapter use RCPC and CRC codes and partition the code words via puncturing. Examples of coded cooperation using turbo codes and iterative decoding are presented in Chapter 4.

Coded cooperation maintains for both users the same overall information rate, code rate, transmit power, and bandwidth as in the comparable non-cooperative system. A key feature of coded cooperation is the ability to vary the code rate between the two codeword partitions in order to adapt to various channel conditions.

We develop tight upper bounds for the performance of coded cooperation, and validate these bounds with simulations. For slow Rayleigh fading, coded cooperation yields impressive gains for both partners, even when the inter-user channel is much worse than the uplink channels, and when one has a much worse uplink channel than the other. For fast i.i.d. Rayleigh fading, coded cooperation provides important gains when the users have different uplink channel qualities. The user with the worse uplink channel experiences significant improvement under these conditions. In Chapter 4, we present an extension of coded cooperation using space-time signaling concepts to improve performance in fast fading.

CHAPTER 4

EXTENSIONS TO CODED COOPERATION: SPACE-TIME TRANSMISSION AND ITERATIVE DECODING

In this chapter, we introduce two extensions to the coded cooperation framework developed in Chapter 3 that significantly improve performance under a variety of scenarios. The first extension uses ideas from space-time coding[1] and MIMO systems, and thus we refer to this technique as *space-time cooperation*. This extension allows the users to capture better space-time diversity in fast fading, compared to coded cooperation.

Second, while examples in Chapter 3 involve coded cooperation implemented using RCPC codes, various channel coding methods can be used within the coded cooperation framework, as discussed in Section 3.2. In particular, since coded cooperation involves two code components, turbo codes are a natural fit. We investigate turbo-coded cooperation in the context of both original coded cooperation and space-time cooperation. We demonstrate that turbo-coded cooperation improves performance over non-cooperative turbo-coded systems that have comparable computational complexity. In addition, our turbo codes are decoded at the destination; the turbo code component does not add to the mobile complexity.

We analyze the performance of space-time cooperation over slow and fast frequency non-selective fading channels. Tight union bounds for bit error rate (BER) and block error rate (BLER), verified through simulations, are developed by again applying the tools and techniques from Simon and Alouini [54] and Malkamäki and Leib [45]. Full diversity order is achieved in slow fading when both users cooperate.

[1]Depending on the multiple access mechanism, an actual space-time code may be used.

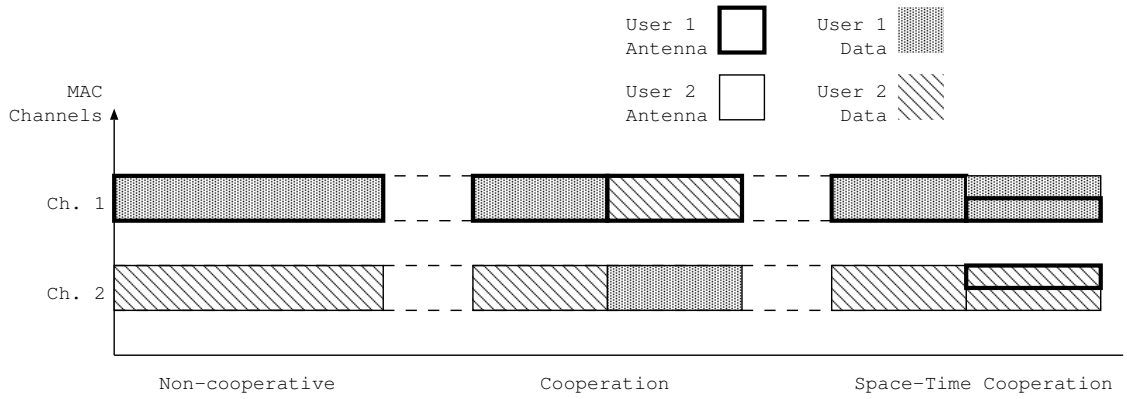

Figure 4.1. Space-time cooperation compared to the original coded cooperation and no cooperation.

In fast fading, higher diversity order is achieved compared with coded cooperation and no cooperation. The BER and BLER bounds are confirmed through simulations.

4.1 Coded Cooperation with Space-Time Transmission

The results developed in this chapter are based on the system model described in Section 3.1. The results for slow fading presented in this chapter correspond to reciprocal inter-user channels, noting that in Section 3.6.1 it is shown that reciprocity or lack of it does not significantly affect the performance of coded cooperation. As in Chapter 3, for fast fading we assume that the inter-user channels are independent.

4.1.1 Space-Time Cooperation

Our extension of the coded cooperation framework is illustrated in Figure 4.1. Unlike the original coded cooperation framework, where users transmit their partner's data in the second frame (whenever possible), in the new method, which we call space-time cooperation, the users send both their own as well as their partner's parity bits in the second frame. This strategy is effective in the fast fading channel for the two reasons given below.

Under fast fading, a user's uplink channel sees independent fading between the first and second frames, thus using the partner's channel in the second frame does not provide any added benefit. In space-time cooperation the second frame by itself enjoys path diversity because each user transmits *both* users' parities during the second frame.

Furthermore, the users, by sending both their own as well as their partner's data, are hedging their bets against adverse conditions in the inter-user channel. Recall that each user makes independent decisions on cooperation, based on the reception of partner's data. If only one of the cooperating users receives the other correctly but not vice versa, then one of the users will benefit from the transmissions of *both* second frames, while the other will not (see Figure 3.4). It has been shown in Chapter 3 that in the context of slow fading, especially with reciprocal inter-user channels, the impact of these imbalances are minimal because their probabilities are very small. In fast fading, that is not so. By using part of their power in the second frame for their own data, the users reduce the impact of such adverse conditions.

The details of the space-time cooperation are as follows. The encoded block for User i, $\boldsymbol{y_i}$, is divided into the two frames, $\boldsymbol{v_i}$ and $\boldsymbol{s_i}$, such that $\boldsymbol{y_i} = [\boldsymbol{v_i}, \boldsymbol{s_i}]$, $i = 1, 2$. For second frame transmission, if User 1 successfully decodes $\boldsymbol{v_2}$, User 1 transmits $\boldsymbol{s_1}$ using User 1's channel and $\boldsymbol{s_2}$ using User 2's channel. Otherwise, User 1 transmits $\boldsymbol{s_1}$ only. In order to maintain the same average power, User i divides his power in the second frame according to the ratio β_i, so that User i's own bits $\boldsymbol{s_i}$ are transmitted with energy $\beta_i E_{b,i}$, and the partner User j's bits are transmitted with energy $(1 - \beta_i)E_{b,i}$.

We denote the additional parity bits of User i which are transmitted by User j as $\boldsymbol{s}_{i,j}$. For the purposes of this work, we assume that the multiple access and coding schemes are such that $\boldsymbol{s}_{i,i}$ and $\boldsymbol{s}_{i,j}$ can be coherently combined at the destination. We

discuss the implementation of this framework for different multiple access and coding schemes in more detail in Section 4.1.2.

As in the original coded cooperation framework, the users act independently in the second frame, with no knowledge of whether their first frame was correctly decoded by their partner. This again gives rise to four possible cooperative cases for the transmission of the second frame. In Case 1, both users successfully decode their partners, so that they each send both their own and their partner's second set of coded bits in the second frame, resulting in the fully cooperative scenario depicted in Figure 4.1. In Case 2, neither user successfully decodes their partner's first frame, and the system reverts to the non-cooperative case for that pair of source blocks, i.e., $\beta_i = 1$, $i = 1, 2$. In Case 3, User 2 successfully decodes User 1, but User 1 does not successfully decode User 2. Consequently, User 1 transmits only his own bits in the second frame, i.e., $\beta_1 = 1$, while User 2 splits his power and transmits the additional parity bits for both himself and User 1. Case 4 is identical to Case 3 with the roles of User 1 and User 2 reversed.

In Section 4.3 we present an analytical methodology for evaluating the performance of space-time cooperation, showing that we achieve full diversity in slow fading (for Cases 1 and 3), and improved diversity over the original coded cooperation in fast fading. We demonstrate the validity of these bounds via simulations as part of the performance results presented in Section 4.4.

4.1.2 Implementation Issues

In this section we briefly visit the implementation of space-time cooperation in different multiple access schemes. The main issues considered here are transmission in both channels during the second frame, and coherent combining at the receiver.

In the case of CDMA, transmission in each channel requires only the use of a

different chip sequence. Since the data of each user is transmitted by two different users, the two transmissions are not time coherent, but they may be resolved at the destination and coherently combined via RAKE fingers. We note that this method was first suggested in the context of the CDMA uncoded cooperation scenario of Sendonaris, Erkip, and Aazhang [52, 53].

In the case of FDMA, the new method entails transmission on two different frequency bands. Each bit in the second frame is transmitted by two antennas, thus the simple but effective code of Alamouti [2] may be used. Alamouti's space-time code requires that the symbols be transmitted from the two antennas in synchronization, otherwise inter-symbol interference will erode the performance of the system. Tight uplink synchronization between users exists in OFDMA systems [65], for example, where training symbols with cyclic prefix and other techniques are used, whose details fall outside the scope of this work.

In the case of TDMA, once again the Alamouti space-time code may be used, and once again the issue of synchronization arises. Unlike OFDMA, in TDMA symbol-level synchronization between users in the uplink is not guaranteed. However, coarse synchronization is usually present: GSM, for example, provides synchronization up to 0.5 of a symbol interval [56], which is not enough for our purposes, but suggests that tighter synchronization is possible. Progress is already being made on the relay synchronization issue [63], but more work is needed in this area.

4.2 Turbo-Coded Cooperation

The implementation of coded cooperation using turbo codes is shown in Figure 4.2. Turbo codes employ two constituent recursive systematic convolutional (RSC) codes with interleaving [10, 8]. The users and the destination have the same random interleaver, shown as π in Figure 4.2. The code word for the first frame is obtained using

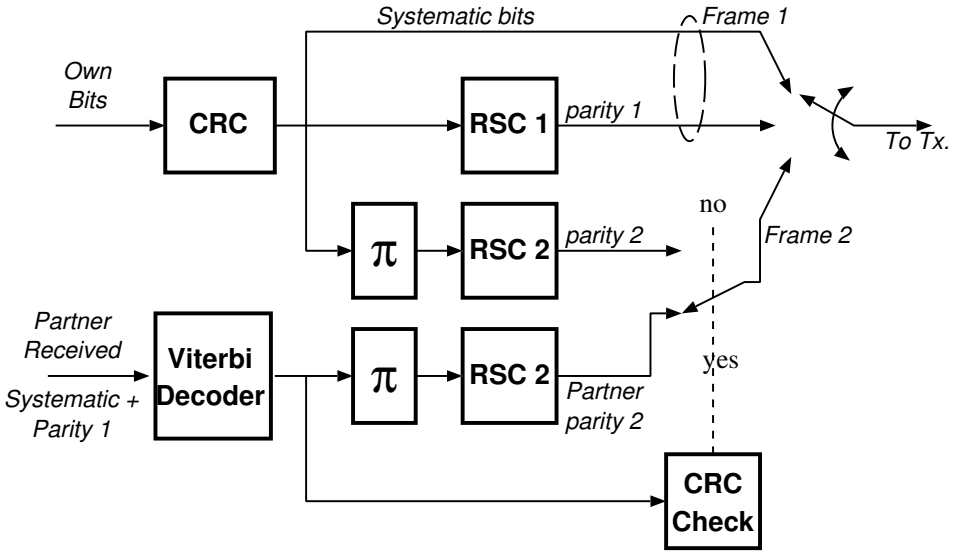

Figure 4.2. Turbo encoding in a coded cooperation scheme.

the first RSC code. Upon successful decoding of the partner, the user interleaves the source bits over the K-bit block and transmits the parity bits corresponding to the second RSC code.

Turbo coding can be used with either coded cooperation or space-time cooperation. The difference between the two cases, as described in Section 4.1.1, is in the second frame. In turbo-coded cooperation, each user transmits its partner's parity bits in the second frame using all available power. In space-time turbo-coded cooperation, each user transmits its own as well as its partner's second set of parity bits, by splitting the available power. In either case, if the first frame of the partner is not successfully decoded, the user will interleave, encode and transmit the second set of parity bits for its own source block using all of its power.

The scheme presented above has a fixed cooperation percentage of 33%. It is possible to have a flexible cooperation percentage, as well as better performance, by using punctured turbo codes or rate compatible punctured turbo codes (RCPT) [49]. However, the mobiles must then perform turbo decoding on the partner's bits, in-

creasing the complexity. In this work we only consider the simpler case with a fixed cooperation percentage, where a user employs the conventional Viterbi decoding for the partner, as shown in Figure 4.2.

At the destination, the combination of the first and second frames offers the possibility of turbo decoding. The low-complexity iterative decoder [10, 26] offers near-optimum decoding performance for turbo codes. For the sake of brevity we omit explanation of the SISO modules and iterative decoding of turbo codes. The interested reader is referred to the rich existing literature; i.e., [26, 6] and references therein.

4.3 Performance Analysis

In this section we present an analytical methodology for evaluating the performance of coded cooperation. In developing pairwise error probabilities in Section 4.3.1, we again use tools and techniques from Craig [18] and Simon and Alouini [54] to modify and extend the results from Section 3.3. We then determine union bounds for the overall bit and block error probabilities in Section 4.3.2 using weight enumerating functions. The validity of the resulting bounds is demonstrated via simulations in Section 4.4.

4.3.1 Pairwise Error Probability

Slow Fading

For space-time cooperation in slow fading, we can rewrite (3.5) for User 1's code word as

$$P(d|\gamma_{1,0}\gamma_{2,0}) = Q\left(\sqrt{2d_1\gamma_{1,0} + 2d_2\beta_1\gamma_{1,0} + 2d_2(1-\beta_2)\gamma_{2,0}}\right), \tag{4.1}$$

where again the subscripts 1, 2, and 0 denote User 1, User 2, and the destination respectively. The variables d_1 and d_2 are the numbers of bits in the Hamming weight

d that are transmitted through User 1's channel and both users' channels respectively, such that $d_1 + d_2 = d$.

To obtain the the unconditional PEP we must take the expected value of (4.1) over the distributions of $\gamma_{1,0}$ and $\gamma_{2,0}$. Using the tools developed by Simon and Alouini [54], we can obtain the following result:

$$P(d) = \frac{1}{\pi} \int_0^{\pi/2} \left(1 + \frac{(d_1 + \beta_1 d_2)\Gamma_{1,0}}{\sin^2\theta}\right)^{-1} \left(1 + \frac{d_2(1-\beta_2)\Gamma_{2,0}}{\sin^2\theta}\right)^{-1} d\theta, \tag{4.2}$$

where $\Gamma_{i,0}$ is the average (over fading) uplink SNR between User i and the destination. Note that (4.2) is an exact expression for the unconditional PEP and is easily evaluated with numerical integration techniques.

The following upper bound is obtained for (4.2) by noting that the integrand is maximized for $\sin^2\theta = 1$,

$$P(d) \leq \frac{1}{2} \left(\frac{1}{1 + (d_1 + \beta_1 d_2)\Gamma_{1,0}}\right) \left(\frac{1}{1 + d_2(1-\beta_2)\Gamma_{2,0}}\right). \tag{4.3}$$

For the cases in which $\beta_2 \neq 1$ (Cases 1 and 3), we see from (4.3) that, for large SNR, the PEP is inversely proportional to the product of the average SNR for the two uplink channels. Thus, provided that d_1 and d_2 are both greater than zero, full diversity order of two is achieved. This is also the same as the original coded cooperation framework, for which (4.3) with $\beta_1 = \beta_2 = 0$ is equal to (3.14).

For no cooperation (which also corresponds to Case 2), we have that $\beta_1 = \beta_2 = 1$ in (4.3), and thus we see that we only have diversity order one. For Case 4, we have $\beta_1 < 1$ and $\beta_2 = 1$, so that again we only have diversity order one.

Fast Fading

For fast fading, the fading coefficients are no longer constant over the code word, but are i.i.d. across the coded bits. Thus we can generalize (4.1) as

$$P(d|\boldsymbol{\gamma}_{1,0},\boldsymbol{\gamma}_{2,0}) = Q\left(\sqrt{2\sum_{n\in\eta_1}\gamma_{1,0}(n) + 2\beta_1\sum_{n\in\eta_2}\gamma_{1,0}(n) + 2\left(1-\beta_2\right)\sum_{n\in\eta_2}\gamma_{2,0}(n)}\right)$$

where the set η_i is the portion of bits of the Hamming weight d transmitted through User i's channel. The cardinalities of η_1 and η_2 are d_1 and d_2 respectively, where again $d_1 + d_2 = d$.

We use the techniques of [54] once more to obtain the following expression for the unconditional PEP:

$$\begin{aligned} P(d) &= \frac{1}{\pi}\int_0^{\pi/2}\left(1+\frac{\Gamma_{1,0}}{\sin^2\theta}\right)^{-d_1}\left(1+\frac{\beta_1\Gamma_{1,0}}{\sin^2\theta}\right)^{-d_2}\left(1+\frac{\left(1-\beta_2\right)\Gamma_{2,0}}{\sin^2\theta}\right)^{-d_2}d\theta \\ &\leq \frac{1}{2}\left(\frac{1}{1+\Gamma_{1,0}}\right)^{d_1}\left(\frac{1}{1+\beta_1\Gamma_{1,0}}\right)^{d_2}\left(\frac{1}{1+\left(1-\beta_2\right)\Gamma_{2,0}}\right)^{d_2}. \end{aligned} \tag{4.4}$$

From (4.4), the diversity order for fast fading in Cases 1 and 3 ($\beta_2 \neq 1$) is $d_1 + 2d_2 = d + d_2$. In contrast, for Cases 2 and 4 ($\beta_2 = 1$), as well as for the original coded cooperation framework ($\beta_1 = \beta_2 = 0$), and for no cooperation ($\beta_1 = \beta_2 = 1$), the diversity order is equal to d. Thus we see that our modified framework involving space-time transmission does indeed provide increased diversity in fast fading.

4.3.2 Bit and Block Error Rate

We can obtain union bounds for the BER and BLER as a function of the PEP using well-known weight enumerating techniques. To obtain tight bounds for the case of slow fading, we again use the limit-before-average technique from Malkamäki and Leib [45].

Convolutional Codes

Since in our framework we always consider terminated convolutional codes with a finite uncoded block length K and coded block length N, we can obtain bounds for the BER and BLER using the weight enumerating function (WEF) of the equivalent block code as

$$\begin{aligned} P_b(\boldsymbol{\gamma}) &\leq \sum_{d=d_f}^{N} \sum_{w=1}^{K} \frac{w}{K} a_{w,d} P(d|\boldsymbol{\gamma}) \\ P_{block}(\boldsymbol{\gamma}) &\leq \sum_{d=d_f}^{N} \sum_{w=1}^{K} a_{w,d} P(d|\boldsymbol{\gamma}), \end{aligned} \tag{4.5}$$

where d_f is the free distance of the code, and $a_{w,d}$ is the multiplicity of code words corresponding to input weight w and output weight d. We note that these forms are alternatives to the BER and BLER bounds for convolutional codes used in the analysis in Section 3.4, and they give equivalent results.

Turbo Codes

For turbo codes, we can similarly consider the WEF for the equivalent block code, as shown in [8],[7]. Using the concept of a *uniform interleaver*[2] [8], the WEF of the overall concatenated code is given based on the WEF of the constituent codes. We follow the same direction of [8] with a minor modification for a turbo code with C_1 and C_2 as the constituent systematic recursive convolutional codes and an interleaver with size K.

The conditional WEF of a block code, $A_w^C(Z)$, gives all possible code words generated by the set of input sequences with weight w (note that Z is only a dummy variable). Assume $A_w^{C_1}(Z)$ is the conditional WEF of C_1 and $A_w^{C_2}(Y)$ for C_2. Then

[2]A uniform interleaver with size K maps a code word of weight w into all its distinct $\binom{K}{w}$ permutations with equal probability $1/\binom{K}{w}$ [8].

using the probabilistic uniform interleaver the conditional WEF of the turbo code is [8]

$$A_w^C(Z,Y) = \frac{A_w^{C_1}(Z) \times A_w^{C_2}(Y)}{\binom{K}{w}}. \tag{4.6}$$

Although we employ the original type of turbo code [10, 8] which has similar constituent convolutional codes, keeping the WEF of C_1 and C_2 separate (with two dummy variables Z and Y) makes it possible to deal with the four different scenarios in the cooperation schemes, which as a sub-case has the analysis of [8]. The BER and BLER of the turbo code are obtained using the union bound argument [8]

$$\begin{aligned} P_b(\boldsymbol{\gamma}) &\leq \sum_{z=0}^{K}\sum_{y=0}^{K}\sum_{w=1}^{K} \frac{w}{K} a_{w,z,y} P(d|\boldsymbol{\gamma}) \\ P_{block}(\boldsymbol{\gamma}) &\leq \sum_{z=0}^{K}\sum_{y=0}^{K}\sum_{w=1}^{K} a_{w,z,y} P(d|\boldsymbol{\gamma}), \end{aligned} \tag{4.7}$$

where $a_{w,z,y}$ denotes the multiplicity of code words corresponding to input weight w and parity weights z and y, obtained from the corresponding code WEF $W^w A_w^C(Z,Y)$, and $P(d|\boldsymbol{\gamma})$ is the corresponding PEP expression from Section 4.3.1. The expressions above assume $R_1 = R_2 = \frac{1}{2}$. Note that d_1 is equal to the summation of the exponents of W and Z (w and z), and d_2 is equal to the exponent of Y (y).

Overall Bit and Block Error Rate

The overall end-to-end unconditional BER is equal to the average of the unconditional BER over the four possible transmission cases discussed in Section 4.1.1

$$P_b = \sum_{i=1}^{4} P_b(\text{Case } i) P(\text{Case } i) \tag{4.8}$$

where $P_b(\text{Case } i)$ denotes the BER corresponding to Case i, and $P(\text{Case } i)$ is the probability of occurrence of Case i. The end-to-end BLER has an identical expression. Bounds on the probabilities $P(\text{Case } i)$ for each of the four cases are obtained from the BLER corresponding to the code used for the first frame transmissions. The

calculation of $P(\text{Case } i)$ is identical to that found in Chapter 3. Based on (4.8), the overall end-to-end diversity achieved via cooperation is similarly a weighted average of the diversity corresponding to each of the four cases, where the relative weights are determined by the inter-user channel conditions. This behavior is illustrated in the performance results given in Section 4.4.

4.4 Performance Evaluation

For our simulations we use a 16-bit CRC code with generator polynomial given by coefficients 15935 (hexadecimal notation). We computed via computer enumeration the WEF of our codes, including the partitioning of the Hamming weights d into d_1 and d_2, corresponding to the source block length K. All comparisons are between systems with equal information rate K and equal code rate R, therefore we plot the error probabilities against channel SNR. Plotting BER or BLER versus the information bit SNR, or E_b/N_0, yields identical results up to an additive constant in the log-SNR domain. The plots apply equally to each of the multiple access schemes, for the following reason: using an orthogonal space-time block code is equivalent to coherently combining multiple copies of each information symbol [2, 59]. Thus, the results for space-time cooperation presented below are equivalent for the case of CDMA, in which coherent combining is achieved via the signature correlation properties, and for TDMA and FDMA, in which an orthogonal space-time block code would be used, as discussed in Section 4.1.2. In addition, all results presented in this section for space-time cooperation are for $\beta_1 = \beta_2 = 0.5$.

4.4.1 Rate Compatible Punctured Convolutional Codes

We use the family of RCPC codes with memory $M = 4$, puncturing period $P = 8$, rate 1/4 mother code, and generator polynomials $\text{G}(23, 35, 27, 33)$ (octal) given by

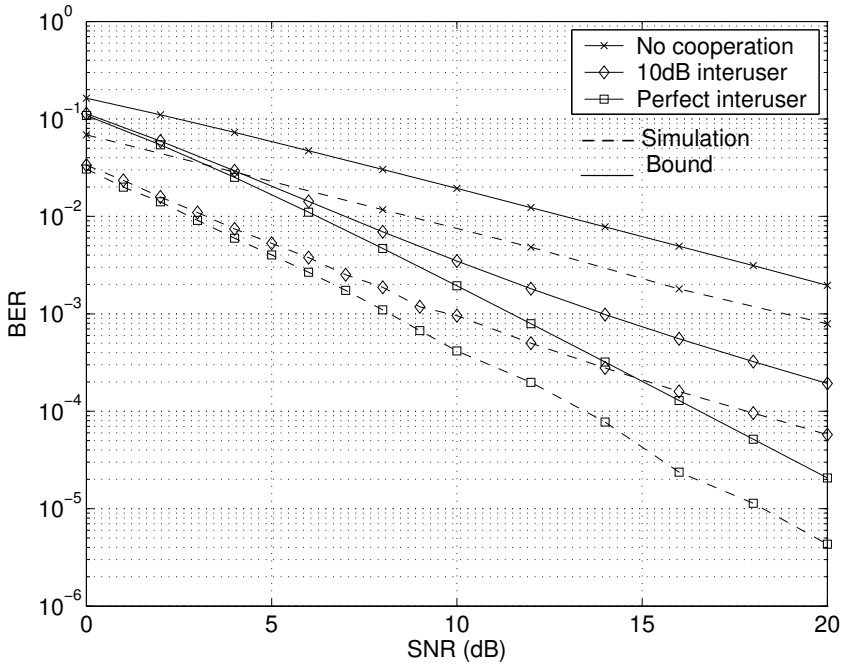

Figure 4.3. Slow Rayleigh fading results. Equal uplink SNR, cooperation at 50%.

Hagenauer [25]. For slow fading, we choose overall code rate $R = 1/4$, while for fast fading we use $R = 2/5$. In all cases, the source block size is $K = 128$ bits.

Figure 4.3 shows analytical bound and simulation results of BER for slow Rayleigh fading with 10dB average SNR inter-user channel and perfect inter-user channel. Both users' uplink channels have the same average SNR (symmetric uplink channels), and the level of cooperation is 50%. Under slow fading, space-time cooperation achieves significant gain over non-cooperative systems, gains that are similar to coded cooperation. As an example, at BER of 10^{-3}, a coding gain of 9dB is achieved over the non-cooperative baseline system of similar rate, bandwidth, and power, when the inter-user channel is at 10dB. The perfect (error free) inter-user channel demonstrates the limits of the gains, which at BER $= 10^{-3}$ is about 11dB.

Figures 4.4 shows BER results for fast Rayleigh fading. The cooperation percentage is at 30%. User 1's uplink channel is fixed at 5dB, while User 2's channel

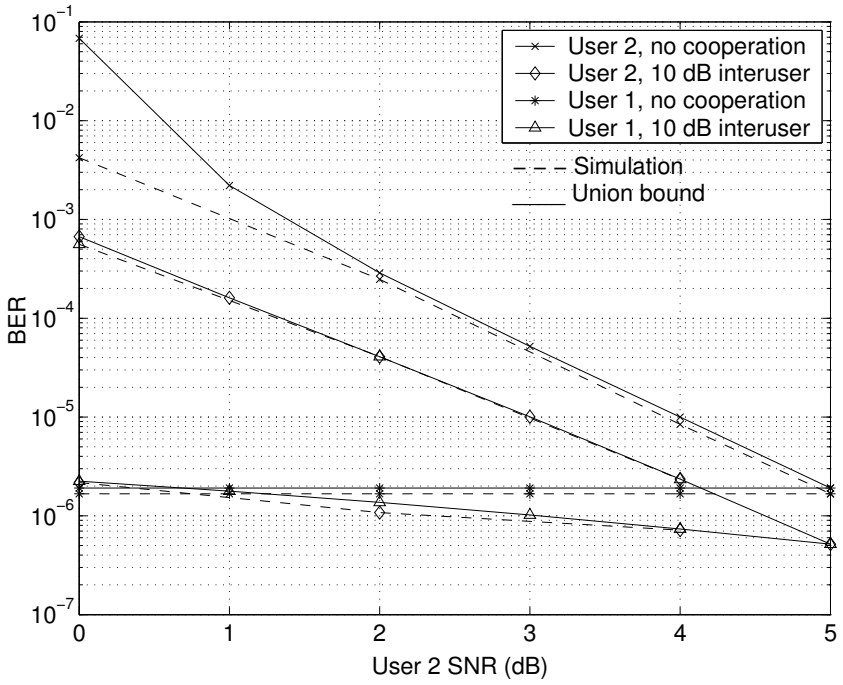

Figure 4.4. Fast Rayleigh fading results. Unequal uplink SNR: User 1 is fixed at 5dB while User 2 varies 0-5dB.

varies from 0dB to 5dB. As shown in Figure 4.4, User 2 realizes a gain of 1dB if the inter-user channel average SNR is 10dB. Interestingly, User 1 which has a better channel also improves somewhat. The union bounds match well to the simulation results.

Figure 4.5 compares the BLER of coded cooperation and space-time coded cooperation, using analytical bounds, for fast Rayleigh fading with 10dB inter-user SNR. Cooperation is at 30% and User 1's SNR is fixed at 10dB. This figure shows that, for space-time cooperation, not only does User 2 improve significantly, but also User 1 does not lose performance by cooperating with User 2, even though User 1 has better SNR to start with. This is a noticeable improvement over the original coded cooperation framework.

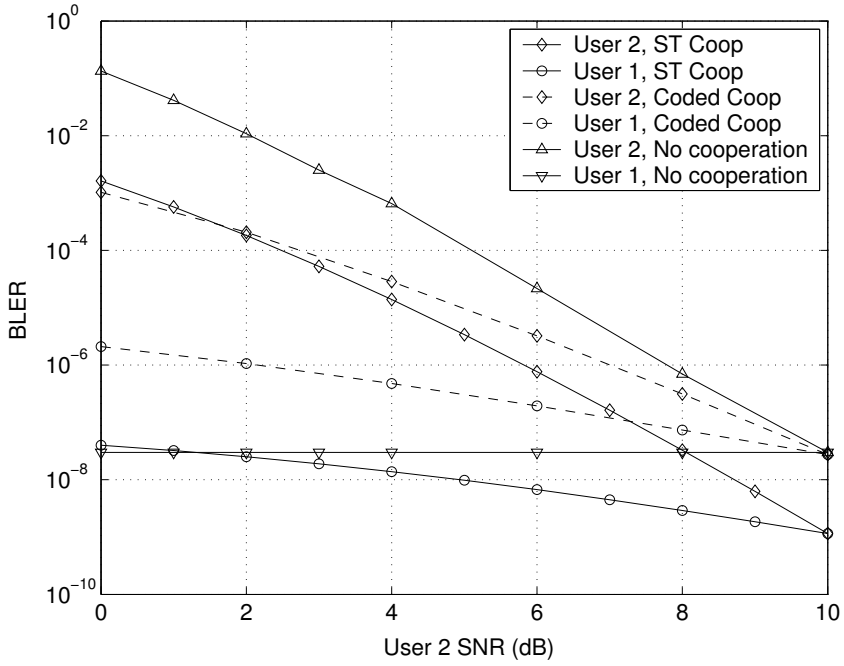

Figure 4.5. Comparing block error rates of coded cooperation versus space-time cooperation (analytical bounds). Inter-user channel at 10dB, cooperation at 30%, and the users have unequal uplink SNR (User 1 at 10dB and User 2 varies 0-10dB).

4.4.2 Turbo Codes

We employ the best reported turbo code with rate-1/2 eight-state constituent codes with generator polynomials $G(1, \frac{17}{13})$ (octal) from [9]. The overall code rate is 1/3. The source block has $K = 128$ bits. The cooperation percentage is 33%. The baseline for all comparisons is a non-cooperative *turbo coded* system, therefore comparisons are fair on the basis of computational complexity as well as rate.

Figure 4.6 shows the simulation results for the BER of turbo coded cooperation compared to non-cooperative turbo coding with various inter-user channel conditions. As shown in Figure 4.6, cooperation yields significant gain in slow fading due to the increased diversity. The gain at BER $=10^{-3}$ is from 5dB (for the case of 6dB inter-user channel) to 8dB (for the perfect inter-user channel).

Figure 4.7 shows the union bounds and simulation results for the BLER of

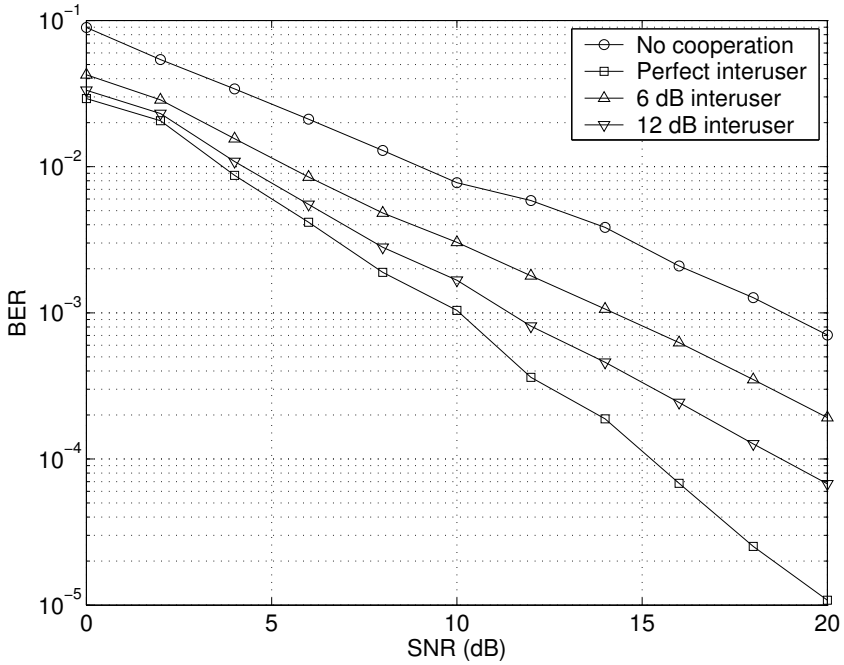

Figure 4.6. Turbo coded cooperation in slow fading. Users have equal uplink SNR.

turbo coded cooperation in fast fading. User 1 has a fixed average uplink SNR at 5dB and the inter-user channel has SNR of 10dB. The union bounds match the simulated results except at very low SNR in the non-cooperative case, a behavior already reported in literature (i.e. [7]). The gain for User 2 is about 3dB at BLER = 10^{-4}, decreasing gradually as User 2's SNR approaches the SNR of User 1. User 1 (who has a better channel) sacrifices performance by cooperation. Nevertheless, provided that User 1's performance remains acceptable, this constitutes a better overall system performance since the worst user has improved significantly.

The performance of the space-time turbo coded cooperation in fast fading channel is demonstrated in Figure 4.8. The channel conditions are the same as Figure 4.7. The gain for User 2 at BLER = 10^{-4} is similar to turbo coded cooperation, but the gain is maintained over a wider range of SNR. Moreover, User 1 gains from cooperation as well, unlike the previous case.

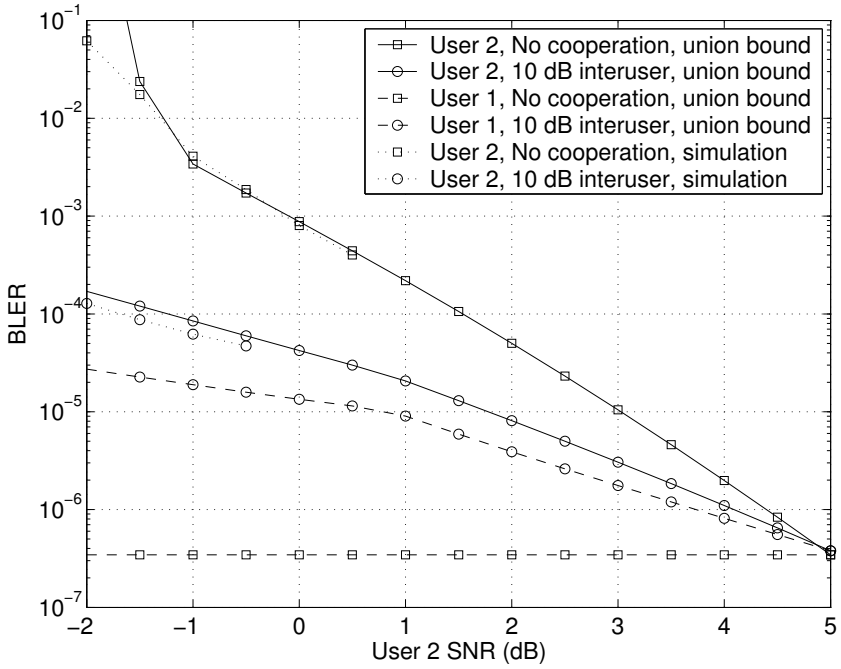

Figure 4.7. Turbo coded cooperation in fast fading, User 1 SNR=5dB.

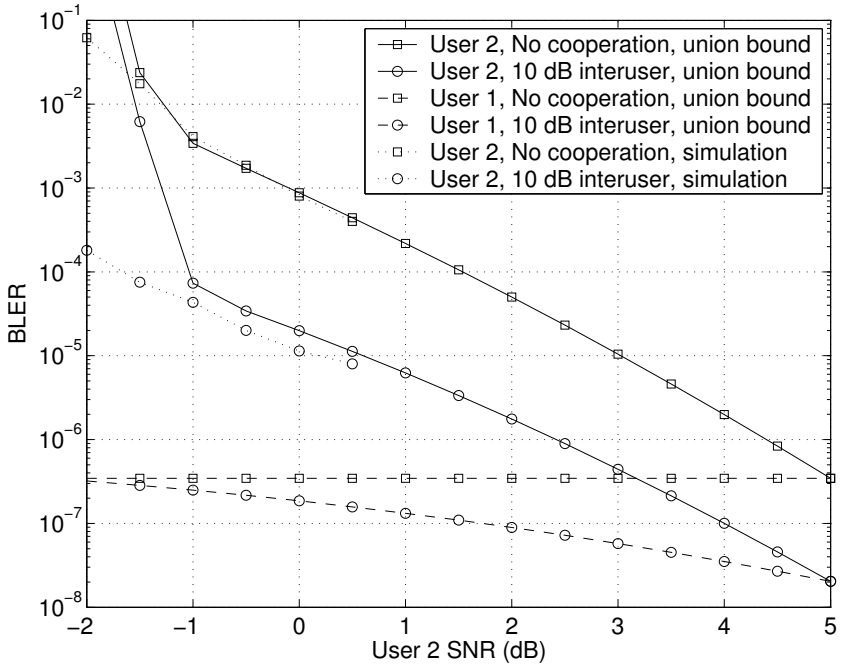

Figure 4.8. Turbo coded *space-time* cooperation in fast fading, User 1 SNR=5dB

4.5 Minimax power splitting

In many applications, the wireless system is required to provide and maintain a minimum quality of service for all users. In a non-cooperative system, one user may have a very good channel that provides a quality of service significantly better than that required for the application. Another user may have a poor channel such that the user is in outage, or must significantly increase power to meet the quality of service requirement. This in turn has a detrimental effect on the other users in the system. Such a scenario represents a poor allocation of system resources.

When the users cooperate, they can share their resources such that all the cooperating users achieve the minimum quality of service more reliably and with less power. Specifically, for the space-time coded cooperation framework introduced in this chapter, we would like to find the user power splitting ratios β_1 and β_2 such that the combined resources for the two users are shared in the most effective way. Guaranteeing a minimum quality of service for both users corresponds to the following minimax criterion for determining β_1 and β_2:

$$\min_{\beta_1,\beta_2}[\max(P_{b_1}, P_{b_2})] \tag{4.9}$$

where P_{b_1} and P_{b_2} are the end-to-end BER of User 1 and User 2 respectively.

In order to solve this optimization problem, we note that P_{b_1} is a monotonically increasing function of β_1 and a monotonically decreasing function of β_2 (similarly P_{b_2} increases with β_2 and decreases with β_1). Thus, the optimum point in (4.9) corresponds to a point for which P_{b_1} and P_{b_2} are equal. If P_{b_1} and P_{b_2} are not equal, clearly we can alter either β_1 or β_2 or both to make them equal and thus reduce the maximum of P_{b_1} and P_{b_2}. We can therefore simplify the criterion of (4.9) as

$$\min_{\substack{\beta_1,\beta_2 \\ P_{b_1}=P_{b_2}}} [\max(P_{b_1}, P_{b_2})] = \min_{\substack{\beta_1,\beta_2 \\ P_{b_1}=P_{b_2}}} (P_{b_1}). \tag{4.10}$$

Using the method of Lagrange multipliers, can write

$$\min_{\beta_1,\beta_2}[P_{b_1} - \lambda(P_{b_1} - P_{b_2})] = \min_{\beta_1,\beta_2}[(1-\lambda)P_{b_1} + \lambda P_{b_2}]. \tag{4.11}$$

Taking derivatives of (4.11) with respect to β_1 and β_2, after some algebraic manipulation we obtain

$$\begin{cases} (P_{b_1})'_{\beta_1} = \frac{(P_{b_1})'_{\beta_2}(P_{b_2})'_{\beta_1}}{(P_{b_2})'_{\beta_2}} \\ P_{b_2} = P_{b_1} \end{cases} \tag{4.12}$$

where $(f)'_x$ is the derivative of f with respect to x. The two equations above can be solved to obtain desired values for β_1 and β_2. These optimal values for β_1 and β_2 are functions of the average inter-user and uplink SNR, as well as the overall coding scheme and percent cooperation. For the results presented in Figure 4.9 and Table 4.1, we solved (4.12) numerically by searching over the region $(\beta_1, \beta_2) \in [0,1] \times [0,1]$. We use the bounds derived in Section 4.3 to obtain P_{b_1}, P_{b_2}, and their derivatives. From an implementation standpoint, the optimal β_1 and β_2 values would be determined at the destination. In practice, a look-up table could be developed to minimize the complexity of this operation.

Figure 4.9 shows the union bounds with the minimax optimization in fast fading with the RCPC code implementation. User 1's average uplink SNR ($\Gamma_{1,0}$) is fixed at 5dB, while User 2's ($\Gamma_{2,0}$) varies from 0 to 5dB. The inter-user channel has 10dB average SNR, and the overall code rate is $R = 2/5$ with 30% cooperation. The optimum values of β_1 and β_2 for each SNR point are shown in Table 4.1. We see that as User 2's uplink channel deteriorates relative to User 1, both users allocate more of their power to User 2's information. The optimum values are $\beta_1 = \beta_2 = 0.5$ when both user's uplink SNR are equal, as expected.

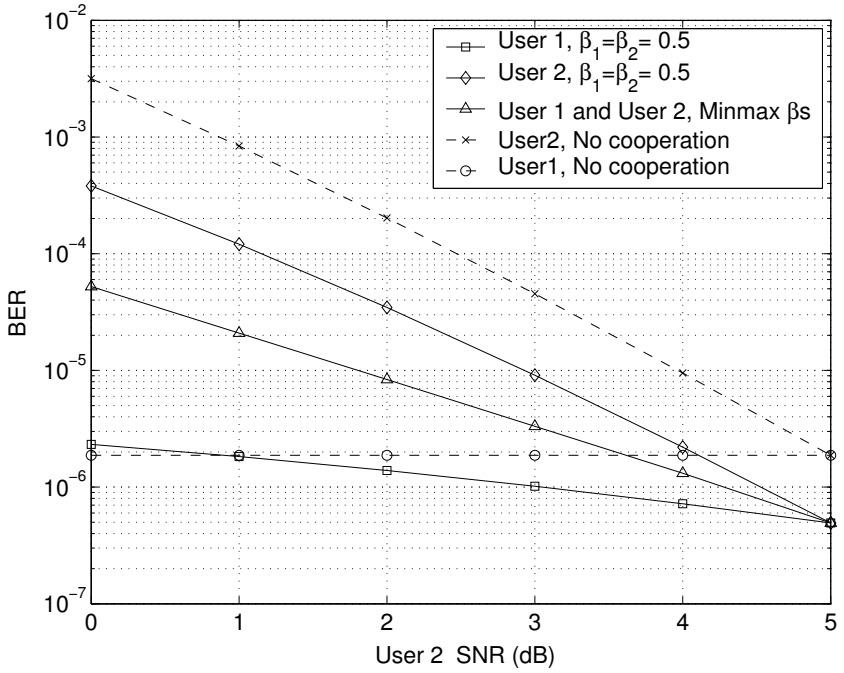

Figure 4.9. Union bounds with minimax criteria for unequal uplink SNR in fast fading.

Table 4.1. Optimum β_1 and β_2 values for minimax criteria, corresponding to Figure 4.9

Γ_2	0dB	1dB	2dB	3dB	4dB	5dB
β_1	0.2	0.2	0.3	0.4	0.4	0.5
β_2	1	0.9	0.8	0.7	0.6	0.5

4.6 Chapter Summary

This chapter develops two extensions to the coded cooperation framework introduced in Chapter 3. The first extension, which we call space-time cooperation, aims to improve upon the performance of coded cooperation in a fast-fading environment. In the second frame, each user transmits additional parity for both itself and its partner. This method is shown to provide improved diversity in fast fading compared to both coded cooperation and no cooperation.

The second extension involves the application of turbo codes to both coded cooperation and space-time cooperation. Since coded cooperation and space-time cooperation involve two code components, turbo codes are a natural fit. Analytical and numerical results demonstrate that turbo-coded cooperation and space-time turbo-coded cooperation achieve significant performance gains over non-cooperative turbo-coded systems with comparable complexity.

For both of these cases, we extend the bit and block error rate analysis from Chapter 3 to obtain tight performance bounds, which are verified by simulations. In Chapter 5, we derive outage probability expressions for both coded cooperation and space-time cooperation. These results provide alternative performance metrics that are independent of any particular coding scheme.

CHAPTER 5
OUTAGE BEHAVIOR OF CODED COOPERATION

In the previous two chapters, we have introduced the coded cooperation framework, as well as an extension which we call space-time cooperation. For both cases, we have derived expressions for pairwise error probability, and developed tight bounds for bit and block error rate. Examples with specific coding schemes show that coded cooperation provides significant improvement for *both* partners, even when the channel between them is poor, or when one partner has a significantly better channel than the other to the destination.

To better understand coded cooperation in a context that is independent of any particular coding scheme, in this chapter we examine the outage behavior of coded cooperation. We consider the case of quasi-static Rayleigh fading, in which the fading remains constant over the transmission of a complete code word. This model is appropriate for many types of ad hoc and sensor networks in which the nodes move slowly, or are fixed but with the exact geometry unknown at the time of design. Such systems present especially attractive applications for cooperative protocols. For a quasi-static (non-ergodic) fading environment, outage probability [46, 13] is an appropriate metric. In addition, this type of analysis facilitates characterization of performance over various rates. Moreover, outage probability has been shown to be a lower bound on block error rate for sufficiently large block lengths [38, 44].

We derive outage probability expressions for coded cooperation in Section 5.1. We consider both the case where the channels between the two users are mutually independent (independent inter-user channels), and the case where the two users see an identical instantaneous signal-to-noise ratio (SNR) between them (reciprocal inter-

user channels).[1] In addition, we demonstrate that coded cooperation achieves full diversity (order two for two users) in the asymptote of user transmit power. In Section 5.2 we present numerical results which illustrate the outage probability behavior of coded cooperation for various channel conditions between the partners and to their destination. These results show the advantages of the coded cooperation framework over non-cooperative transmission and repetition-based cooperative protocols.

5.1 Outage Probability Analysis

As a baseline, we consider non-cooperative direct transmission between source and destination. With quasi-static fading, the capacity conditioned on the channel realization, characterized by the instantaneous SNR γ, can be expressed by the familiar Shannon formula $C(\gamma) = \log_2(1+\gamma)$ b/s/Hz. The channel is *in outage* if the conditional capacity falls below a selected threshold rate R, and the corresponding *outage event* is $\{C(\gamma) < R\}$, or equivalently $\{\gamma < 2^R - 1\}$. The *outage probability* is thus defined as

$$P_{out} = \Pr\{\gamma < 2^R - 1\} = \int_0^{2^R-1} p_\gamma(\gamma) d\gamma, \tag{5.1}$$

where $p_x(x)$ denotes the probability density function (pdf) of random variable x. For the case of Rayleigh fading, γ has an exponential pdf with parameter $1/\Gamma$, where Γ denotes the mean value of SNR over the fading and accounts for the combination of transmit power and large-scale path loss and shadowing effects. The outage probability for Rayleigh fading can thus be evaluated as

$$P_{out} = \int_0^{2^R-1} \frac{1}{\Gamma} \exp\left(-\frac{\gamma}{\Gamma}\right) d\gamma = 1 - \exp\left(-\frac{2^R-1}{\Gamma}\right). \tag{5.2}$$

[1] The nature of the inter-user channel, i.e., independent, reciprocal, or correlated to some degree, depends in part on the multiple access scheme employed. This issue is discussed in more detail in Section 3.6.1

5.1.1 Coded Cooperation

For a detailed description of the coded cooperation framework, we refer the reader to Section 3.2. The users are allocated overall information rate R, which corresponds to N total coded symbols per source block. The user code words are transmitted over two successive time segments, or frames. In the first frame each user transmits a rate $R_1 = R/\alpha$ code word consisting of N_1 code symbols, where we have defined α as

$$\alpha = N_1/N = R/R_1, \tag{5.3}$$

the portion each user's N total channel symbols allocated for the first frame.[2]

Recall that there are four possible cases for second-frame transmission based on whether each user successfully decodes the partner's first-frame code word (see Section 3.2 and Figure 3.4). We parameterize the four cases by $\Theta \in \{1, 2, 3, 4\}$ and express the corresponding conditional capacities and outage events as follows:

- **Case 1 ($\Theta = 1$)**: In this case, both partners correctly decode each other. This corresponds to the following outage events:

$$\begin{aligned} C_{1,2}(\gamma_{1,2}) &= \log_2(1 + \gamma_{1,2}) > R/\alpha \\ C_{2,1}(\gamma_{2,1}) &= \log_2(1 + \gamma_{2,1}) > R/\alpha, \end{aligned} \tag{5.4}$$

  where the subscript form i, j denotes transmission from User i to User j. In the second frame both users transmit additional parity for each other. For a given user, the destination will receive a transmission from both the user (first frame) and the partner (second frame). The first frame uses a fraction α of the total N allocated bits, while the second frame uses $1 - \alpha$. These two transmissions can thus be viewed as parallel (conditionally) Gaussian channels, whose capacities add together [17, Section 10.4]. Equivalently, the two transmissions can

[2] In Chapters 3 and 4, we define the level of cooperation as $N_2/N = 1 - \alpha$. For the analysis in this chapter, it is more convenient to parameterize the cooperation level by α.

be viewed as time sharing between two independent channels, where the first channel is used a fraction α of the time. We can thus write the outage events for Users 1 and 2 as

$$\begin{aligned} C_{1,d}(\gamma_{1,d}, \gamma_{2,d}|\Theta = 1) &= \alpha \log_2(1 + \gamma_{1,d}) + (1 - \alpha) \log_2(1 + \gamma_{2,d}) < R \\ C_{2,d}(\gamma_{1,d}, \gamma_{2,d}|\Theta = 1) &= \alpha \log_2(1 + \gamma_{2,d}) + (1 - \alpha) \log_2(1 + \gamma_{1,d}) < R, \end{aligned} \tag{5.5}$$

where the subscript d denotes the destination.

- **Case 2 ($\Theta = 2$)**: In this case, neither user correctly decodes their partner. This corresponds to both users being in outage with respect to their partner,

$$\begin{aligned} C_{1,2}(\gamma_{1,2}) &= \log_2(1 + \gamma_{1,2}) < R/\alpha \\ C_{2,1}(\gamma_{2,1}) &= \log_2(1 + \gamma_{2,1}) < R/\alpha. \end{aligned} \tag{5.6}$$

  In the second frame both users transmit additional parity for their own data. The corresponding outage events are

$$\begin{aligned} C_{1,d}(\gamma_{1,d}|\Theta = 2) &= \log_2(1 + \gamma_{1,d}) < R \\ C_{2,d}(\gamma_{2,d}|\Theta = 2) &= \log_2(1 + \gamma_{2,d}) < R. \end{aligned} \tag{5.7}$$

- **Case 3 ($\Theta = 3$)**: In this case, User 2 correctly decodes User 1, but User 1 does not correctly decode User 2. This corresponds to the events

$$\begin{aligned} C_{1,2}(\gamma_{1,2}) &= \log_2(1 + \gamma_{1,2}) > R/\alpha \\ C_{2,1}(\gamma_{2,1}) &= \log_2(1 + \gamma_{2,1}) < R/\alpha. \end{aligned} \tag{5.8}$$

  In the second frame, User 1 and User 2 both transmit the same additional parity for User 1, while no additional parity is transmitted for User 2. The corresponding outage events are

$$\begin{aligned} C_{1,d}(\gamma_{1,d}, \gamma_{2,d}|\Theta = 3) &= \alpha \log_2(1 + \gamma_{1,d}) \\ &\quad + (1 - \alpha) \log_2(1 + \gamma_{1,d} + \gamma_{2,d}) < R \\ C_{2,d}(\gamma_{2,d}|\Theta = 3) &= \log_2(1 + \gamma_{2,d}) < R/\alpha. \end{aligned} \tag{5.9}$$

- **Case 4 ($\Theta = 4$)**: This case is identical to Case 3 with the roles of Users 1 and 2 reversed. Thus for the first frame we have the events

$$\begin{aligned} C_{1,2}(\gamma_{1,2}) &= \log_2(1+\gamma_{1,2}) < R/\alpha \\ C_{2,1}(\gamma_{2,1}) &= \log_2(1+\gamma_{2,1}) > R/\alpha, \end{aligned} \tag{5.10}$$

and the outage events for Users 1 and 2 are

$$\begin{aligned} C_{1,d}(\gamma_{1,d}|\Theta=4) &= \log_2(1+\gamma_{1,d}) < R/\alpha \\ C_{2,d}(\gamma_{1,d},\gamma_{2,d}|\Theta=4) &= \alpha\log_2(1+\gamma_{2,d}) \\ &\quad + (1-\alpha)\log_2(1+\gamma_{1,d}+\gamma_{2,d}) < R. \end{aligned} \tag{5.11}$$

Note that the above assumes an independent inter-user channel ($\gamma_{1,2}$ and $\gamma_{2,1}$ independent), the most general condition. Since the four cases are disjoint, and assuming that $\{\gamma_{1,2}, \gamma_{2,1}, \gamma_{1,d}, \gamma_{2,d}\}$ are all mutually independent, we can write the overall outage probability for User 1 as

$$\begin{aligned} P_{out,1} &= \Pr\{\gamma_{1,2} > 2^{R/\alpha}-1\}\cdot\Pr\{\gamma_{2,1} > 2^{R/\alpha}-1\} \\ &\qquad \cdot \Pr\{(1+\gamma_{1,d})^{\alpha}(1+\gamma_{2,d})^{1-\alpha} < 2^R\} \\ &\quad + \Pr\{\gamma_{1,2} < 2^{R/\alpha}-1\}\cdot\Pr\{\gamma_{2,1} < 2^{R/\alpha}-1\}\cdot\Pr\{\gamma_{1,d} < 2^R-1\} \\ &\quad + \Pr\{\gamma_{1,2} > 2^{R/\alpha}-1\}\cdot\Pr\{\gamma_{2,1} < 2^{R/\alpha}-1\} \\ &\qquad \cdot \Pr\{(1+\gamma_{1,d})^{\alpha}(1+\gamma_{1,d}+\gamma_{2,d})^{1-\alpha} < 2^R\} \\ &\quad + \Pr\{\gamma_{1,2} < 2^{R/\alpha}-1\}\cdot\Pr\{\gamma_{2,1} > 2^{R/\alpha}-1\}\cdot\Pr\{\gamma_{1,d} < 2^{R/\alpha}-1\}. \end{aligned} \tag{5.12}$$

Due to symmetry, we can obtain an identical expression for User 2 by simply reversing the roles of Users 1 and 2. In the remainder of this chapter, we derive various outage probability expressions for User 1 only, with the understanding that the corresponding expressions for User 2 are identical.

For the case of Rayleigh fading, we can evaluate (5.12) as

$$\begin{aligned}
P_{out,1} &= \exp\left(\frac{1-2^{R/\alpha}}{\Gamma_{1,2}}\right)\cdot\exp\left(\frac{1-2^{R/\alpha}}{\Gamma_{2,1}}\right) \\
&\quad\cdot\iint_A \Phi(\gamma_{1,d},\gamma_{2,d},\Gamma_{1,d},\Gamma_{2,d})d\gamma_{1,d}d\gamma_{2,d} \\
&+\left[1-\exp\left(\frac{1-2^{R/\alpha}}{\Gamma_{1,2}}\right)\right]\cdot\left[1-\exp\left(\frac{1-2^{R/\alpha}}{\Gamma_{2,1}}\right)\right] \\
&\quad\cdot\left[1-\exp\left(\frac{1-2^{R}}{\Gamma_{1,d}}\right)\right] \\
&+\exp\left(\frac{1-2^{R/\alpha}}{\Gamma_{1,2}}\right)\left[1-\exp\left(\frac{1-2^{R/\alpha}}{\Gamma_{2,1}}\right)\right] \\
&\quad\cdot\iint_B \Phi(\gamma_{1,d},\gamma_{2,d},\Gamma_{1,d},\Gamma_{2,d})d\gamma_{1,d}d\gamma_{2,d} \\
&+\left[1-\exp\left(\frac{1-2^{R/\alpha}}{\Gamma_{1,2}}\right)\right]\cdot\exp\left(\frac{1-2^{R/\alpha}}{\Gamma_{2,1}}\right)\cdot\left[1-\exp\left(\frac{1-2^{R/\alpha}}{\Gamma_{1,d}}\right)\right],
\end{aligned} \tag{5.13}$$

where

$$\begin{aligned}
A &\equiv \{(1+\gamma_{1,d})^{\alpha}(1+\gamma_{2,d})^{1-\alpha} < 2^{R}\} \\
B &\equiv \{(1+\gamma_{1,d})^{\alpha}(1+\gamma_{1,d}+\gamma_{2,d})^{1-\alpha} < 2^{R}\} \\
\Phi(\gamma_{1,d},\gamma_{2,d},\Gamma_{1,d},\Gamma_{2,d}) &= \frac{1}{\Gamma_{1,d}}\exp\left(-\frac{\gamma_{1,d}}{\Gamma_{1,d}}\right)\cdot\frac{1}{\Gamma_{2,d}}\exp\left(-\frac{\gamma_{2,d}}{\Gamma_{2,d}}\right).
\end{aligned} \tag{5.14}$$

Using the results of Appendix A, we can simplify (5.13) to obtain

$$\begin{aligned}
P_{out,1} &= \exp\left(\frac{1-2^{R/\alpha}}{\Gamma_{2,1}}\right) \\
&\quad\cdot\left[1-\exp\left(\frac{1-2^{R/\alpha}}{\Gamma_{1,d}}\right)-\exp\left(\frac{1-2^{R/\alpha}}{\Gamma_{1,2}}\right)\cdot\Psi_1(\Gamma_{1,d},\Gamma_{2,d},R,\alpha)\right] \\
&+\left[1-\exp\left(\frac{1-2^{R/\alpha}}{\Gamma_{2,1}}\right)\right] \\
&\quad\cdot\left[1-\exp\left(\frac{1-2^{R}}{\Gamma_{1,d}}\right)-\exp\left(\frac{1-2^{R/\alpha}}{\Gamma_{1,2}}\right)\cdot\Psi_2(\Gamma_{1,d},\Gamma_{2,d},R,\alpha)\right]
\end{aligned} \tag{5.15}$$

where

$$\begin{aligned}
\Psi_1(\Gamma_{1,d},\Gamma_{2,d},R,\alpha) &= \int_0^{2^{R/\alpha}-1} \frac{1}{\Gamma_{1,d}} \exp\left(-\frac{\gamma_{1,d}}{\Gamma_{1,d}} - \frac{a}{\Gamma_{2,d}}\right) d\gamma_{1,d} \\
\Psi_2(\Gamma_{1,d},\Gamma_{2,d},R,\alpha) &= \int_0^{2^{R}-1} \frac{1}{\Gamma_{1,d}} \exp\left(-\frac{\gamma_{1,d}}{\Gamma_{1,d}} - \frac{b}{\Gamma_{2,d}}\right) d\gamma_{1,d} \\
a &= \frac{2^{R/(1-\alpha)}}{(1+\gamma_{1,d})^{\alpha/(1-\alpha)}} - 1 \\
b &= \frac{2^{R/(1-\alpha)}}{(1+\gamma_{1,d})^{\alpha/(1-\alpha)}} - 1 - \gamma_{1,d}.
\end{aligned} \tag{5.16}$$

In the case of reciprocal inter-user channels ($\gamma_{1,2} = \gamma_{2,1}$), the events (5.8) and (5.10) (Cases 3 and 4) do not occur. As a result, (5.12) simplifies to

$$\begin{aligned}
P_{out,1} = &\Pr\{\gamma_{1,2} > 2^{R/\alpha} - 1\} \cdot \Pr\{(1+\gamma_{1,d})^{\alpha}(1+\gamma_{2,d})^{1-\alpha} < 2^R\} \\
&+ \Pr\{\gamma_{1,2} < 2^{R/\alpha} - 1\} \cdot \Pr\{\gamma_{1,d} < 2^R - 1\}.
\end{aligned} \tag{5.17}$$

Using results from Appendix A, we can evaluate (5.17) for Rayleigh fading as

$$\begin{aligned}
P_{out,1} = &\exp\left(\frac{1-2^{R/\alpha}}{\Gamma_{1,2}}\right)\left[1 - \exp\left(\frac{1-2^{R/\alpha}}{\Gamma_{1,d}}\right) - \Psi_1(\Gamma_{1,d},\Gamma_{2,d},R,\alpha)\right] \\
&+ \left[1 - \exp\left(\frac{1-2^{R/\alpha}}{\Gamma_{1,2}}\right)\right]\left[1 - \exp\left(\frac{1-2^{R}}{\Gamma_{1,d}}\right)\right].
\end{aligned} \tag{5.18}$$

where $\Psi_1(\Gamma_{1,d},\Gamma_{2,d},R,\alpha)$ is the same as in (5.16).

We see from (5.15) and (5.18) that the outage probability for coded cooperation is a function of the mean channel SNR values $\{\Gamma_{1,2},\Gamma_{2,1},\Gamma_{1,d},\Gamma_{2,d}\}$, the allocated rate R, and the cooperation level α. While the channel SNR and allocated rate may often be set by environmental or system constraints, α is a parameter that can be varied to optimize performance. Obtaining a general expression for an optimal α as a function of the other parameters is complicated by the fact that α appears in the limits of integrals in (5.15) and (5.18). Nevertheless, for any given parameter set, an optimal α may be determined through iteration. We show examples of this in Section 5.2.

5.1.2 Asymptotic Analysis and Diversity Order

We would like to examine the behavior of the outage probability in the high-SNR regime to determine the diversity order achieved by coded cooperation. To facilitate this, we re-parameterize the mean SNR $\Gamma_{i,j}$ as follows:

$$\Gamma_{i,j} \Longrightarrow \Gamma_T \cdot \Gamma_{i,j} \tag{5.19}$$

where now Γ_T is the ratio of the user transmit power to the received noise, and $\Gamma_{i,j}$ is a finite constant accounting for large-scale path loss and shadowing effects. For the purposes of this work we assume that Γ_T is the same for both users. Relative differences in quality between the various channels are still captured by the $\Gamma_{i,j}$ values. This re-parameterization decouples the user transmit power from the physical impairments of the channel itself. Thus, by expressing outage probability as a function of $1/\Gamma_T$, and then letting $\Gamma_T \to \infty$ (e.g., the high-SNR regime), the diversity order is given by the smallest exponent of $1/\Gamma_T$.

To obtain the outage probability as a function of $1/\Gamma_T$ for the case of independent inter-user channels, we expand each exponential term in (5.15) using the equivalent Taylor's series representation (e.g. [11, p. 299]) and collect like-order terms. This results in the following expression for User 1:

$$P_{out,1} = \frac{1}{\Gamma_T^2} \cdot \left[\frac{(2^{R/\alpha} - 1)^2}{\Gamma_{1,d}\Gamma_{1,2}} + \frac{\Lambda(R,\alpha)}{\Gamma_{1,d}\Gamma_{2,d}} \right] + O\left(\frac{1}{\Gamma_T^3}\right), \tag{5.20}$$

where

$$\Lambda(R,\alpha) = \begin{cases} 2^{R/(1-\alpha)} \left(\frac{1-\alpha}{1-2\alpha}\right) \left(2^{R(1-2\alpha)/\alpha(1-\alpha)} - 1\right) - 2^{R/\alpha} + 1 & \alpha \neq 1/2 \\ R \cdot 2^{2R+1} \cdot \ln 2 - 2^{2R} + 1 & \alpha = 1/2 \end{cases}, \tag{5.21}$$

and $O\left(\frac{1}{\Gamma_T^3}\right)$ denotes the higher-order terms from the Taylor's series expansion.[3] Appendix B provides details of how (5.20) is obtained. It is interesting to note that,

[3] Throughout this chapter, $O(\cdot)$ denotes the familiar order notation; see for example [34, pp. 2–3].

in the high-SNR regime, the dependence of outage probability for User 1 on $\Gamma_{2,1}$ appears only in the terms of third-order and higher. Appendix B demonstrates why this occurs.

For the case of reciprocal inter-user channels, we can obtain a similar expression using the results in Appendix B:

$$P_{out,1} = \frac{1}{\Gamma_T^2} \cdot \left[\frac{(2^R - 1)(2^{R/\alpha} - 1)}{\Gamma_{1,d}\Gamma_{1,2}} + \frac{\Lambda(R,\alpha)}{\Gamma_{1,d}\Gamma_{2,d}} \right] + O\left(\frac{1}{\Gamma_T^3}\right) \tag{5.22}$$

where $\Lambda(R,\alpha)$ is given in (5.21).

We see from (5.20) and (5.22) that, as $\Gamma_T \to \infty$, the outage probability is a function of $1/\Gamma_T^2$. This shows that coded cooperation achieves full diversity, in this case diversity order two for two cooperating users.

5.1.3 Space-Time Cooperation

For a detailed description of space-time cooperation, we refer the reader to Section 4.1. Recall that in the second frame, instead of allocating all power to transmitting additional parity for the partner, the user splits the power according to the ratio β_i ($i \in \{1,2\}$ denotes User i). The user's own additional parity symbols are transmitted with power $\beta_i P$ and additional parity for the partner is transmitted with power $(1-\beta_i)P$, where P denotes the user's total average transmit power. If the partner is not successfully decoded all the power is allocated the the user's own parity.

The original motivation for space-time cooperation was to provide improved performance over coded cooperation in a fast-fading environment; i.e., when the fading coefficients are i.i.d. for each transmitted symbol. Our interest in space-time cooperation in the context of this chapter stems from the fact that in a sense it represents a generalization of the original framework. Coded cooperation can be viewed as

a special case for $\beta_i = 0$, $i = 1, 2$, and thus we would like to see if this power splitting (e.g. $\beta_i \neq 0$) provides any advantages.

Space-time cooperation involves the same four cases, resulting from the first frame transmissions, as coded cooperation. The outage events for User 1 become

$$\begin{aligned}
C_{1,d}(\gamma_{1,d}, \gamma_{2,d}|\Theta = 1) &= \alpha \log_2(1 + \gamma_{1,d}) \\
&\quad + (1 - \alpha) \log_2 \left[1 + \beta_1 \gamma_{1,d} + (1 - \beta_2)\gamma_{2,d}\right] < R \\
C_{1,d}(\gamma_{1,d}|\Theta = 2) &= \log_2(1 + \gamma_{1,d}) < R \\
C_{1,d}(\gamma_{1,d}, \gamma_{2,d}|\Theta = 3) &= \alpha \log_2(1 + \gamma_{1,d}) \\
&\quad + (1 - \alpha) \log_2 \left[1 + \gamma_{1,d} + (1 - \beta_2)\gamma_{2,d}\right] < R \\
C_{1,d}(\gamma_{1,d}|\Theta = 4) &= \alpha \log_2(1 + \gamma_{1,d}) + (1 - \alpha) \log_2(1 + \beta_1 \gamma_{1,d}) < R.
\end{aligned} \tag{5.23}$$

For the case of independent inter-user channels, the outage probability for User 1 is

$$\begin{aligned}
P_{out,1} &= \Pr\{\gamma_{1,2} > 2^{R/\alpha} - 1\} \cdot \Pr\{\gamma_{2,1} > 2^{R/\alpha} - 1\} \\
&\qquad \cdot \Pr\{(1 + \gamma_{1,d})^{\alpha}(1 + \beta_1 \gamma_{1,d} + (1 - \beta_2)\gamma_{2,d})^{1-\alpha} < 2^R\} \\
&\quad + \Pr\{\gamma_{1,2} < 2^{R/\alpha} - 1\} \cdot \Pr\{\gamma_{2,1} < 2^{R/\alpha} - 1\} \cdot \Pr\{\gamma_{1,d} < 2^R - 1\} \\
&\quad + \Pr\{\gamma_{1,2} > 2^{R/\alpha} - 1\} \cdot \Pr\{\gamma_{2,1} < 2^{R/\alpha} - 1\} \\
&\qquad \cdot \Pr\{(1 + \gamma_{1,d})^{\alpha}(1 + \gamma_{1,d} + (1 - \beta_2)\gamma_{2,d})^{1-\alpha} < 2^R\} \\
&\quad + \Pr\{\gamma_{1,2} < 2^{R/\alpha} - 1\} \cdot \Pr\{\gamma_{2,1} > 2^{R/\alpha} - 1\} \\
&\qquad \cdot \Pr\{(1 + \gamma_{1,d})^{\alpha}(1 + \beta_1 \gamma_{1,d})^{1-\alpha} < 2^R\}.
\end{aligned} \tag{5.24}$$

For Rayleigh fading we can evaluate (5.24) as

$$\begin{aligned} P_{out,1} = & \exp\left(\frac{1-2^{R/\alpha}}{\Gamma_{1,2}}\right) \cdot \exp\left(\frac{1-2^{R/\alpha}}{\Gamma_{2,1}}\right) \\ & \cdot \iint_C \Phi(\gamma_{1,d}, \gamma_{2,d}, \Gamma_{1,d}, \Gamma_{2,d}) d\gamma_{1,d} d\gamma_{2,d} \\ & + \left[1 - \exp\left(\frac{1-2^{R/\alpha}}{\Gamma_{1,2}}\right)\right] \left[1 - \exp\left(\frac{1-2^{R/\alpha}}{\Gamma_{2,1}}\right)\right] \\ & \cdot \left[1 - \exp\left(\frac{1-2^{R}}{\Gamma_{1,d}}\right)\right] \\ & + \exp\left(\frac{1-2^{R/\alpha}}{\Gamma_{1,2}}\right) \cdot \left[1 - \exp\left(\frac{1-2^{R/\alpha}}{\Gamma_{2,1}}\right)\right] \\ & \cdot \iint_D \Phi(\gamma_{1,d}, \gamma_{2,d}, \Gamma_{1,d}, \Gamma_{2,d}) d\gamma_{1,d} d\gamma_{2,d} \\ & + \left[1 - \exp\left(\frac{1-2^{R/\alpha}}{\Gamma_{1,2}}\right)\right] \cdot \exp\left(\frac{1-2^{R/\alpha}}{\Gamma_{2,1}}\right) \\ & \cdot \int_E \frac{1}{\Gamma_{1,d}} \exp\left(-\frac{\gamma_{1,d}}{\Gamma_{1,d}}\right) d\gamma_{1,d} \end{aligned} \tag{5.25}$$

where

$$\begin{aligned} C &\equiv \{(1+\gamma_{1,d})^{\alpha}(1+\beta_1\gamma_{1,d}+(1-\beta_2)\gamma_{2,d})^{1-\alpha} < 2^R\} \\ D &\equiv \{(1+\gamma_{1,d})^{\alpha}(1+\gamma_{1,d}+(1-\beta_2)\gamma_{2,d})^{1-\alpha} < 2^R\} \\ E &\equiv \{(1+\gamma_{1,d})^{\alpha}(1+\beta_1\gamma_{1,d})^{1-\alpha} < 2^R\} \end{aligned} \tag{5.26}$$

and $\Phi(\gamma_{1,d}, \gamma_{2,d}, \Gamma_{1,d}, \Gamma_{2,d})$ is the same as (5.14). We can simplify (5.25) in a manner similar to that described in Appendix A for (5.13) to obtain

$$\begin{aligned} P_{out,1} = & \exp\left(\frac{1-2^{R/\alpha}}{\Gamma_{2,1}}\right) \\ & \cdot \left[\int_E \frac{1}{\Gamma_{1,d}} \exp\left(-\frac{\gamma_{1,d}}{\Gamma_{1,d}}\right) d\gamma_{1,d} - \exp\left(\frac{1-2^{R/\alpha}}{\Gamma_{1,2}}\right) \cdot \Psi_5(\Gamma_{1,d}, \Gamma_{2,d}, R, \alpha)\right] \\ & + \left[1 - \exp\left(\frac{1-2^{R/\alpha}}{\Gamma_{2,1}}\right)\right] \\ & \cdot \left[1 - \exp\left(\frac{1-2^{R}}{\Gamma_{1,d}}\right) - \exp\left(\frac{1-2^{R/\alpha}}{\Gamma_{1,2}}\right) \cdot \Psi_6(\Gamma_{1,d}, \Gamma_{2,d}, R, \alpha)\right] \end{aligned} \tag{5.27}$$

where

$$\Psi_5(\Gamma_{1,d},\Gamma_{2,d},R,\alpha)=\int_E \frac{1}{\Gamma_{1,d}}\exp\left(-\frac{\gamma_{1,d}}{\Gamma_{1,d}}-\frac{c}{(1-\beta_2)\Gamma_{2,d}}\right)d\gamma_{1,d}$$
$$\Psi_6(\Gamma_{1,d},\Gamma_{2,d},R,\alpha)=\int_0^{2^R-1} \frac{1}{\Gamma_{1,d}}\exp\left(-\frac{\gamma_{1,d}}{\Gamma_{1,d}}-\frac{b}{(1-\beta_2)\Gamma_{2,d}}\right)d\gamma_{1,d} \qquad (5.28)$$
$$c=\frac{2^{R/(1-\alpha)}}{(1+\gamma_{1,d})^{\alpha/(1-\alpha)}}-1-\beta_1\gamma_{1,d}$$

and b is the same as (5.16).

For reciprocal inter-user channels, (5.24) simplifies to

$$\begin{aligned}P_{out,1}&=\Pr\{\gamma_{1,2}>2^{R/\alpha}-1\}\\&\quad\cdot\Pr\{(1+\gamma_{1,d})^{\alpha}(1+\beta_1\gamma_{1,d}+(1-\beta_2)\gamma_{2,d})^{1-\alpha}<2^R\} \qquad (5.29)\\&\quad+\Pr\{\gamma_{1,2}<2^{R/\alpha}-1\}\cdot\Pr\{\gamma_{1,d}<2^R-1\},\end{aligned}$$

and using the above results we obtain for Rayleigh fading

$$\begin{aligned}P_{out,1}&=\exp\left(\frac{1-2^{R/\alpha}}{\Gamma_{1,2}}\right)\left[\int_E\frac{1}{\Gamma_{1,d}}\exp\left(-\frac{\gamma_{1,d}}{\Gamma_{1,d}}\right)d\gamma_{1,d}-\Psi_5(\Gamma_{1,d},\Gamma_{2,d},R,\alpha)\right]\\&\quad+\left[1-\exp\left(\frac{1-2^{R/\alpha}}{\Gamma_{1,2}}\right)\right]\left[1-\exp\left(\frac{1-2^{R}}{\Gamma_{1,d}}\right)\right]\end{aligned} \qquad (5.30)$$

where $\Psi_5(\Gamma_{1,d},\Gamma_{2,d},R,\alpha)$ is the same as in (5.28).

In addition to the cooperation level α, with space-time cooperation we have two additional free parameters, the power splitting ratios β_1 and β_2. Determining optimal values for β_1 and β_2 is beyond the scope of this chapter. In all the results for space-time cooperation presented in Section 5.2, we use $\beta_1=\beta_2=0.5$. Some preliminary results on optimal power splitting are given in Section 4.5.

To determine the diversity achieved by space-time cooperation, we re-parameterize $\Gamma_{i,j}$ and expand the exponential terms using Taylor's series as we did for coded cooperation (Section 5.1.2 and Appendix B). For the case of independent inter-user channels, we obtain

$$P_{out,1}=\frac{1}{\Gamma_T^2}\cdot\left[\int_E\left(\frac{2^{R/\alpha}-1}{\Gamma_{1,d}\Gamma_{1,2}}+\frac{c}{\Gamma_{1,d}\cdot(1-\beta_2)\Gamma_{2,d}}\right)d\gamma_{1,d}\right]+O\left(\frac{1}{\Gamma_T^3}\right), \qquad (5.31)$$

and for the case of reciprocal inter-user channels we have

$$P_{out,1} = \frac{1}{\Gamma_T^2} \cdot \left[\frac{(2^R - 1)(2^{R/\alpha} - 1)}{\Gamma_{1,d}\Gamma_{1,2}} + \int_E \frac{c}{\Gamma_{1,d} \cdot (1 - \beta_2)\Gamma_{2,d}} d\gamma_{1,d} \right] + O\left(\frac{1}{\Gamma_T^3}\right), \quad (5.32)$$

where c is the same as in (5.28). We see from (5.31) and (5.32) that space-time cooperation also achieves full diversity order.

5.2 Numerical Results

In this section we present outage probability results for coded cooperation. For each of the curves shown, the outage probabilities for coded cooperation and space-time cooperation at each point correspond to the cooperation level α which minimizes the average outage probability over both the users. This value of α is determined iteratively as discussed in Section 5.1.1. As mentioned in Section 5.1.3, we use $\beta_1 = \beta_2 = 0.5$ for space-time cooperation. For ease of exposition, we set $\Gamma_{1,2} = \Gamma_{2,1}$ for all cases (obviously true for reciprocal inter-user channels, and reasonable for independent inter-user channels since path loss is a reciprocal phenomenon, and large-scale shadowing, i.e. from buildings or other large obstructions, is also in many cases). As a result of this, we note that the outage probabilities for both users are equal if their channels to the destination (uplink channels) have equal mean SNR ($\Gamma_{1,d} = \Gamma_{2,d}$).

The first set of plots focuses on the low-rate regime. Specifically, we consider as an example rate $R = 1/2$ b/s/Hz. Figure 5.1 shows outage probability vs. mean uplink SNR ($\Gamma_{1,d} = \Gamma_{2,d}$) for various conditions of the inter-user channel. The different sets of curves correspond to the inter-user mean SNR equal to the mean uplink SNR, 10dB less than the mean uplink SNR, and equal to ∞; e.g., a noiseless inter-user channel. This latter case represents a lower bound on the achievable outage probability for the coded cooperation framework.

All of the cases in Figure 5.1 clearly show that coded cooperation achieves

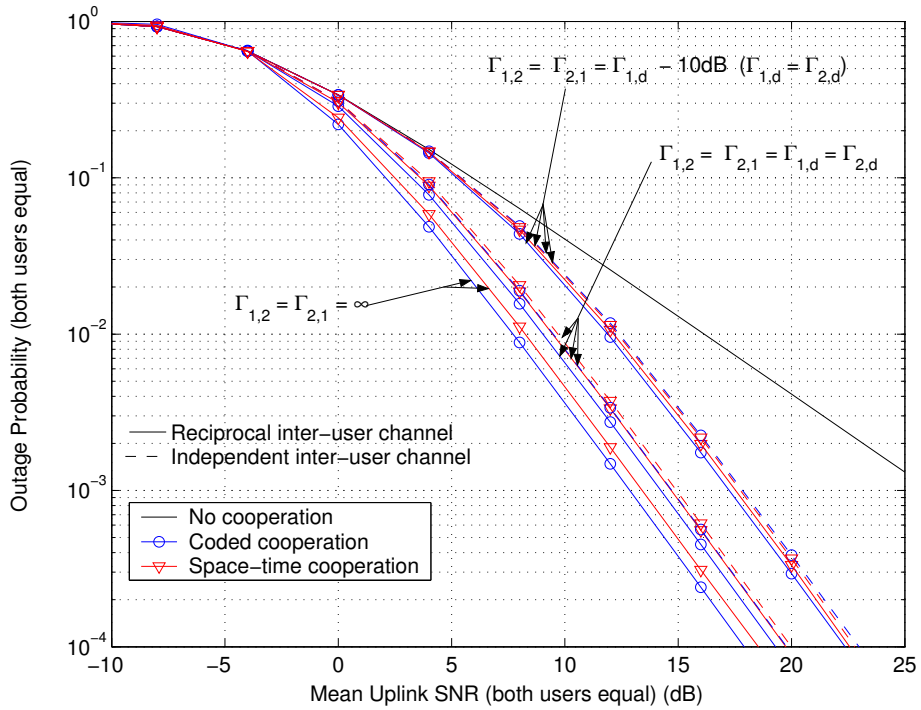

Figure 5.1. Outage probability vs. SNR for rate $R = 1/2$ b/s/Hz. Various sets of curves correspond to the inter-user channel mean SNR equal to the mean uplink SNR, 10dB less than the mean uplink SNR, and equal to ∞; e.g., a noiseless inter-user channel.

diversity order two (compared with diversity order one for non-cooperative transmission). The outage probability with reciprocal inter-user channels is always less than that with independent inter-user channels, since the latter admits Cases 3 and 4, in which no additional parities are transmitted for one of the users. Nevertheless, the difference between reciprocal and independent inter-user channels is quite small compared to the overall gain relative to the non-cooperative system. Coded cooperation generally maintains an advantage over space-time cooperation in the slow fading environment, although again the difference is small. It is interesting to note, however, that the difference in outage probability for reciprocal vs. independent inter-user channels is actually smaller with space-time cooperation. This indicates that a user always transmitting its own parities with some power in the second frame pro-

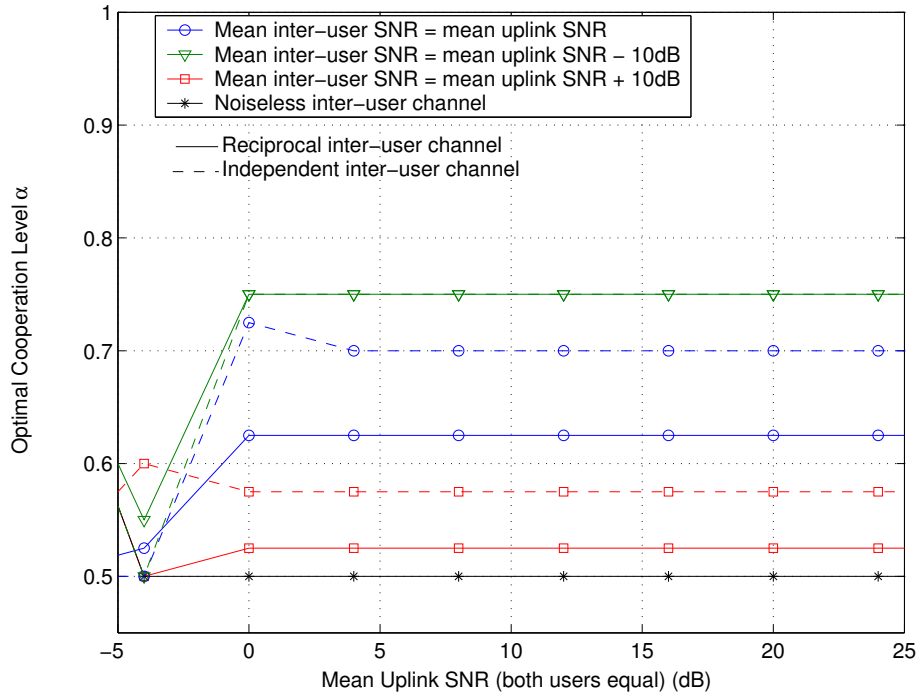

Figure 5.2. Optimal cooperation level α vs. SNR for coded cooperation, rate $R = 1/2$ b/s/Hz. The different curves represent various inter-user channel qualities. For all cases $\Gamma_{1,d} = \Gamma_{2,d}$.

vides a degree robustness against the deleterious effects of Cases 3 and 4. Finally, we note two interesting points about the effect of the inter-user channel quality. First, that coded cooperation can provide significant gains even if the inter-user mean SNR is less than that of the uplink channels. Second, as the inter-user channel quality improves relative to the uplink channels, we observe diminishing returns. Having a mean inter-user SNR equal to that of the uplink channels provides most of the achievable gain; increasing the mean inter-user SNR further provides minimal additional improvement.

Figure 5.2 shows optimal values of cooperation level α for coded cooperation corresponding to various degrees of inter-user channel quality. Again we consider rate $R = 1/2$ and $\Gamma_{1,d} = \Gamma_{2,d}$. With the exception of extreme conditions (e.g., very high mean inter-user SNR or very low mean uplink SNR), the optimal α value is almost

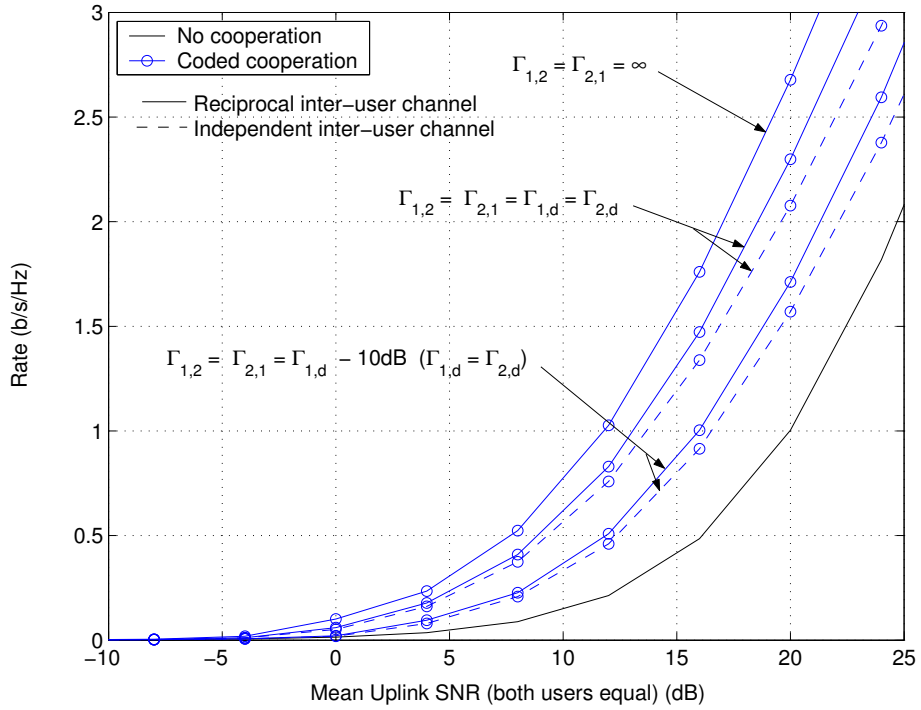

Figure 5.3. Rate vs. SNR for outage probability 10^{-2}. Various sets of curves correspond to the inter-user channel mean SNR equal to the mean uplink SNR, 10dB less than the mean uplink SNR, and equal to ∞; e.g., a noiseless inter-user channel. For simplicity, only results for coded cooperation are shown. Results for space-time cooperation are similar.

always greater than 1/2. This indicates that it is generally better to allocate a higher portion of the total rate R to the first frame, which improves the chances of successful detection of a user by its partner. As the inter-user channel quality decreases relative to the uplink channels, the optimal α value increases correspondingly, which allocates even more rate to the first frame. Finally, we note that, for a fixed inter-user channel quality relative to the uplink channels, the optimal α value for independent inter-user channels is greater than for reciprocal inter-user channels. This difference corresponds to trying to reduce the probability of occurrence for Cases 3 and 4 for independent inter-user channels.

Figure 5.3 shows rate vs. mean uplink SNR (both users equal) with fixed out-

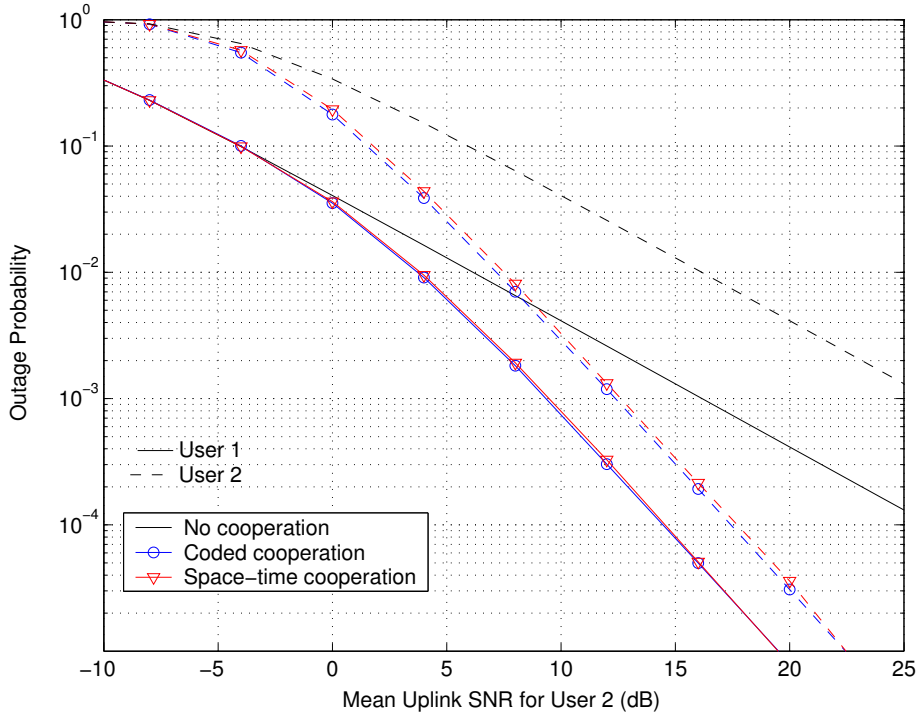

Figure 5.4. Outage probability vs. SNR for rate $R = 1/2$ b/s/Hz and unequal mean SNR for the uplink channels. The mean SNR of the inter-user channel is equal to that of User 2. The mean SNR of User 1's uplink channel is 10dB higher. For simplicity, only results for reciprocal inter-user channels are shown. Results for independent inter-user channels are similar.

age probability for various conditions of the inter-user channel (the same as those in Figure 5.1). These results indicate the improvement in throughput that coded cooperation provides over the non-cooperative system. Again we see that, even when the inter-user channel quality is poor relative to the uplink channels, coded cooperation still provides a significant improvement.

Figure 5.4 shows outage probability vs. uplink SNR for unequal mean uplink SNR ($\Gamma_{1,d} \neq \Gamma_{2,d}$). The x-axis is the mean uplink SNR for User 2, $\Gamma_{2,d}$. In this case, User 1 has a better uplink channel, with mean SNR $\Gamma_{1,d} = \Gamma_{2,d} + 10$dB. The mean inter-user SNR is equal to $\Gamma_{2,d}$. As one might expect, User 2 improves significantly relative to the non-cooperative system by cooperating with a partner that has a better

quality uplink channel. More interesting is the fact that User 1 also achieves significant gain, despite cooperating with User 2 that has a poorer uplink channel. This illustrates that even a user with a very good uplink channel has a strong motivation to cooperate, which is an important practical result. In addition, we observe that the difference in outage probability between Users 1 and 2 is noticeably reduced in the cooperative system. This shows that cooperation inherently re-allocates the system resources in a more effective manner.

5.2.1 Comparison with Repetition-Based Methods

Next, we compare coded cooperation with two repetition-based methods; namely, the amplify-and-forward and selection decode-and-forward protocols introduced in [40]. For both of these schemes, the cooperation level α is 1/2 by definition. The outage probability of amplify-and-forward (with respect to User 1; the outage probability for User 2 is similar) is given by [40]

$$P_{out,1} = \Pr\left\{\gamma_{1,d} + \frac{\gamma_{1,2}\gamma_{2,d}}{\gamma_{1,2} + \gamma_{2,d} + 1} < 2^{2R} - 1\right\}. \tag{5.33}$$

Though obtaining an expression for Rayleigh fading is difficult, outage probability can be estimated via Monte Carlo simulation of (5.33). Note also that (5.33) applies for both reciprocal and independent inter-user channels; i.e., for given $\Gamma_{1,2}$ and $\Gamma_{2,1}$ the performance of amplify-and-forward does not depend on the correlation between $\gamma_{1,2}$ and $\gamma_{2,1}$. This is because a user always amplifies and forwards the partner's signal regardless of the channel conditions. The partnering users are effectively decoupled, in the sense that we do not have the four cases that characterize coded cooperation.

Selection decode-and-forward is similar to coded cooperation, except that the user repeats the first-frame symbols in the second frame (the partner's if correctly decoded, otherwise the user's own) instead of transmitting additional parity. Based on [40], we can generalize selection decode-and-forward for independent inter-user

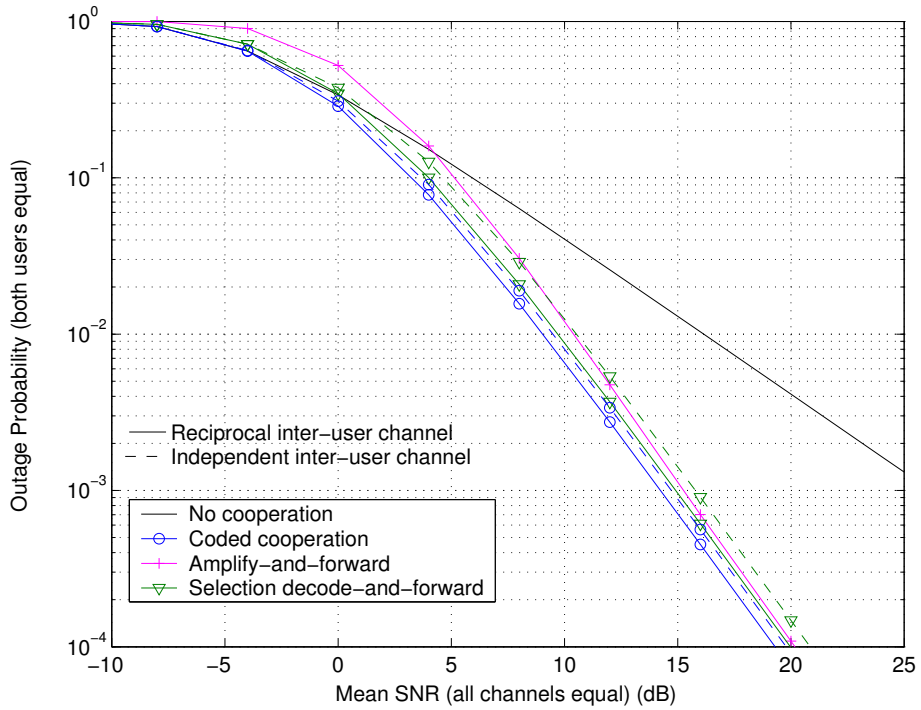

Figure 5.5. Outage probability vs. SNR for rate $R = 1/2$ b/s/Hz. All channels have equal mean SNR. Comparison of coded cooperation, amplify-and-forward, and selection decode-and-forward.

channels and derive outage probability expressions in a manner similar to that which we have used for coded cooperation. We refer the interested reader to Appendix C for the details of this derivation.

Figure 5.5 compares outage probability vs. mean uplink SNR for coded cooperation, amplify-and-forward, and selection decode-and-forward (for simplicity we do not show space-time cooperation). Again we consider the low-rate regime with rate $R = 1/2$, with all channels having equal mean SNR ($\Gamma_{1,2} = \Gamma_{2,1} = \Gamma_{1,d} = \Gamma_{2,d}$). Coded cooperation maintains a slight advantage over the two repetition-based methods, regardless of whether the inter-user channels are independent or reciprocal. At low mean uplink SNR, amplify-and-forward and selection decode-and-forward are worse than no cooperation, which is a result of the inefficiency of repetition coding in this region (noise amplification by the partner adds to this effect in the case of amplify-and-

forward). An inherent property of coded cooperation is that it never performs worse than no cooperation. Another interesting observation for the repetition-based schemes is that selection decode-and-forward becomes worse than amplify-and-forward with increasing uplink SNR for the case of independent inter-user channels.

Figure 5.6 compares outage probability vs. rate for the various cooperative schemes. In the low-rate regime, highlighted in Figure 5.6(a), all of the methods provide significant improvement, with coded cooperation generally performing slightly better overall. As the rate increases, the outage probability of the repetition-based methods exceeds that of the non-cooperative system. This is again a manifestation of the inefficiency of repetition coding. The higher-rate region also highlights the main strength of space-time cooperation, namely its robustness in the case of independent inter-user channels. The outage probability for coded cooperation exceeds that of space-time cooperation at higher rates when the inter-user channels are independent, a result of Cases 3 and 4 having a significant impact in this region. The power splitting that occurs in space-time cooperation noticeably retards this effect. As in Figure 5.5, we note here that coded cooperation, as well as space-time cooperation, in the worst case always performs at least as well as no cooperation.

5.3 Chapter Summary

To understand coded cooperation in a more general context that is independent of any particular coding scheme, in this chapter we examine the outage probability of coded cooperation. We derive expressions for outage probability in the case of quasi-static Rayleigh fading, and show that coded cooperation achieves full diversity (order two for two cooperating users) in the high-SNR regime. We perform a similar analysis for space-time cooperation, an extension of coded cooperation in which each user splits its power in the second frame and transmits for both itself and the partner.

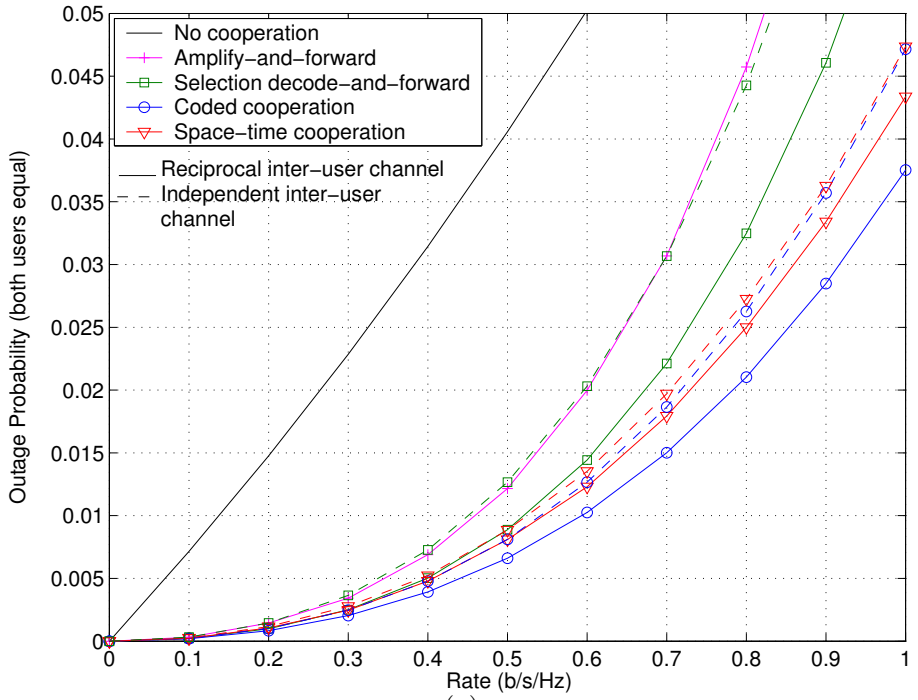

(a)

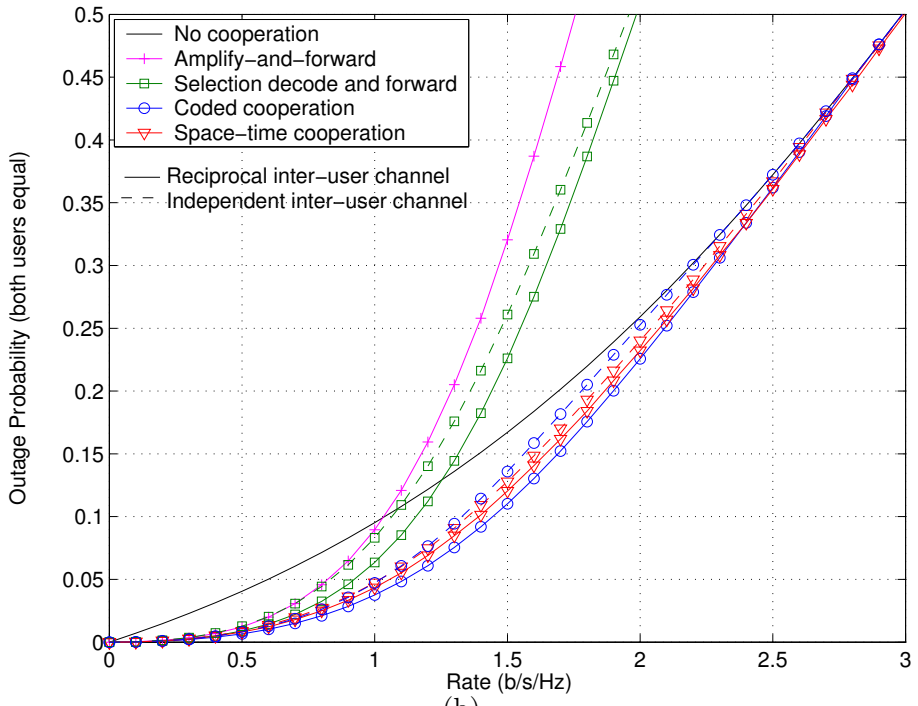

(b)

Figure 5.6. Outage probability vs. rate. All channels have mean SNR of 10dB. In (a) the focus is on the low-rate regime, while (b) shows a broader range for rate.

Numerical outage probability results demonstrate that both coded cooperation and space-time cooperation provide significant gains over non-cooperation transmission, especially in the low-rate regime ($R \leq 1$ b/s/Hz). Coded cooperation generally performs slightly better than space-time cooperation, except at higher rates when the inter-user channels are independent. Under these conditions, space-time cooperation provides increased robustness against the effects of independent inter-user channels. The results also show that coded cooperation performs better than repetition-based cooperative protocols. Due to the inefficiency of repetition coding, the repetition based schemes are worse than no cooperation for low SNR or higher rates. In contrast, we see that coded cooperation and space-time cooperation in the worst case always perform at least as well as non-cooperative transmission.

Thusfar in this dissertation, we have considered coded cooperation in the context of two users that are paired together and cooperate with each other. In Chapter 6, we extend the coded cooperation framework to multi-user networks, and develop protocols for partner selection in such an environment.

CHAPTER 6

CODED COOPERATION IN MULTI-USER WIRELESS NETWORKS

Previous works on user cooperation [51, 52, 53, 50, 41, 43, 39, 40] discussed in Chapter 2, as well as the coded cooperation framework as developed in Chapters 3 through 5, consider a scenario in which two users are paired together and cooperate with each other in a reciprocal fashion. Each of these works demonstrates that the performance (i.e, outage probability or bit/block error rate) is significantly improved compared to non-cooperative transmission. These results motivate the extension of user cooperation to multi-user wireless networks, and the study of protocols for partner allocation. Of particular interest are wireless ad hoc networks, in which the mobility of the users, the lack of centralized control, and the impairments of the wireless channel combine to present significant challenges to reliable communication throughout the network. A notable first step in the application of user cooperation to network applications has been made by Laneman and Wornell [42]. In this work, repetition-based cooperative protocols developed in [40] are applied to a multi-user network, in which each user attempts to cooperate with all the other users. It is shown that the diversity order achieved is equal to the number of users in the network, a significant improvement over non-cooperative transmission.

In this chapter, we extend the two-user coded cooperation framework from the previous chapters to a multi-user scenario. We consider M transmitting users randomly distributed within a finite area, and propose distributed protocols in which each user individually and independently decides with whom to cooperate at any given time. These protocols are general in the sense that a user can cooperate with any n $(0 \leq n \leq M-1)$ of the $M-1$ other users, which presents a diversity vs. complexity

tradeoff that we examine. We consider the case of quasi-static Rayleigh fading, and compare the performance of these protocols in terms of outage probability [46, 13], in order to remove any dependence on a particular coding scheme. Results show that full diversity is achieved, as well as significant gains compared to a non-cooperative system. In addition, we propose a centralized algorithm, in which a central node or destination, that maintains some knowledge of all the channels between the users, assigns partners based on minimizing the average outage probability over all the users. This algorithm represents a lower bound on performance for the distributed protocols (for a given n), which primarily have a view toward ad hoc networks, as well as having applicability to cellular and other networks that have some centralized control.

The remainder of this chapter is organized as follows. Section 6.1 defines the system model, introduces cooperative transmission, and describes performance characterization for the network under consideration. Section 6.2 considers distributed protocols for partner selection, and examines their performance in terms of outage probability. In Section 6.3 we propose an algorithm for partner assignment based on some central knowledge of all channels between users. We again examine the outage probability and compare the results with those of the distributed protocols. Finally, we summarize in Section 6.4.

6.1 System Model and Characterization

6.1.1 Network Realization and Channel Model

Our network model consists of multiple nodes, or users, randomly distributed over a two-dimensional circular region. A given user is equally likely to be located at any point in the region, and the user locations are all mutually independent. We consider a group of M users that have data to transmit. Each of these users has a destination node (not part of the set of M transmitting users) at another random location in

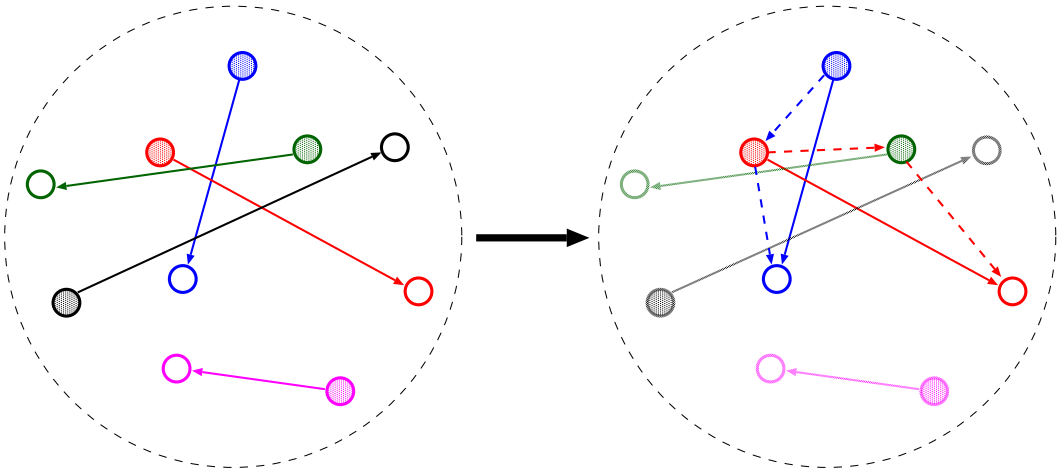

(a) (b)

Figure 6.1. (a) Illustration of a given network realization. The shaded circles represent the transmitting users, while the empty circles represent their corresponding destinations. (b) Example of partner selection and cooperation (for simplicity only two of the transmitting users are shown with partners).

the space. We define a given placement of the M users and their corresponding destination nodes as a *network realization*. This is illustrated in Figure 6.1(a).

Each of the users is assigned a unique, orthogonal (i.e., in time, frequency, or spreading code) multiple-access channel. The physical channel from User i to User j has instantaneous signal-to-noise ratio (SNR)

$$\gamma_{i,j} = \Gamma_{i,j} \cdot |h_{i,j}|^2, \tag{6.1}$$

where $|h_{i,j}|$ is the Rayleigh-distributed fading magnitude, with $E\{|h_{i,j}|^2\} = 1$. The term $\Gamma_{i,j}$ represents the average SNR of the channel over fading, and is modeled as

$$\Gamma_{i,j} = \left(\frac{P}{N_0}\right) K S_{i,j} d_{i,j}^{\beta} \tag{6.2}$$

where P is the transmit power (equal for all users), N_0 is the additive white Gaussian noise power at the receiver (equal for each receiver), K is the path loss for an arbitrary reference distance, $S_{i,j}$ is a zero-mean log-normal shadowing component with standard

deviation σ_S (dB), $d_{i,j}$ is the distance between nodes i and j (normalized by the reference distance), and β is the path loss exponent. The numerical results in this chapter are obtained using $\sigma_S = 8$ dB and $\beta = 4$. Both the fading and and shadowing components are i.i.d. for each $\{i, j\}$ pair. The shadowing components are assumed to be reciprocal ($S_{i,j} = S_{j,i}$). We consider quasi-static fading, such that the fading coefficients $\{\alpha_{i,j}\}$ are constant for a given transmitted block, or code word, but are i.i.d. for different blocks. The shadowing components are constant for a given network realization.

6.1.2 Cooperative Transmission

Cooperative transmission for the network model defined above is based on the coded cooperation framework developed in Chapters 3 through 5. Each user segments its data into coded transmit blocks, consisting of N code symbols, such that the allocated rate for each block is R b/s/Hz. Users cooperate by dividing the transmission of each N-symbol block over two successive time segments, or frames. In the first frame each user transmits a rate R/α code word ($N_1 = \alpha N$ symbols). This itself is a valid (albeit weaker) code word which can be decoded to obtain the original information. If a user successfully decodes a selected partner's (another of the M transmitting users) first-frame transmission, in the second frame the user transmits N_2 additional parity symbols for the partner's data according to some overall coding scheme, where $N_1 + N_2 = N$. Otherwise, if a user selects no partners for that block (for example, if the user cannot successfully decode any of the other users), the user transmits N_2 additional parity symbols for its own data. Each user always transmits a total of N bits per source block over the two frames. If a user selects multiple partners with which to cooperate in the second frame, the second-frame transmit power allocated to each partner is scaled accordingly to maintain total transmit power P. Thus, cooperation works within the identical multiple-access framework as a comparable

non-cooperative system, and no additional bandwidth or power is required. The parameter α gives the degree of cooperation; e.g., the portion of each user's N total channel symbols per block allocated for the first frame.

Previous works on two-user cooperation, as well as the previous chapters of this dissertation, generally consider reciprocal partnerships; in other words, two users are paired together and serve as partners for each other. In the multi-user network scenario, it is not necessary (and may not be desireable) to constrain partnerships to be reciprocal. Spatial diversity does not require reciprocal partnerships, but only that additional parities for a user are transmitted in the second frame by at least one of the other M transmitting users. As a result, in this work we do not restrict protocols to produce reciprocal partnerships. Figure 6.1(b) gives an example of non-reciprocal partnerships for a given network realization.

6.1.3 System Characterization

Performance results for the protocols developed in the following sections are obtained by averaging metrics of interest (i.e., user outage probability) for an arbitrary user over fading and network realizations. We obtain results via Monte Carlo simulation. Each iteration consists of the following steps:

1. Randomly place $2M$ nodes (M transmitting users and their corresponding destinations).

2. Apply random shadowing and fading to each link.

3. Select partners according to a given protocol.

4. Compute desired metrics for an arbitrary user based on the given partner selection.

The results of Step 4 are then averaged over all the iterations to produce the desired result.

A key system performance metric is outage probability. As in Chapter 5, we consider as a baseline non-cooperative direct transmission between source and destination. Recall (see Section 5.1) that the outage probability for non-cooperative transmission is given by

$$P_{out} = \Pr\{\gamma < 2^R - 1\} = \int_0^{2^R-1} p_\gamma(\gamma) d\gamma, \tag{6.3}$$

where $p_x(x)$ denotes the probability density function (pdf) of random variable x. For the case of Rayleigh fading, γ has an exponential pdf with parameter $1/\Gamma$, where Γ is the mean value of SNR over the fading as described in (6.1) and (6.2). The outage probability for Rayleigh fading is thus evaluated as

$$P_{out} = \int_0^{2^R-1} \frac{1}{\Gamma} \exp\left(-\frac{\gamma}{\Gamma}\right) d\gamma = 1 - \exp\left(-\frac{2^R-1}{\Gamma}\right). \tag{6.4}$$

Averaging this result over several network realizations gives the average outage probability of an arbitrary user in the network for the case of non-cooperative transmission.

6.2 Distributed Protocols

In this section, we consider various protocols for partner selection in which each of the M transmitting users individually decides which of the other users to cooperate with for a given transmit block. Each acts autonomously, with no knowledge of the actions of the other users. We therefore we refer to these as *distributed protocols*, as they are suitable for applications such as wireless ad hoc networks and sensor networks, in which there is little centralized control over the operation of the network.

6.2.1 Protocol Description

For each transmit block, a user attempts to select n of the other $M-1$ users to transmit for in the second frame. Let n_d be the number of other users whose first frame a given user can successfully decode, and n_s be the number of of users actually selected by the given user. We assume that each user has no knowledge of the locations of the other users.

A user selects for whom to transmit based on a priority list of the other $M-1$ transmitting users. In this work we consider the following methods for creating the priority lists:

1. *Random selection:* For each transmit block, a user randomly orders the other $M-1$ users, such that a given user has equal probability of occupying any position in the list.

2. *Received SNR selection:* For each transmit block, a user prioritizes the other $M-1$ users in order from highest to lowest received SNR for their first-frame transmissions.

3. *Fixed priority selection:* A user has a fixed priority list that remains constant for all transmit blocks. For partner selection to be fair, the user lists should be such that a given user occupies a different position in each of the other user's lists. Without loss of generality, we can define such a list for User i as $\{i+1, i+2, \ldots, M, 1, \ldots, i-1\}$ (i.e., User 5's list is $\{6, 7, \ldots, M, 1, \ldots, 4\}$).

After all the users have transmitted their first frames, a given user may attempt to decode each user according to its priority list until n have been decoded successfully, in which case $n_s = n$, or until the list is exhausted, in which case $n_s = n_d$. With this strategy we say that the user makes all possible decoding attempts. Alternatively,

the user may simply attempt to decode the first n users in the list, and select for cooperation those who are successfully decoded. In this case, $0 \leq n_s \leq \min[n, n_d]$ (for example, if $n = 1$, and the first user in the list is not successfully decoded, then $n_s = 0$ even though $n_d \neq 0$, e.g., other users could be decoded successfully if attempted). We can characterize the complexity of the protocol by the number of decoding attempts for an arbitrary user averaged over multiple transmit blocks and network realizations. Even for $n = 1$, for a given block User i may have multiple partners that transmit its additional parities in the second frame. We assume that these multiple copies of User i's parity symbols are optimally combined (i.e., maximal ratio combining) at User i's destination prior to decoding. We discuss further in Section 6.2.4 some practical issues implied by this optimal combining.

6.2.2 Outage Probability Characterization

For a given transmit block, let $\mathcal{S}_i$ be the set of users that select and transmit additional parity for User i in the second frame. In the first frame, User i transmits αN coded symbols, while in the second frame the users in $\mathcal{S}_i$ (the partners) each transmit the same $(1-\alpha)N$ additional parity symbols for User i, which are then optimally combined at User i's destination. The first and second frames can be viewed as parallel (conditionally) Gaussian channels, whose capacities add together [17, Section 10.4]. Equivalently, they can be viewed as time sharing between sets of independent channels. We can thus write the outage event for User i conditioned on $\mathcal{S}_i$ as

$$C_{i,d}(\gamma_{i,d}, \{\gamma_{p,d}\}|\mathcal{S}_i) = \alpha \log_2(1+\gamma_{i,d}) + (1-\alpha)\log_2\left(1 + \sum_{p\in\mathcal{S}_i} \gamma_{p,d}\right) < R, \qquad (6.5)$$

where the subscript d denotes User i's destination, and the subscript p denotes a given partner in the set $\mathcal{S}_i$. The corresponding outage probability conditioned on $\mathcal{S}_i$

is

$$P_{out,i}(\mathcal{S}_i) = \Pr\left\{(1+\gamma_{i,d})^{\alpha}\left(1+\sum_{p\in\mathcal{S}_i}\gamma_{p,d}\right)^{1-\alpha} < 2^R\right\}. \tag{6.6}$$

We use the outage event in (6.6) for Step 4 of the Monte Carlo simulation described in Section 6.1.3.

For Rayleigh fading we can evaluate (6.6) as

$$P_{out,i}(\mathcal{S}_i) = \int_A \cdots \int \frac{1}{\Gamma_{i,d}} \exp\left(-\frac{\gamma_{i,d}}{\Gamma_{i,d}}\right) d\gamma_{i,d} \cdot \prod_{p\in\mathcal{S}_i} \frac{n_{s,p}}{\Gamma_{p,d}} \exp\left(-\frac{n_{s,p}\gamma_{p,d}}{\Gamma_{p,d}}\right) d\gamma_{p,d} \tag{6.7}$$

where

$$A \equiv \left\{(1+\gamma_{i,d})^{\alpha}\left(1+\sum_{p\in\mathcal{S}_i}\gamma_{p,d}\right)^{1-\alpha} < 2^R\right\}, \tag{6.8}$$

and $n_{s,p}$ denotes the total number of users (including User i) selected by partner p.

While (6.7) can be simplified further, the result is not useful for this work, and we omit the details here. What is instructive, however, is to examine (6.7) in the high-SNR regime to determine the achieved diversity. To facilitate this, we re-parameterize the mean channel SNR $\Gamma_{i,j}$ as we did in Section 5.1.2:

$$\Gamma_{i,j} \Longrightarrow \Gamma_T \cdot \Gamma_{i,j}, \tag{6.9}$$

where now $\Gamma_T = \left(\frac{P}{N_0}\right)$, the ratio of user transmit power to the received noise, and $\Gamma_{i,j} = KS_{i,j}d_{i,j}^{\beta}$ is a finite constant accounting for large-scale path loss and shadowing (see (6.2)). By expressing outage probability as a function of $1/\Gamma_T$, and then letting $\Gamma_T \to \infty$ (e.g., the high-SNR regime), the diversity order is given by the smallest exponent of $1/\Gamma_T$.

The outage probability as a function of $1/\Gamma_T$, is obtained by rewriting (6.7) as

$$\begin{aligned} P_{out,i}(\mathcal{S}_i) = & \frac{1}{\Gamma_T^{|\mathcal{S}_i|+1}} \int_A \cdots \int \frac{\prod_{p\in\mathcal{S}_i} n_{s,p}}{\Gamma_{i,d}\cdot\prod_{p\in\mathcal{S}_i}\Gamma_{p,d}} \exp\left(-\frac{\gamma_{i,d}}{\Gamma_T\Gamma_{i,d}} - \sum_{p\in\mathcal{S}_i}\frac{n_{s,p}\gamma_{p,d}}{\Gamma_T\Gamma_{p,d}}\right) \\ & \cdot d\gamma_{i,d}\prod_{p\in\mathcal{S}_i} d\gamma_{p,d}, \end{aligned} \tag{6.10}$$

where $|\mathcal{S}_i|$ denotes the number of partners in the set $\mathcal{S}_i$. We can expand the exponential term in (6.10) using the equivalent Taylor's series representation (i.e., [11, p. 299]) to obtain

$$P_{out,i}(\mathcal{S}_i) = \left(\frac{1}{\Gamma_T^{|\mathcal{S}_i|+1}}\right) \cdot \left(\frac{\prod_{p\in\mathcal{S}_i} n_{s,p}}{\Gamma_{i,d} \cdot \prod_{p\in\mathcal{S}_i} \Gamma_{p,d}}\right) \cdot \left(\int_A \cdots \int d\gamma_{i,d} \prod_{p\in\mathcal{S}_i} d\gamma_{p,d}\right) + O\left(\frac{1}{\Gamma_T^{|\mathcal{S}_i|+2}}\right). \tag{6.11}$$

Note that the integral term represents the first term in the Taylor's series expansion of $\exp(\cdot)$ (namely 1), while $O\left(\frac{1}{\Gamma_T^{|\mathcal{S}_i|+2}}\right)$ denotes the order of the remaining terms.[1] The integral term, which is a function of the rate R, the cooperation level α, and the number of partners $|\mathcal{S}_i|$, can be simplified to a single integral; however, as this does not further the objectives of this work, we do not include the details here.

We see from (6.11) that, as $\Gamma_T \to \infty$, the outage probability is a function of $1/\Gamma_T^{|\mathcal{S}_i|+1}$, which demonstrates that the achieved diversity, conditioned on $\mathcal{S}_i$, is $|\mathcal{S}_i| + 1$. For example, if $|\mathcal{S}_i| = 2$ for a given transmit block, User i achieves diversity order 3 for that block. This is the result of portions of User i's N code symbols arriving at User i's destination via three independent physical channels. Specifically, αN symbols travel directly through User i's own channel, and $(1-\alpha)N$ symbols travel from each of the two partners in $\mathcal{S}_i$ to User i's destination.

User i's overall outage probability can be expressed as

$$P_{out,i} = \sum_{\mathcal{S}_i} \Pr\{\mathcal{S}_i\} \cdot P_{out,i}(\mathcal{S}_i), \tag{6.12}$$

where the summation is over all possible partner sets $\mathcal{S}_i$. The overall diversity order achieved by User i is thus equal to the smallest $|\mathcal{S}_i|+1$ for which $\Pr\{\mathcal{S}_i\} > 0$ as $\Gamma_T \to \infty$. Closed-form expressions for $\Pr\{\mathcal{S}_i\}$ depend on the selection protocol (specifically,

[1] Throughout this chapter, $O(\cdot)$ denotes the familiar order notation; see for example [34, pp. 2–3].

the method of generating the priority lists), and in general are difficult to obtain for $n < M - 1$. Nevertheless, it is clear that in order to achieve *full* diversity, which we define as diversity order $n + 1$, we must have $\Pr\{|\mathcal{S}_i| < n\} \to 0$ as $\Gamma_T \to \infty$, or equivalently $\Pr\{\mathcal{S}_i\} \to 0$ as $\Gamma_T \to \infty$ for all sets $\mathcal{S}_i$ such that $|\mathcal{S}_i| < n$. Furthermore, in order to obtain any diversity improvement, we require that $\Pr\{|\mathcal{S}_i| = 0\} \to 0$ as $\Gamma_T \to \infty$. In other words, the probability of User i not being selected by any of the other users must go to zero in the high-SNR regime. Otherwise, if $\Pr\{|\mathcal{S}_i| = 0\} > 0$ for all Γ_T, we can achieve at best diversity order one, which is the same as for non-cooperative transmission. We will discuss this issue further in the following section, as we compare the diversity achieved by the various protocols.

6.2.3 Results and Discussion

Figure 6.2 compares the outage probability of the three distributed protocols for the case of $n = 1$, and users making all possible decoding attempts. We see that the fixed priority protocol performs significantly better than the other two protocols. In Figure 6.2(a), the fixed priority protocol has a gain of approximately 8dB over no cooperation for outage probability 10^{-2}. In contrast, the other two protocols have a gain of only 2-3dB. Figure 6.2(b) shows that the fixed priority protocol provides significant improvement over no cooperation, and maintains its superiority over the other protocols, for a wide range of rates.

Furthermore, Figure 6.2(a) shows that the fixed priority protocol is the only one of the three that achieves full diversity (in this case diversity order two for $n = 1$). Figure 6.3 shows $\Pr\{|\mathcal{S}_i| < n\}$ vs. average source-to-destination SNR for fixed rate $R = 1/3$, $M = 10$, and $n = 1$ and 3 (again the users are making all possible decoding attempts). In the high-SNR regime ($\Gamma_T \to \infty$), it becomes highly likely that User i's first-frame transmission can be successfully decoded by all the other users. Thus,

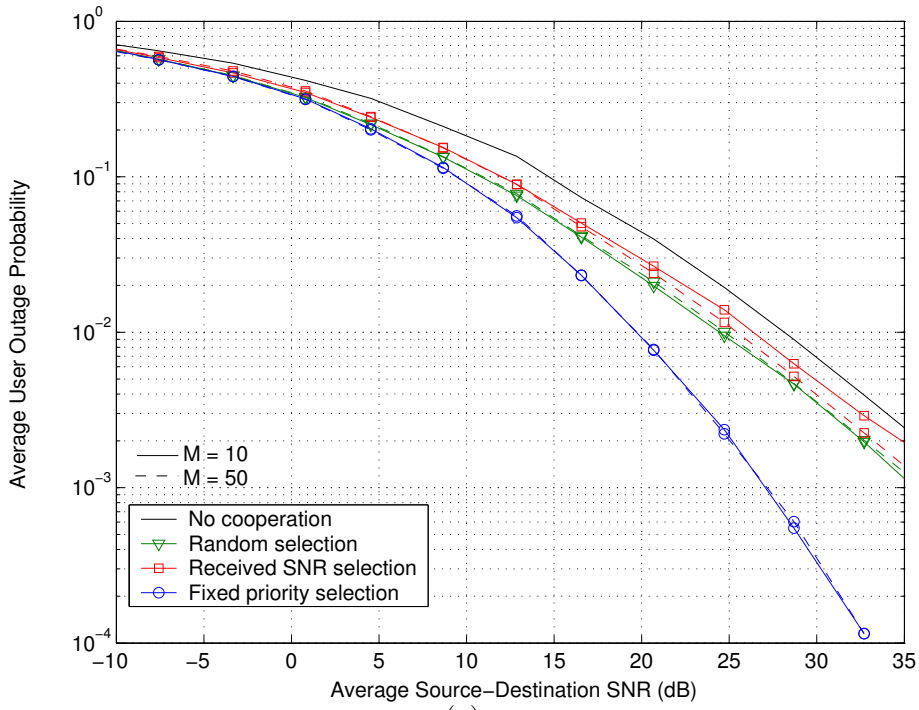

(a)

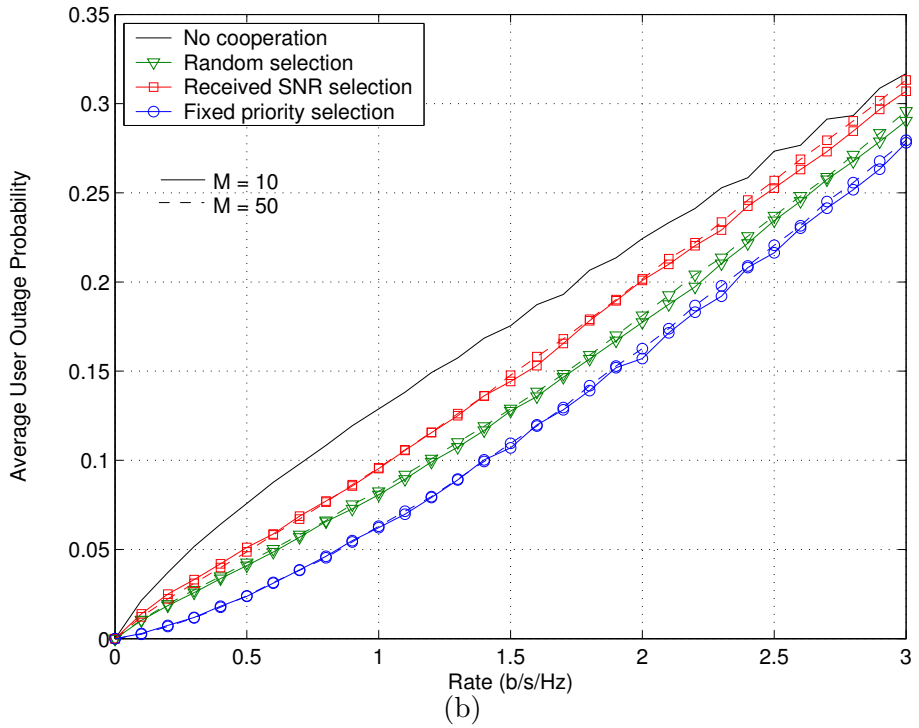

(b)

Figure 6.2. Comparison of distributed protocols for $\alpha = 0.75$, $n = 1$ (users make all possible decoding attempts), and $M = 10$ and 50: (a) outage probability vs. average source-destination SNR for rate $R = 1/3$; (b) outage probability vs. rate for average source-destination SNR of 20dB.

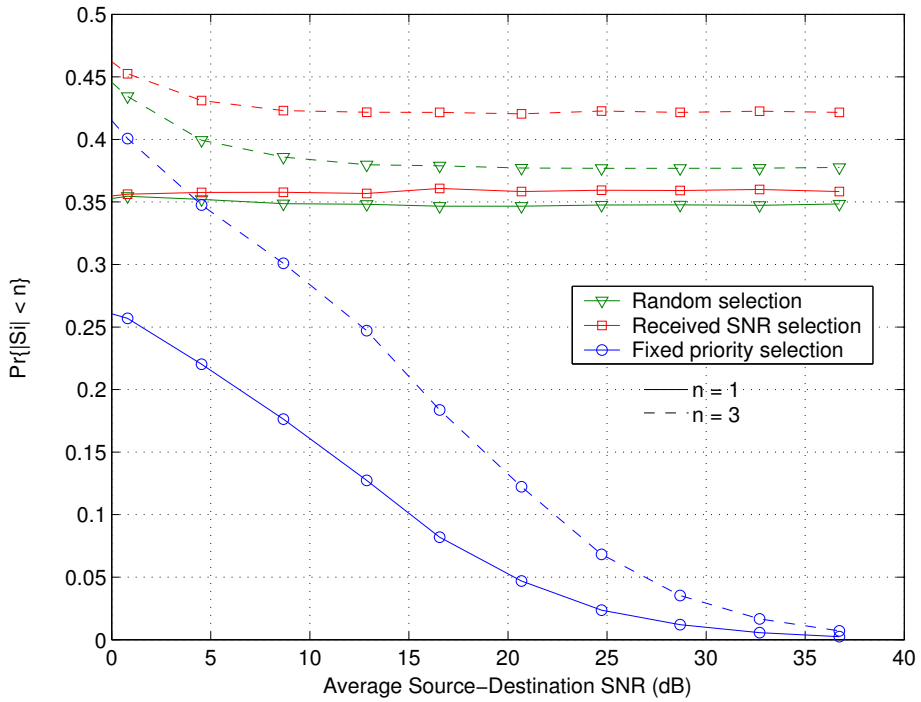

Figure 6.3. $\Pr\{|\mathcal{S}_i| < n\}$ vs. average source-destination SNR for rate $R = 1/3$, $\alpha = 0.75$, $M = 10$, and $n = 1$ and 3 (users make all possible decoding attempts).

with the fixed priority protocol, for a given n the probability approaches 1 that Users $i-1$, $i-2$,..., $i-n$, will select and transmit for User i in the second frame, and thus User i will achieve full diversity $n+1$. In other words, $\Pr\{|\mathcal{S}_i| < n\} \to 0$ as $\Gamma_T \to \infty$ for the fixed priority protocol. This is illustrated in Figure 6.3.

For the random selection protocol, assuming that all users can successfully decode User i, the probability that User j ($j \neq i$) does not select User i is

$$\begin{aligned} \Pr\{j \notin \mathcal{S}_i\} &= \left(\frac{M-2}{M-1}\right)\left(\frac{M-3}{M-2}\right)\cdots\left(\frac{M-n-1}{M-n}\right) \\ &= \frac{M-n-1}{M-1} = 1 - \frac{n}{M-1}. \end{aligned} \tag{6.13}$$

Since each user selects independently of all other users, the probability that User i is not selected by any other user is

$$\Pr\{|\mathcal{S}_i| = 0\} = \left(1 - \frac{n}{M-1}\right)^{M-1}. \tag{6.14}$$

From (6.14), we see that $\Pr\{|\mathcal{S}_i| = 0\} > 0$ for the random selection protocol for all $n < M - 1$ (for $n = M - 1$, all of the protocols become the same), even as $\Gamma_T \to \infty$. Furthermore, Figure 6.3 shows that $\Pr\{|\mathcal{S}_i| < n\}$ is bounded away from zero regardless of SNR. Thus, the random selection protocol does not achieve full diversity, and in fact at best achieves only diversity order 1 for $n < M - 1$. The fact that $\Pr\{|\mathcal{S}_i| = 0\}$ is bounded away from zero also accounts for its poor performance relative to the fixed priority protocol for moderate SNR.

While one may expect that random selection would not perform particularly well, it is initially surprising that selection based on the best received SNR actually performs worse than random selection. However, with this protocol the particular users selected by a potential partner in the second frame actually depend on the random spatial distribution of the users in the given network realization, as well as the random shadowing and fading components, which are completely independent of Γ_T. In this respect, the behavior of received SNR selection is similar to that of random selection, and empirically we observe that $\Pr\{|\mathcal{S}_i| < n\}$ is again bounded away from zero (see Figure 6.3). In fact, we observe that $\Pr\{|\mathcal{S}_i| = 0\}$ is greater for received SNR selection than random selection for a given n. This is because the respective probabilities of User i being selected by Users j and k are not uncorrelated. With $n = 1$ and $\gamma_{i,j} < \gamma_{k,j}$, User j will likely not select User i, and in addition it is more likely (although not a certainty because of random fading) that $\gamma_{i,k} < \gamma_{j,k}$, in which case User k will likely not select User i either. One example of such a scenario is that User i is isolated near the boundary of the region, while the other users are clustered relatively close together in another part of the region.

Figure 6.2 also shows that, for a given $n < M - 1$, the number of transmitting users M has little effect on the performance. In the random selection and fixed priority selection protocols, the priority list order is uncorrelated with the physical

locations of the users. Thus, the partners in $\mathcal{S}_i$ are located randomly with respect to User i and its destination, and the probability of their locations is independent of M. Consequently, the outage probability of User i is not significantly affected by M. Figure 6.2(a) shows that received SNR selection improves slightly as M increases. With more users, it becomes less likely that, for User i, received SNR $\gamma_{i,j}$ is small for all j. However, at best received SNR selection approaches the performance of random selection, and thus, since fixed priority selection still performs much better, this is not a significant result. Obviously, for $n = M$, increasing M increases the achievable diversity according to (6.11), and thus improves performance, but this comes at the expense of increased complexity, as each user attempts to decode all $M - 1$ other users each transmit block.

Figure 6.4 compares the outage probability of the fixed priority selection protocol for $M = 10$ and various values of n. In addition, for each n curves are shown corresponding to users making all possible decoding attempts (solid curves), and making only n attempts (dashed curves). As noted in Section 6.2.1, we can characterize the complexity as the expected number of decoding attempts per transmit block made by a user. Figure 6.5 compares complexities for various n values when users make all possible decoding attempts. We note from Figure 6.5(a) that random selection and fixed priority selection have identical complexity. The complexity of received SNR selection is less and converges much faster to the minimum value n, which makes sense since a user in this protocol attempts to decode first those users for which it sees the highest received SNR.

In Figure 6.4, we see that as n increases, the diversity increases and the outage probability decreases relative to non-cooperative transmission. However, the additional gain obtained from incrementing n to $n + 1$ decreases as n increases, while the complexity increases approximately linearly, illustrating a case of diminishing returns.

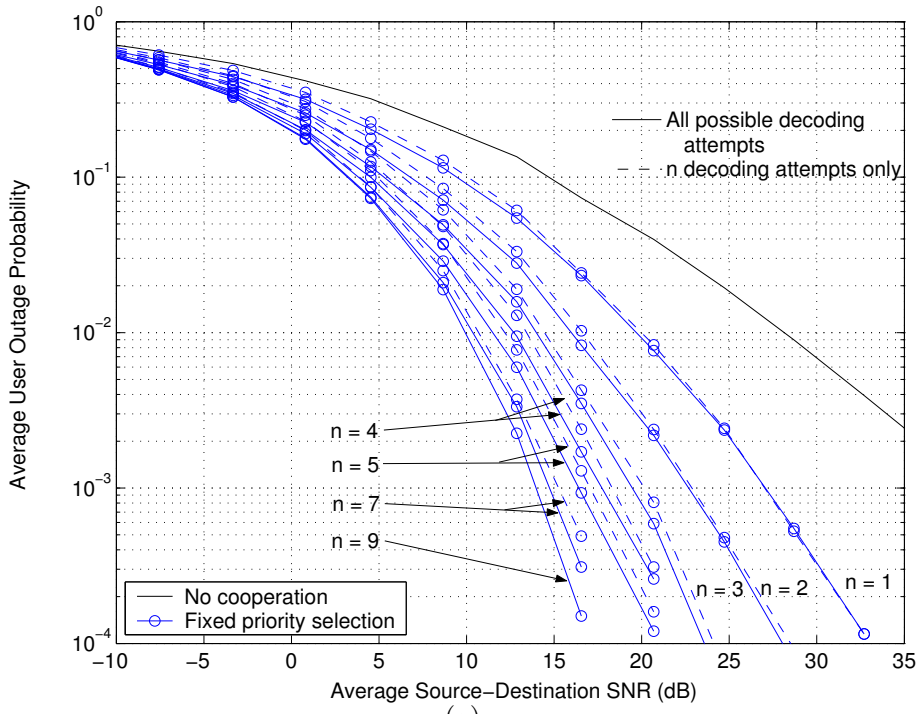

(a)

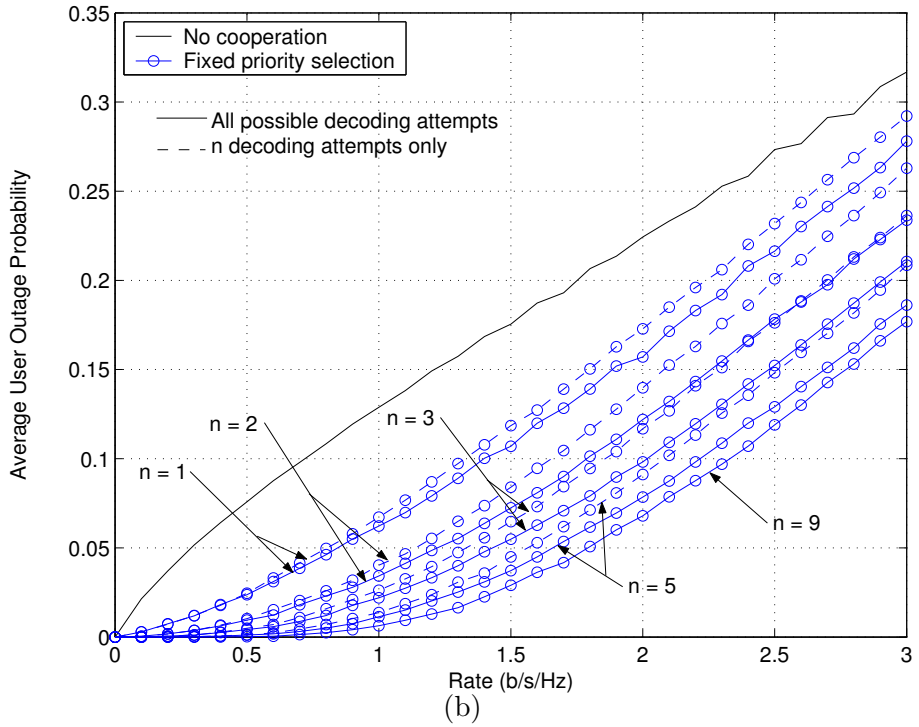

(b)

Figure 6.4. Comparison of fixed priority protocol for various n with $\alpha = 0.75$ and $M = 10$: (a) outage probability vs. average source-destination SNR for rate $R = 1/3$; (b) outage probability vs. rate for average source-destination SNR of 20dB.

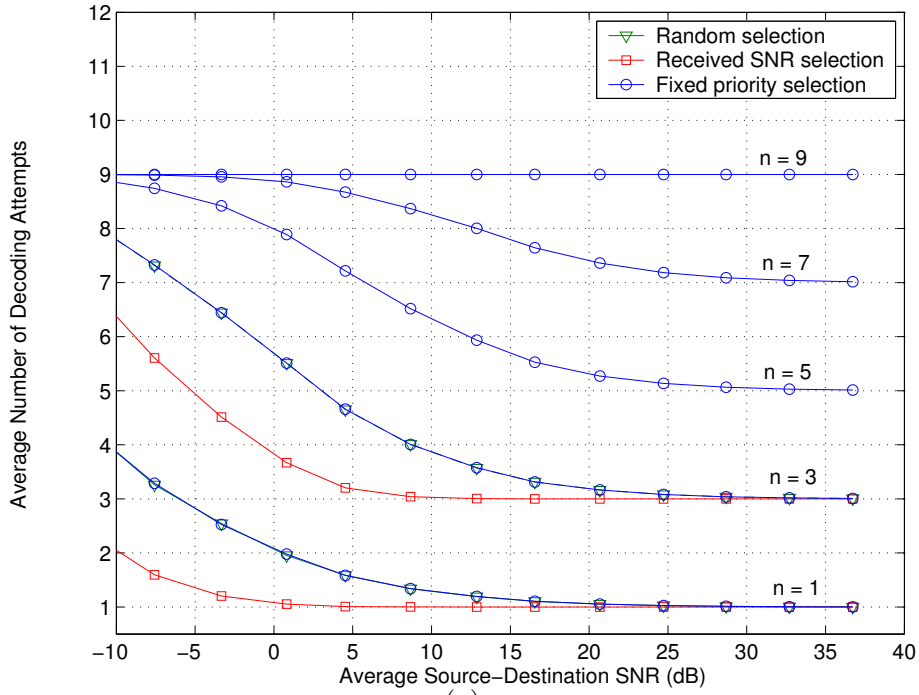

(a)

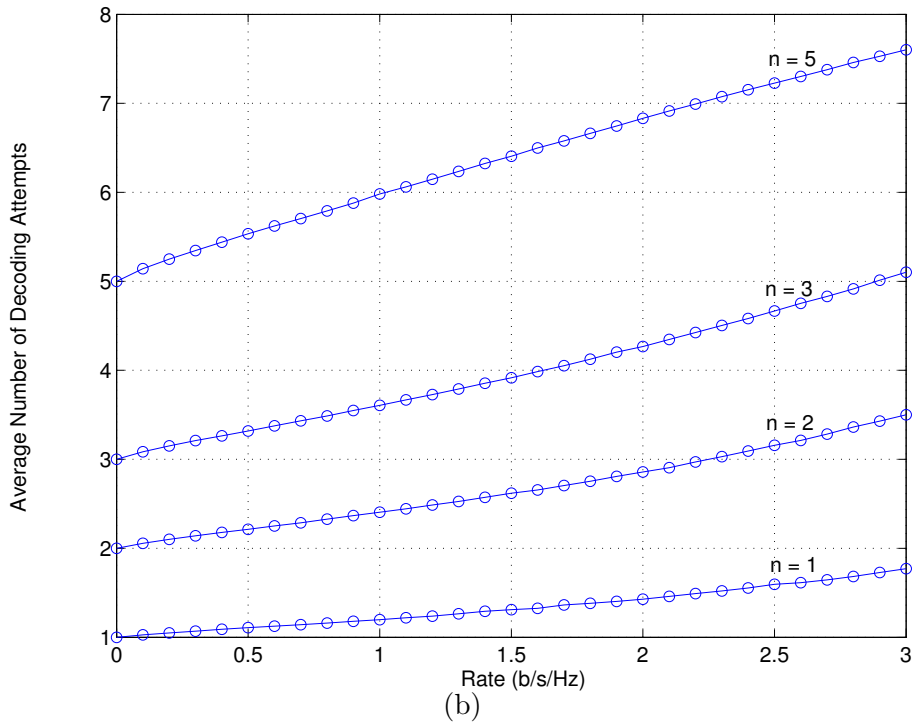

(b)

Figure 6.5. Complexity (average number of decoding attempts per transmit block) for various n, when users make all possible decoding attempts, with $\alpha = 0.75$ and $M = 10$: (a) complexity vs. average source-destination SNR for rate $R = 1/3$ (for simplicity only the fixed priority protocol is shown for $n > 3$); (b) complexity vs. rate of fixed priority protocol with average source-destination SNR of 20dB.

For example, in Figure 6.4(a), $n = 9$ (the maximum n value) provides an additional 10dB gain over $n = 1$ for outage probability 10^{-2}. Setting $n = 5$ provides roughly 85% of this additional gain, with 30%-45% less complexity (depending on whether users make all possible decoding attempts, or only n attempts).

In the low rate regime, characterized by Figure 6.4(a), we see that there is little difference in performance when a user makes n decoding attempts only vs. all possible attempts. For outage probability of 10^{-2}, the gain with n attempts only is within roughly 0.5dB of that given by making all possible attempts for all the n values. As the SNR increases, the performance of the two cases converges, since, as shown in Figure 6.5(a), with all possible decoding attempts the average number of attempts converges to n. Thus, for low rates the complexity vs. performance tradeoff favors each user making only n decoding attempts in each transmit block.

At higher rates, shown in Figure 6.4(b), the outage probability at a given rate is simply determined by the average number of decoding attempts, regardless of whether a user makes all possible attempts, or n attempts only. For example, the outage probabilities for $n = 2$ with all possible decoding attempts and for $n = 3$ with n attempts only are roughly equal for rates around 2.5 b/s/Hz. We see from Figure 6.5(b) that this corresponds to the rates for which the average number of decoding attempts with $n = 2$ is close to 3.

6.2.4 Practical Issues

To enable optimal combining at User i's destination of second-frame transmissions by multiple partners, the partners can transmit in their own multiple-access channels, allowing separate detection. The partners would have to include an additional header in the second frame to inform the destination that they are transmitting for User i. This header would need error protection, which in turn leads to a tradeoff between

the additional overhead imposed and the performance gain compared with a non-cooperative system. Examination of this tradeoff is beyond the scope of this work.

Alternatively, the partners can avoid the need for additional headers by transmitting in User i's multiple-access channel in the second frame. Two or more users attempting to transmit in the same multiple-access channel leads to implementation issues similar to those discussed in Section 4.1.2 for two-user space-time cooperation. In the case of CDMA, the partners are transmitting with User i's spreading code, and their transmissions can be resolved and coherently combined at the destination using RAKE fingers provided that they are not exactly chip-synchronized. This method was first suggested by Sendonaris, Erkip, and Aazhang [52, 53] for their CDMA-based uncoded two-user cooperation scheme. To avoid the issue of simultaneous transmission and reception on the same carrier frequency, we can consider that the group of transmitting users is divided into two subgroups, each of which transmits on a different carrier in the first frame. The results in this chapter would thus correspond to each subgroup containing $M-1$ users (e.g., each user has $M-1$ potential partners).

In the case of TDMA or FDMA, a suitable space-time code may be used to achieve full diversity from the partners' transmissions. This has been suggested in Section 4.1.2 for two-user space-time cooperation, and by Laneman and Wornell [42] for a multi-user decode-and-forward protocol. Some preliminary work on suitable space-time codes in this type of environment has been done by El Gamal and Aktas [19]. As noted in Section 4.1.2 and [42], effective use of a space-time code in this context requires that the second-frame transmissions of the partners be synchronized at the symbol level. While certainly non-trivial, progress in this type of synchronization is already being made, as noted in Section 4.1.2; see for example [65] in the context of OFDM systems, and [63] for a TDMA-based system. Detailed treatment of the synchronization issue is beyond the scope of this work.

6.3 Centralized Protocol

In this section, we consider a protocol in which a central node or controller, that maintains some knowledge of all the channels between the users, assigns partners for a given network realization based on optimizing a selected criterion. This type of protocol would be suitable for applications such as cellular networks, in which all communications are supervised by a base station, or other types of networks which are coordinated by a centralized controller or master node. In addition, since this protocol attempts to optimize partner assignment, it provides a bound for the performance of the distributed protocols for a given value of n. Thus, we can evaluate the tradeoff in performance compared with the convenience of a distributed implementation.

6.3.1 Protocol Description

For the purposes of exposition, we consider that each user has one partner ($n = 1$). While the protocol described below can be extended for $n > 1$, this increases the complexity and complicates the decoding process, and thus we consider only $n = 1$ in this work. As the optimality criterion, we consider minimizing the average outage probability over the M transmitting users for a given network realization. As noted in Section 6.1.2, we do not require that partnerships be reciprocal. Figure 6.6 illustrates a situation in which non-reciprocal partner assignment is more desirable. In this example, the best partner for User 1, based on optimizing the selected criterion, is determined to be User 2. However, the channels between the users are such that the best partner for User 2 is actually User 3, rather than User 1.

In our centralized protocol, partners are assigned for a given network realization using the following algorithm (note that this corresponds to Step 3 of the Monte Carlo iteration given in Section 6.1.3):

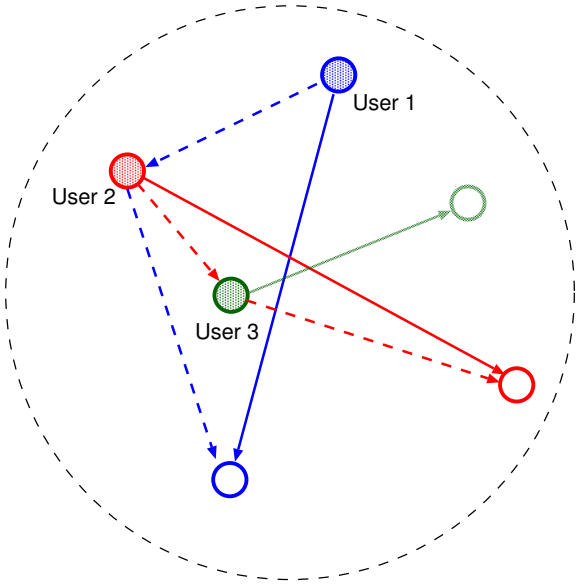

Figure 6.6. Example of a situation in which non-reciprocal partner assignment is more desirable.

1. Initially assign partners randomly, such that each user has exactly one parter, and each user is a partner for only one other user.

2. Compute the average outage probability over the M users for the initial partner assignment using the available channel knowledge.

3. For User i:

   (a) Determine all users with whom User i could potentially exchange partners. It is not possible to exchange with the user for whom User i is already the partner, or with the user who is also User i's current partner.

   (b) For each candidate exchange, compute the average outage probability over the M users using the available channel knowledge.

   (c) Reassign partners according to the candidate exchange that minimizes the average outage probability (if none of the candidate exchanges reduce the average outage probability, do not change the partner assignment).

4. Repeat Step 3 for all M users.

5. If partner reassignment has occurred, repeat Steps 3 and 4. Otherwise, if no exchanges are made in the latest pass through Steps 3 and 4, terminate the algorithm.

The complexity of this algorithm is $O(M^2)$. We consider that the central controller performing partner assignment may have three levels of channel knowledge: (a) no channel knowledge, in which case partner assignment is random (e.g., the above algorithm terminates after Step 1); (b) user locations only are known, thus path loss components are known but shadowing components are not; and (c) user locations and shadowing components for all channels are known.

As stated in Section 6.1.2, if User i's designated partner does not successfully decode User i's first-frame transmission, the partner transmits additional parity for its own data in the second frame. This gives rise to four possible cases for what User i's destination receives in the second frame, as illustrated in Figure 6.7. For purposes of exposition, User j is User i's assigned partner, while User i is the partner for User k. In Case 1, User j successfully decodes User i, and User i successfully decodes User k, so that additional parity for User i is transmitted by User j in the second frame. In Case 2, User j does not successfully decode User i, and User i does not successfully decode User k. Thus, User j does not transmit additional parity for User i, but User i does transmit its own additional parity. In Case 3, User j successfully decodes User i, but User i does not successfully decode User k, resulting in User i's additional parity being transmitted by both Users i and j. Finally, in Case 4 User j does not successfully decode User i, but User i successfully decodes User k. As a result, none of the users transmit additional parity for User i in the second frame. We note that these four cases are analogous to those for two-user coded

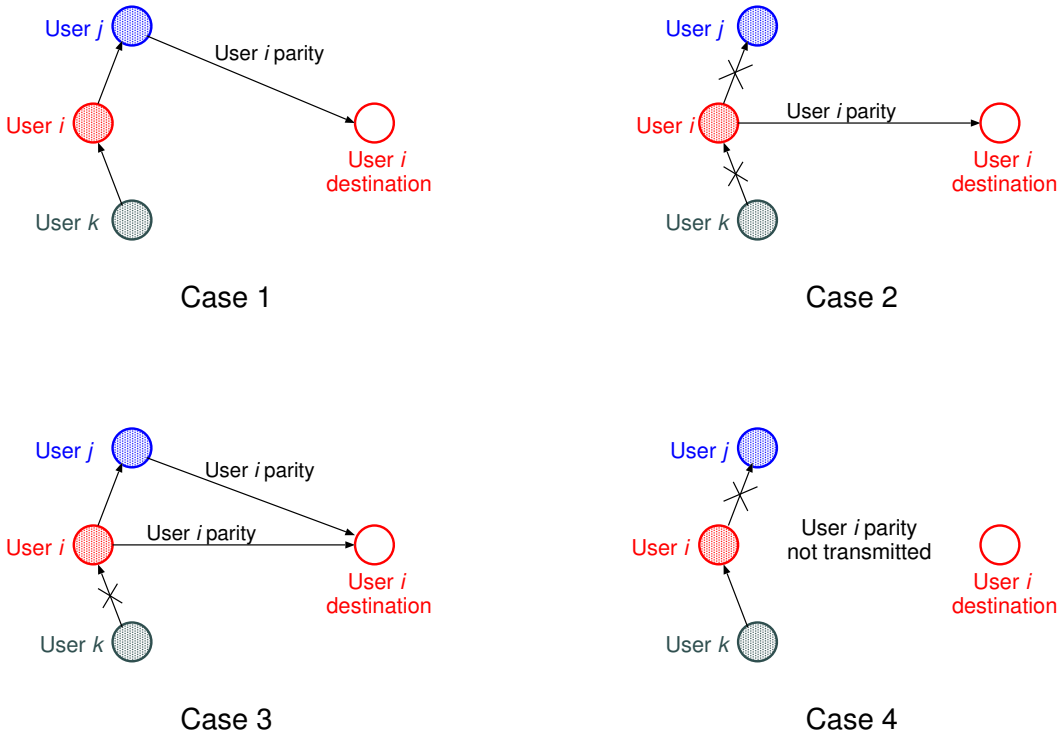

Figure 6.7. Four cases for second-frame transmission of additional parity for User i. In this example, User j is User i's assigned partner, while User i is the partner for User k

cooperation discussed in Chapter 3 (see Section 3.2 and Figure 3.4). Consequently, since the centralized protocol assigns partners *a priori*, for $n = 1$ each user can transmit in its own multiple-access channel in the second frame, and, given the four cases, User i's destination can decode the transmissions using the same methodology as described in Section 3.6.3.

6.3.2 Outage Probability Characterization

In the following analysis, we apply the notational convention of Figure 6.7, denoting User j as User i's partner, and User i as User k's partner. We parameterize the four cases described above by $\Theta \in \{1, 2, 3, 4\}$ and express the corresponding conditional capacities and outage events for each case relative to User i as follows:

- **Case 1 ($\Theta = 1$)**: In this case, Users i and j both correctly decode the rate R/α first-frame transmissions of their respective partners. In an information-theoretic sense, correct decoding corresponds to the following events:

$$\begin{aligned} C_{i,j}(\gamma_{i,j}) &= \log_2(1+\gamma_{i,j}) > R/\alpha \\ C_{k,i}(\gamma_{k,i}) &= \log_2(1+\gamma_{k,i}) > R/\alpha, \end{aligned} \tag{6.15}$$

  In the second frame User j transmits additional parity for User i. As with the distributed protocols, the first and second frame transmissions of User i's coded symbols can be viewed as parallel channels, or equivalently, as time sharing between channels. Thus, we can write the outage event for User i as

$$C_{1,d}(\gamma_{i,d}, \gamma_{j,d}|\Theta = 1) = \alpha \log_2(1+\gamma_{i,d}) + (1-\alpha)\log_2(1+\gamma_{j,d}) < R \tag{6.16}$$

  where again the subscript d denotes User i's destination.

- **Case 2 ($\Theta = 2$)**: In this case, neither User i nor j correctly decodes its respective partner. This corresponds to the events,

$$\begin{aligned} C_{i,j}(\gamma_{i,j}) &= \log_2(1+\gamma_{i,j}) < R/\alpha \\ C_{k,i}(\gamma_{k,i}) &= \log_2(1+\gamma_{k,i}) < R/\alpha. \end{aligned} \tag{6.17}$$

  In the second frame, User i transmits its own additional parity symbols, which corresponds to the outage event

$$C_{i,d}(\gamma_{i,d}|\Theta = 2) = \log_2(1+\gamma_{i,d}) < R \tag{6.18}$$

- **Case 3 ($\Theta = 3$)**: In this case, User j correctly decodes User i, but User i does not correctly decode User k. This corresponds to the events

$$\begin{aligned} C_{i,j}(\gamma_{i,j}) &= \log_2(1+\gamma_{i,j}) > R/\alpha \\ C_{k,i}(\gamma_{k,i}) &= \log_2(1+\gamma_{k,i}) < R/\alpha. \end{aligned} \tag{6.19}$$

  In the second frame, User i's additional parity is transmitted by both User j and User i. The corresponding outage event is

$$C_{i,d}(\gamma_{i,d}, \gamma_{j,d}|\Theta = 3) = \alpha \log_2(1+\gamma_{i,d}) + (1-\alpha)\log_2(1+\gamma_{i,d}+\gamma_{j,d}) < R \tag{6.20}$$

- **Case 4 ($\Theta = 4$)**: In this case, User j does not correctly decode User i, but User i does correctly decode User k. The corresponding events are

$$\begin{aligned} C_{i,j}(\gamma_{i,j}) &= \log_2(1+\gamma_{i,j}) < R/\alpha \\ C_{k,i}(\gamma_{k,i}) &= \log_2(1+\gamma_{k,i}) > R/\alpha, \end{aligned} \tag{6.21}$$

  In the second frame, no additional parity symbols for User i are transmitted, resulting in the outage event

$$C_{i,d}(\gamma_{i,d}|\Theta = 4) = \log_2(1+\gamma_{i,d}) < R/\alpha \tag{6.22}$$

Since the four cases are disjoint, and $\{\gamma_{i,j}, \gamma_{k,i}, \gamma_{i,d}, \gamma_{i,d}\}$ are all mutually independent, we can write the overall outage probability for User i as

$$\begin{aligned} P_{out,i} = {} & \Pr\{\gamma_{i,j} > 2^{R/\alpha} - 1\} \cdot \Pr\{\gamma_{k,i} > 2^{R/\alpha} - 1\} \\ & \quad \cdot \Pr\{(1+\gamma_{i,d})^{\alpha}(1+\gamma_{j,d})^{1-\alpha} < 2^R\} \\ & + \Pr\{\gamma_{i,j} < 2^{R/\alpha} - 1\} \cdot \Pr\{\gamma_{k,i} < 2^{R/\alpha} - 1\} \cdot \Pr\{\gamma_{i,d} < 2^R - 1\} \\ & + \Pr\{\gamma_{i,j} > 2^{R/\alpha} - 1\} \cdot \Pr\{\gamma_{k,i} < 2^{R/\alpha} - 1\} \\ & \quad \cdot \Pr\{(1+\gamma_{i,d})^{\alpha}(1+\gamma_{i,d}+\gamma_{j,d})^{1-\alpha} < 2^R\} \\ & + \Pr\{\gamma_{i,j} < 2^{R/\alpha} - 1\} \cdot \Pr\{\gamma_{k,i} > 2^{R/\alpha} - 1\} \cdot \Pr\{\gamma_{i,d} < 2^{R/\alpha} - 1\}. \end{aligned} \tag{6.23}$$

The form of (6.23) is analogous to the outage probability expression for two-user reciprocal cooperation derived in Section 5.1.1, equation (5.12). As a result, based on Section 5.1.1, equations (5.13)–(5.15), and Appendix A, we can evaluate (6.23) for the case of Rayleigh fading as

$$\begin{aligned} P_{out,i} = {} & \exp\left(\frac{1-2^{R/\alpha}}{\Gamma_{k,i}}\right) \\ & \quad \cdot \left[1 - \exp\left(\frac{1-2^{R/\alpha}}{\Gamma_{i,d}}\right) - \exp\left(\frac{1-2^{R/\alpha}}{\Gamma_{i,j}}\right) \cdot \Psi_1(\Gamma_{i,d}, \Gamma_{j,d}, R, \alpha)\right] \\ & + \left[1 - \exp\left(\frac{1-2^{R/\alpha}}{\Gamma_{k,i}}\right)\right] \\ & \quad \cdot \left[1 - \exp\left(\frac{1-2^{R}}{\Gamma_{i,d}}\right) - \exp\left(\frac{1-2^{R/\alpha}}{\Gamma_{i,j}}\right) \cdot \Psi_2(\Gamma_{i,d}, \Gamma_{j,d}, R, \alpha)\right] \end{aligned} \tag{6.24}$$

where

$$\begin{aligned}
\Psi_1(\Gamma_{i,d}, \Gamma_{j,d}, R, \alpha) &= \int_0^{2^{R/\alpha}-1} \frac{1}{\Gamma_{i,d}} \exp\left(-\frac{\gamma_{i,d}}{\Gamma_{i,d}} - \frac{a}{\Gamma_{j,d}}\right) d\gamma_{i,d} \\
\Psi_2(\Gamma_{i,d}, \Gamma_{j,d}, R, \alpha) &= \int_0^{2^{R}-1} \frac{1}{\Gamma_{i,d}} \exp\left(-\frac{\gamma_{i,d}}{\Gamma_{i,d}} - \frac{b}{\Gamma_{j,d}}\right) d\gamma_{i,d} \\
a &= \frac{2^{R/(1-\alpha)}}{(1+\gamma_{i,d})^{\alpha/(1-\alpha)}} - 1 \\
b &= \frac{2^{R/(1-\alpha)}}{(1+\gamma_{i,d})^{\alpha/(1-\alpha)}} - 1 - \gamma_{i,d}.
\end{aligned} \tag{6.25}$$

We use (6.24) in the Monte Carlo simulation to evaluate the performance of the centralized protocol. Note that the average SNR values $\Gamma_{i,j}$ used in (6.24) for Steps 2 and 3 of the partner selection algorithm (Section 6.3.1) depend on the level of channel knowledge. If only the user locations are known, then $\Gamma_{i,j}$ does not contain the shadowing component. If all the shadowing components are known, then $\Gamma_{i,j}$ is as defined in (6.2).

To determine the achieved diversity, we again re-parameterize $\Gamma_{i,j}$ as shown in (6.9), and obtain outage probability as a function of $1/\Gamma_T$ by expanding the exponential terms using the equivalent Taylor's series representation. For the centralized protocol, this is analogous to the procedure in Section 5.1.2 and Appendix B, and we obtain the following result:

$$P_{out,i} = \frac{1}{\Gamma_T^2} \cdot \left[\frac{(2^{R/\alpha}-1)^2}{\Gamma_{i,d}\Gamma_{i,j}} + \frac{\Lambda(R,\alpha)}{\Gamma_{i,d}\Gamma_{j,d}}\right] + O\left(\frac{1}{\Gamma_T^3}\right), \tag{6.26}$$

where

$$\Lambda(R,\alpha) = \begin{cases} 2^{R/(1-\alpha)}\left(\frac{1-\alpha}{1-2\alpha}\right)\left(2^{R(1-2\alpha)/\alpha(1-\alpha)}-1\right) - 2^{R/\alpha} + 1 & \alpha \neq 1/2 \\ R \cdot 2^{2R+1} \cdot \ln 2 - 2^{2R} + 1 & \alpha = 1/2 \end{cases}. \tag{6.27}$$

Equation (6.26) is thus analogous to equation (5.20) in Section 5.1.2, and we see that, as $\Gamma_T \to \infty$, the outage probability is a function of $1/\Gamma_T^2$. This shows that the centralized protocol achieves full diversity, in this case diversity order two for $n = 1$.

6.3.3 Results and Discussion

Figure 6.8 compares the outage probability for the centralized protocol with different levels of channel knowledge and different values of M. We see that the centralized protocol does achieve full diversity regardless of the level of channel knowledge. Clearly, more channel information allows for better partner assignment, and in turn better performance. In the low-rate regime, illustrated in Figure 6.8(a) with $R = 1/3$, random partner assignment provides a gain of roughly 8dB at outage probability 10^{-2}. While this is certainly not insignificant, knowledge of the user locations gives an additional gain of 3dB over random partner assignment for $M = 10$. Full channel knowledge (e.g., knowledge of all user locations and shadowing components of each link) provides an additional gain of 8dB. Figure 6.8(b) shows that the relative performance for different levels of channel knowledge is similar for higher rates.

With regard to the number of users M, Figure 6.8 shows that the outage probability with random partner assignment is unaffected by the value of M, which makes sense since in this case partners are located randomly according to a distribution that does not depend on M. When the user locations are known, increasing M provides a small improvement, while with full channel knowledge the improvement is much more significant. In this case, increasing the number possible partners to choose from clearly allows for a better partner assignment, and thus better performance, at the expense of increased complexity for the partner assignment algorithm.

Figure 6.9 compares the centralized protocol with $n = 1$ to the fixed priority selection distributed protocol for various n values. For purposes of comparison, the number of users M is fixed at 10, and curves for fixed priority selection correspond to users making n decoding attempts only. Not surprisingly, we see that the fixed priority protocol with $n = 1$ is equivalent to the centralized protocol with no channel knowledge, e.g. random partner assignment. When the centralized protocol uses

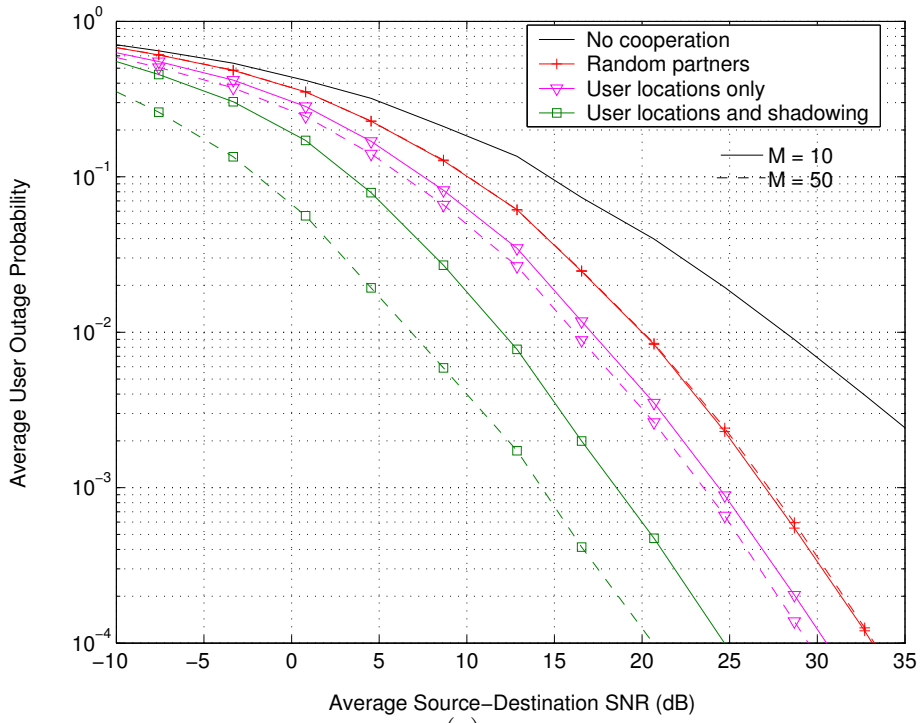

(a)

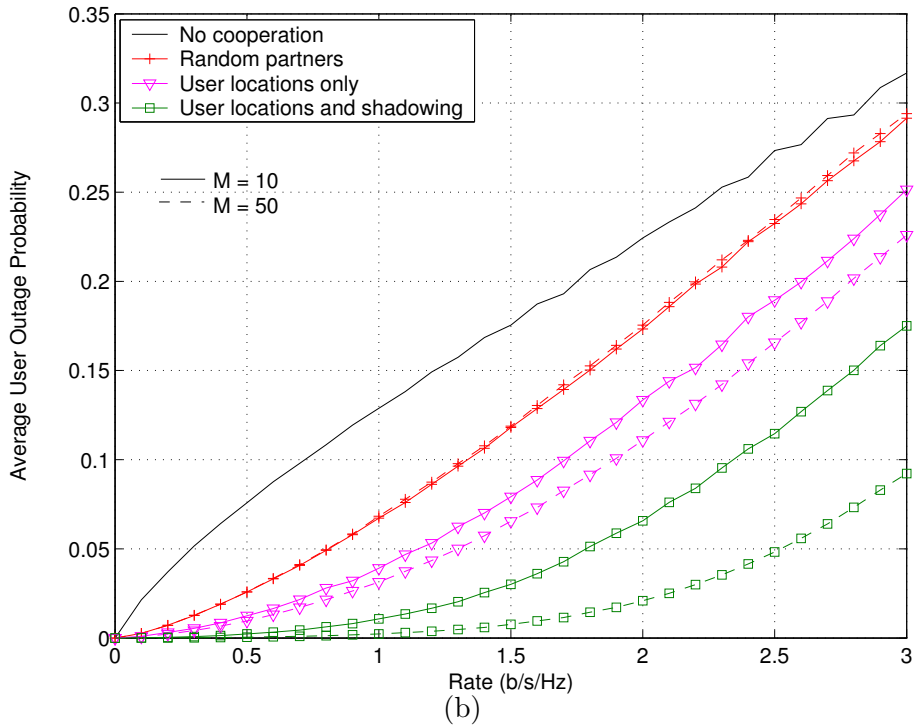

(b)

Figure 6.8. Centralized protocol for $\alpha = 0.75$ and $M = 10$ and 50: (a) outage probability vs. average source-destination SNR for rate $R = 1/3$; (b) outage probability vs. rate for average source-destination SNR of 20dB.

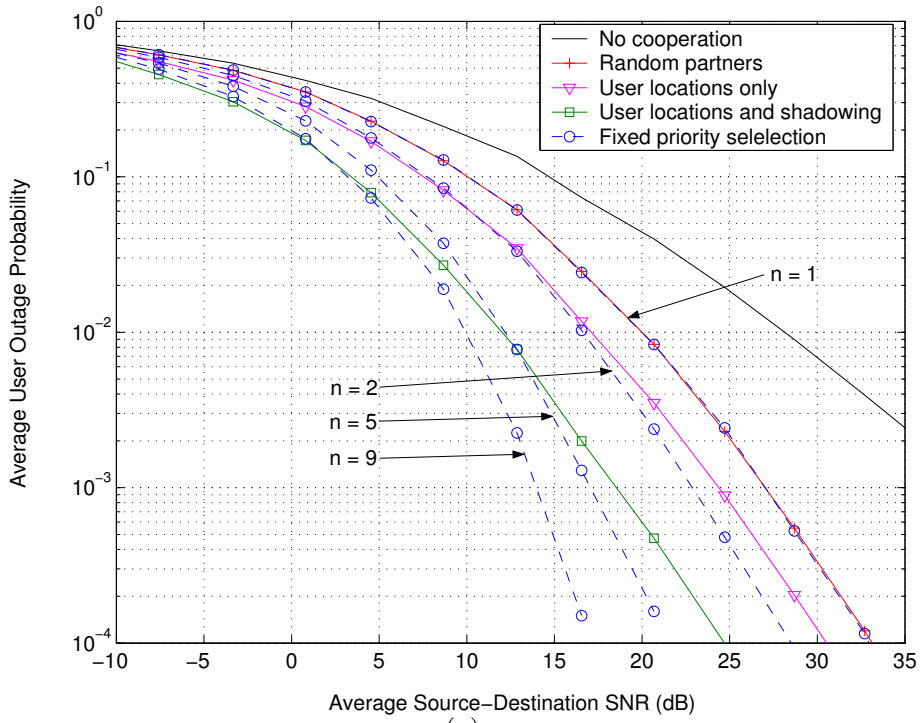

(a)

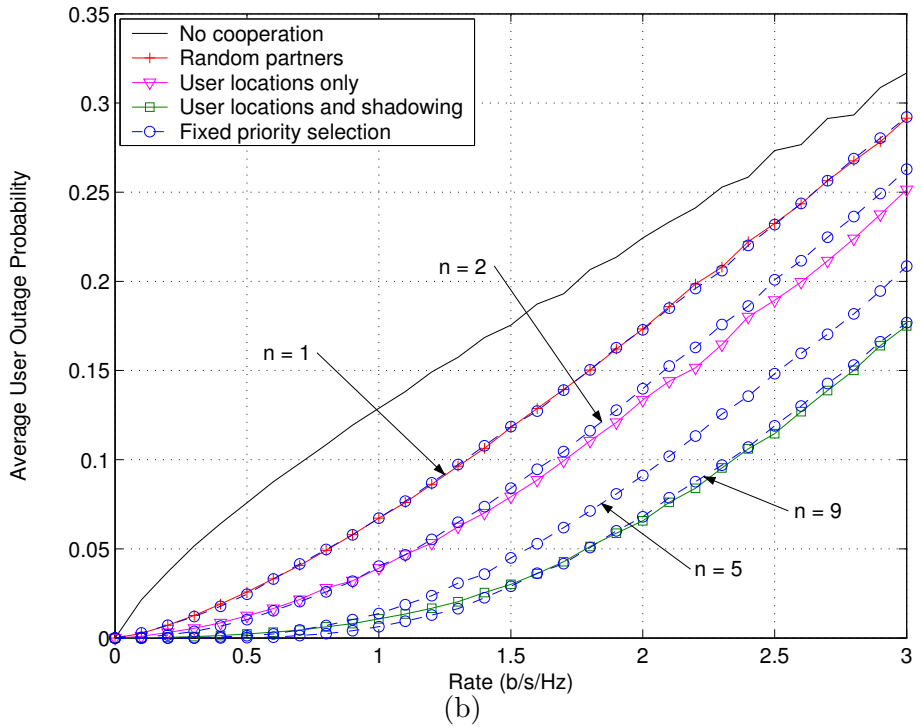

(b)

Figure 6.9. Comparison of centralized protocol and fixed priority selection distributed protocol (n decoding attempts only) for $\alpha = 0.75$ and $M = 10$: (a) outage probability vs. average source-destination SNR for rate $R = 1/3$; (b) outage probability vs. rate for average source-destination SNR of 20dB.

some level of channel knowledge, we see that the distributed protocol can still achieve comparable performance with increased complexity (larger n, or more decoding attempts) for the individual users. There is no single answer to which protocol is best, as the particular application will dictate whether a distributed or centralized protocol is preferred. These results show that both types of protocols are capable of achieving similar performance with appropriate parameter selection.

6.4 Chapter Summary

In this chapter, we extend the two-user coded cooperation framework developed in Chapters 3 through 5 to a multi-user wireless network. We consider distributed protocols for partner selection, in which users act autonomously in deciding which other user or users to cooperate with for each transmitted block. We examine the outage probability for these protocols, demonstrating that full diversity in the number of cooperating users is achieved, as well as significant improvement compared to a non-cooperative system. In addition, we explore the performance vs. complexity tradeoff, where complexity is characterized as the number of other users that each user attempts to cooperate with in each transmitted block. We also propose a centralized algorithm that assigns partners to minimize the average outage probability over all the users, based on some knowledge all the channels between the users. Outage probability results show again that full diversity is achieved, as well as significant gains compared to no cooperation.

In our network model we consider that each transmitting user has a unique destination node at another random location in the network for each transmit block. We adopt this convention in order to have a general model the represents wireless ad hoc networks. However, we note that the results would not change significantly if all users had a common destination located at the center of the network. This

type of model would represent a cellular system, or an ad hoc network that employs clustering. In addition, all the examples presented in this chapter use degree of cooperation $\alpha = 0.75$, which generally gives the best performance based on empirical observations. While it is difficult to obtain a general closed-form expression for the optimal value of α, for any given set of conditions the optimal α may be determined through iteration, similar to the discussion in Section 5.1.1.

The results of this chapter are significant in that they demonstrate that coded cooperation can be implemented in a multi-user environment, and that it can provide noticeable gains in performance. However, there are many more issues related to user cooperation in multi-user wireless networks, of which the results presented here have merely scratched the surface. Chapter 7 summarizes the contributions presented in this and the preceding chapters, and then discusses possible future directions for research on these issues and others related to coded cooperation.

CHAPTER 7
CONCLUSIONS AND FUTURE WORK

In this final chapter, we summarize the contributions of the work presented in this dissertation. In addition, we discuss several avenues for future research in the area of cooperative communications.

7.1 Contributions of this Research

Previously proposed cooperation techniques involve a user repeating the symbols transmitted by its partner. This repetition typically takes one of two forms. The user can simply retransmit, or forward, the noisy analog signal received from the partner. This technique is generally known as amplify-and-forward. Alternatively, the user can attempt to detect each symbol transmitted by the partner, and then forward its estimate on to the destination. This method is referred to as detect-and-forward. With both of these methods, improved diversity relative to non-cooperative direct transmission is achieved by each symbol from a given user being transmitted through multiple independent fading paths.

From a channel coding point of view, repetition coding is not the most efficient use of the available bandwidth. In this dissertation, we present a new framework for cooperative communications, which we call coded cooperation. In this framework, cooperative signaling is integrated with channel coding in the following way. Each user attempts to decode its partner's transmission. If the decoding is successful (determined through error checking via, i.e., an outer CRC code), the user transmits additional parity symbols for its partner according to some overall coding scheme. Otherwise, the user transmits additional parity for its own data. A key benefit of

this framework is that coded cooperation automatically, with no feedback between partners, reverts to non-cooperative transmission when the inter-user channel is poor. This results in a graceful degradation behavior, such that under worst case conditions (i.e., very low SNR for the channel between partners) the performance is never worse than for non-cooperative transmission in a quasi-static fading environment. This is a notable improvement over previous user cooperation methods.

The coded cooperation framework is quite flexible in the sense that it can be implemented with either block or convolutional codes, and the additional parity transmitted by the partner may be obtained through the use of punctured codes, product codes, or other forms of concatenation. In this work we have given examples of coded cooperation using RCPC codes (Chapter 3) and turbo codes (Chapter 4). In addition, the framework allows for variation of the degree of cooperation between partners, which provides for adaptability to various channel conditions.

Coded cooperation does achieve full diversity; however, it does so in a slightly less direct way than the repetition-based methods. Although each symbol transmitted by a user does not travel through multiple fading paths, the nature of channel coding is such that a given information symbol is correlated with multiple coded symbols. These coded symbols are divided between user and partner by the coded cooperation framework, and travel through multiple independent fading paths to the destination, thus effectively providing diversity for the information symbol with which they are correlated.

To characterize the performance of coded cooperation, in Chapter 3 we derive tight bounds for bit and block error rates, for both quasi-static and fast-fading scenarios. We do this by first deriving appropriate pairwise error probability expressions for coded cooperation, and then applying known union-bounding techniques. Numerical results demonstrate that coded cooperation provides significant improvement in

error rate performance over a comparable non-cooperative system. In particular, two key results emerge for the quasi-static fading case that have not appeared in previous work. First, both of the cooperating users experience some improvement even when the average SNR of the inter-user channel is significantly less (i.e. 10-20dB lower) than the average SNR for the user uplink channels. Second, both users improve significantly even when one has an average uplink SNR that is much greater (i.e., 10-20dB higher) than the other. Both of these results have important practical implications. The first result illustrates that, while ideally one would want to assign partners intelligently to maximize performance, coded cooperation nevertheless exhibits a degree of robustness to the quality of the inter-user channel. The second result shows that even a user with a very good channel to its destination has a strong motivation to cooperate, and can benefit by sharing its resources with other users.

In Chapter 4 we present an extension to the coded cooperation framework designed to improve the performance in a fast fading environment, e.g., when the fading coefficients are i.i.d for each transmitted symbol. This extension, which we call *space-time cooperation*, borrows ideas from space-time coding and MIMO system, and operates as follows. In the second frame, instead of transmitting additional parity only for its partner as in coded cooperation, a user divides its power and transmits additional parity for both its partner (in the partner's multiple-access channel) and for itself (in its own multiple-access channel). We extend the error rate analysis from Chapter 3 to develop tight bounds for bit and block error rate for space-time cooperation. Numerical results confirm that space-time cooperation does indeed provide better performance than coded cooperation in fast fading when the two user uplink channels have unequal average SNR. With coded cooperation, the user with the better uplink channel sacrifices its performance in order to help its partner. With space-time cooperation, *both* users have improved performance.

In Chapter 5 we develop information-theoretic bounds for the coded cooperation framework. In particular, since cooperation provides the most improvement for a quasi-static fading environment, we develop outage probability expressions for the case of a Rayleigh fading distribution. These results are important for three reasons. First, outage probability is a performance metric that is independent of any particular coding scheme, and is also a lower bound to block error rate, a practical performance measure. Second, the outage probability results show that coded cooperation does achieve full diversity; i.e., diversity order two for two cooperating users. Third, with outage probability we can examine the behavior of coded cooperation for different rates much more easily than we can with bit or block error rate.

In this analysis we consider both coded cooperation and space-time cooperation, in order to determine if there are any advantages to space-time cooperation's power splitting in the second frame. Numerical results show that in general coded cooperation performs slightly better than space-time cooperation for quasi-static fading; however, space-time cooperation does exhibit more robustness when the channels between the users are independent (the instantaneous SNR are uncorrelated). The results also show that coded cooperation performs better than repetition-based cooperation methods. In particular, outage probability vs. rate curves highlight the inefficiency of repetition-based methods, especially for higher rates.

Finally, in Chapter 6 we extend the coded cooperation framework to a multi-user network scenario. We consider M users randomly distributed within a finite area, and propose distributed protocols in which each user can individually and independently decide with whom to cooperate at any given time. These protocols are general in that a user can choose to cooperate with multiple other users (up to $M-1$) simultaneously, which presents a diversity vs. complexity tradeoff that we examine. We compare the performance of these protocols based on average outage probability

of an arbitrary user in the network, and show that full diversity can be achieved, as well as significant gains vs. non-cooperative transmission. In addition, we propose a centralized algorithm that, using knowledge of all the channels between the users, assigns partners based on minimizing the average outage probability over all the users. This algorithm represents a lower bound on performance for the distributed protocols (which primarily have a view toward wireless ad hoc networks). This algorithm may also be useful in cellular and other networks that have some centralized control.

Given the rapidly growing importance of wireless ad hoc networks, sensor networks, etc., in the digital world of tomorrow, the results of Chapter 6 are particularly relevant. In a cellular network, a base station with multiple antennas can provide transmit diversity in the downlink and receive diversity in the uplink. While the results presented here show that coded cooperation can offer significant performance improvements for cellular systems, we believe that cooperative communication in general, and coded cooperation in particular, can have the greatest impact on wireless ad hoc networks. The results of Chapter 6 demonstrate that coded cooperation can be implemented in this environment, and that it can provide significant performance improvements.

7.2 Future Work

While several key results for cooperative communication have already been obtained, many more issues remain to be addressed, and many possible directions for future research exist.

Throughout this dissertation, we have considered the case of flat Rayleigh fading. We have done this primarily to highlight the spatial diversity provided by coded cooperation. While we believe that our results extend the the case of frequency-selective channels, further investigation is needed to better characterize how these

two forms of diversity interact. It would also be interesting to extend the results and examine the performance of coded cooperation for other fading distributions, such as Ricean and Nakagami fading.

Also in this work we consider that the users transmit with equal and constant power, equal rate, and with a constant modulation and coding scheme. A large body of work exists, going back more than thirty years, on improving the capacity and performance of conventional non-cooperative wireless systems through real-time feedback and adaptation of transmit power [27, 21, 13], information rate [14], modulation scheme [69], coding scheme and rate [68], and various combinations of these parameters [29, 20, 3, 12]. In the context of cooperative communication, the scheme of Sendonaris, Erkip, and Aazhang [51, 52, 53] allows users to vary their power between cooperative and non-cooperative periods to achieve the best overall rate. Recently, a similar power adaptation idea has been proposed for amplify-and-forward cooperation [4]. Thus, a rich area for future research would be to consider for coded cooperation the adaptation of transmit power, both the overall power (subject to an average power constraint), as well as the relative power allocations between the first and second frames. Similarly, one could also consider adapting the cooperation level (e.g., the relative rates allocated to the first and second frames), information rate, modulation scheme, and coding rate/scheme. These parameters could be considered individually, but even more interesting might be the joint adaptation of some or all of these parameters. In the context of multi-user systems, it may be possible to develop adaptive scheduling algorithms based on the idea of multi-user diversity [37, 66], except that the unit of consideration could be a cooperating pair or group of users, rather than a single user.

Somewhat related is the issue of power control. In CDMA-based systems, for example, power control is critical in order to manage the near-far effect, minimize

interference between users, and maintain the desired quality of service for all users. Therefore, power control schemes that work effectively in the context of cooperative communication have great practical importance. Some preliminary results [32] suggest that conventional power control (e.g. equalizing the received SNR for all users) is not an ideal strategy in a cooperative system, indicating that more work in this area is warranted.

Examples in this work apply standard channel coding schemes designed for non-cooperative communication to the coded cooperation framework. Indeed, one of the advantages of coded cooperation is that it works very well with existing channel codes. Nevertheless, an interesting open problem is the development of design criteria specifically for codes that optimize the performance of coded cooperation.

A related issue is the use of space-time codes with coded cooperation. We have suggested this in Chapter 4 for space-time cooperation in a TDMA or FDMA system, and in Chapter 6 in the context of cooperation in multi-user networks (as has [42]). In [57] space-time codes are applied to a scenario in which the cooperating users each have multiple antennas. Despite this preliminary work, the interaction of user cooperation and space-time coding, and the design of space-time codes especially suitable for the cooperative scenario, remain to be fully explored.

Finally, the results in this dissertation have merely scratched the surface of the issues related to user cooperation in multi-user wireless networks. For example, a source-destination pair in our network model of Chapter 6 may be viewed as one hop in a routing path that has been determined through some higher-layer mulithop routing protocol (see for example [61] and references therein). Alternatively, user cooperation itself may be viewed as a mulithop routing protocol that provides two hops from a source to its final destination. The relationship between user cooperation and network scheduling and routing merits further exploration. A result of such work

could be algorithms and protocols that jointly allocate partners or cooperative groups and determine routing paths. Given that wireless ad hoc networks seem to offer the best opportunities for exploiting the benefits of user cooperation, research along these lines may well prove particularly fruitful for the future of cooperative communication.

APPENDICES

APPENDIX A

OUTAGE PROBABILITY EXPRESSIONS

Consider the first integral in (5.13). We can rewrite the constraint A as

$$\gamma_{2,d} < \frac{2^{R/(1-\alpha)}}{(1+\gamma_{1,d})^{\alpha/(1-\alpha)}} - 1 = a. \tag{A.1}$$

Since $\gamma_{2,d}$ is always greater than zero, this in turn leads to

$$\begin{aligned} (1+\gamma_{1,d})^{\alpha/(1-\alpha)} &< 2^{R/(1-\alpha)} \\ \gamma_{1,d} &< 2^{R/\alpha} - 1. \end{aligned} \tag{A.2}$$

We can now rewrite the first integral in (5.13) as

$$\begin{aligned} &\iint_A \Phi(\gamma_{1,d}, \gamma_{2,d}, \Gamma_{1,d}, \Gamma_{2,d}) d\gamma_{1,d} d\gamma_{2,d} = \\ &\qquad \int_0^{2^{R/\alpha}-1} \frac{1}{\Gamma_{1,d}} \exp\left(-\frac{\gamma_{1,d}}{\Gamma_{1,d}}\right) \left[\int_0^a \frac{1}{\Gamma_{2,d}} \exp\left(-\frac{\gamma_{2,d}}{\Gamma_{2,d}}\right) d\gamma_{2,d}\right] d\gamma_{1,d} \\ &= \int_0^{2^{R/\alpha}-1} \frac{1}{\Gamma_{1,d}} \exp\left(-\frac{\gamma_{1,d}}{\Gamma_{1,d}}\right) \left[1 - \exp\left(-\frac{a}{\Gamma_{2,d}}\right)\right] d\gamma_{1,d} \\ &= \left[1 - \exp\left(\frac{1-2^{R/\alpha}}{\Gamma_{1,d}}\right)\right] - \int_0^{2^{R/\alpha}-1} \frac{1}{\Gamma_{1,d}} \exp\left(-\frac{\gamma_{1,d}}{\Gamma_{1,d}} - \frac{a}{\Gamma_{2,d}}\right) d\gamma_{1,d}. \end{aligned} \tag{A.3}$$

Next, consider the second integral in (5.13). We can rewrite the constraint B as

$$\gamma_{2,d} < \frac{2^{R/(1-\alpha)}}{(1+\gamma_{1,d})^{\alpha/(1-\alpha)}} - 1 - \gamma_{1,d} = b. \tag{A.4}$$

Since $\gamma_{2,d}$ is always greater than zero, this in turn leads to

$$\begin{aligned} \frac{2^{R/(1-\alpha)}}{(1+\gamma_{1,d})^{\alpha/(1-\alpha)}} &> (1+\gamma_{1,d}) \\ \gamma_{1,d} &< 2^R - 1. \end{aligned} \tag{A.5}$$

We can now rewrite the second integral in (5.13) as

$$\begin{aligned}\iint_B \Phi(\gamma_{1,d},\gamma_{2,d},\Gamma_{1,d},\Gamma_{2,d})d\gamma_{1,d}d\gamma_{2,d} = \\ &\int_0^{2^R-1} \frac{1}{\Gamma_{1,d}} \exp\left(-\frac{\gamma_{1,d}}{\Gamma_{1,d}}\right)\left[\int_0^b \frac{1}{\Gamma_{2,d}} \exp\left(-\frac{\gamma_{2,d}}{\Gamma_{2,d}}\right) d\gamma_{2,d}\right] d\gamma_{1,d} \\ &= \int_0^{2^R-1} \frac{1}{\Gamma_{1,d}} \exp\left(-\frac{\gamma_{1,d}}{\Gamma_{1,d}}\right)\left[1-\exp\left(-\frac{b}{\Gamma_{2,d}}\right)\right] d\gamma_{1,d} \\ &= \left[1-\exp\left(\frac{1-2^R}{\Gamma_{1,d}}\right)\right] - \int_0^{2^R-1} \frac{1}{\Gamma_{1,d}} \exp\left(-\frac{\gamma_{1,d}}{\Gamma_{1,d}} - \frac{b}{\Gamma_{2,d}}\right) d\gamma_{1,d}.\end{aligned} \tag{A.6}$$

We see that the second terms of (A.3) and (A.6) are Ψ_1 and Ψ_2 respectively, defined in (5.16). Equation (5.15) is thus obtained by substituting (A.3) and (A.6) into (5.13) and factoring like terms. We can apply similar techniques to obtain (5.18), the corresponding expression for reciprocal inter-user channels.

APPENDIX B
ASYMPTOTIC ANALYSIS OF OUTAGE PROBABILITY

The Taylor's series representation of $\exp(x)$ is given by [11, p. 299]

$$\exp(x) = 1 + x + \frac{x^2}{2!} + \frac{x^3}{3!} + \frac{x^4}{4!} + \dots \tag{B.1}$$

Thus, for terms of the form $\exp(\frac{1-2^r}{\Gamma_T \Gamma_{i,j}})$ and $1 - \exp(\frac{1-2^r}{\Gamma_T \Gamma_{i,j}})$ ($r = R$ or R/α), we can write

$$\begin{aligned} \exp\left(\frac{1-2^r}{\Gamma_T\Gamma_{i,j}}\right) &= 1 - \frac{2^r-1}{\Gamma_T\Gamma_{i,j}} + \frac{(2^r-1)^2}{2\Gamma_T^2\Gamma_{i,j}^2} + O\left(\frac{1}{\Gamma_T^3}\right) \\ 1 - \exp\left(\frac{1-2^r}{\Gamma_T\Gamma_{i,j}}\right) &= \frac{2^r-1}{\Gamma_T\Gamma_{i,j}} - \frac{(2^r-1)^2}{2\Gamma_T^2\Gamma_{i,j}^2} + O\left(\frac{1}{\Gamma_T^3}\right). \end{aligned} \tag{B.2}$$

Note that for this analysis, since we expect to have diversity order two for coded cooperation, we are primarily interested in the terms of first and second-order in $1/\Gamma_T$. For the integral term Ψ_1 (5.15),(5.16), applying (B.1) gives

$$\begin{aligned} \Psi_1(\gamma_{1,d}, \Gamma_{1,d}, \Gamma_{2,d}, R, \alpha) = \frac{1}{\Gamma_T\Gamma_{1,d}} \int_0^{2^{R/\alpha}-1} \left[1 - \frac{\gamma_{1,d}}{\Gamma_T\Gamma_{1,d}} - \frac{a}{\Gamma_T\Gamma_{2,d}}\right] d\gamma_{1,d} \\ + O\left(\frac{1}{\Gamma_T^3}\right), \end{aligned} \tag{B.3}$$

where the argument of the integral results from the first two terms of the Taylor's series expansion of $\exp(\cdot)$ (B.1). The remaining terms are represented by $O\left(\frac{1}{\Gamma_T^3}\right)$. We evaluate the integral term to obtain

$$\Psi_1(\gamma_{1,d}, \Gamma_{1,d}, \Gamma_{2,d}, R, \alpha) = \frac{2^{R/\alpha}-1}{\Gamma_T\Gamma_{1,d}} - \frac{(2^{R/\alpha}-1)^2}{2\Gamma_T^2\Gamma_{1,d}^2} - \frac{\Lambda(R,\alpha)}{\Gamma_T^2\Gamma_{1,d}\Gamma_{2,d}} + O\left(\frac{1}{\Gamma_T^3}\right), \tag{B.4}$$

where $\Lambda(R,\alpha)$, defined in (5.21), is the integral of a (5.16) from 0 to $2^{R/\alpha}-1$. Similarly, for Ψ_2 (5.15),(5.16) we obtain

$$\begin{aligned}\Psi_2(\gamma_{1,d},\Gamma_{1,d},\Gamma_{2,d},R,\alpha) &= \frac{1}{\Gamma_T\Gamma_{1,d}}\int_0^{2^R-1}\left[1-\frac{\gamma_{1,d}}{\Gamma_T\Gamma_{1,d}}-\frac{b}{\Gamma_T\Gamma_{2,d}}\right]d\gamma_{1,d} \\ &\quad + O\left(\frac{1}{\Gamma_T^3}\right) \\ &= \frac{2^R-1}{\Gamma_T\Gamma_{1,d}}-\frac{(2^R-1)^2}{2\Gamma_T^2\Gamma_{1,d}^2}-\frac{\Delta(R,\alpha)}{\Gamma_T^2\Gamma_{1,d}\Gamma_{2,d}}+O\left(\frac{1}{\Gamma_T^3}\right),\end{aligned} \tag{B.5}$$

where

$$\Delta(R,\alpha)=\begin{cases}2^{R/(1-\alpha)}\left(\frac{1-\alpha}{1-2\alpha}\right)\left(2^{R(1-2\alpha)/(1-\alpha)}-1\right)-2^R+1-\frac{(2^R-1)^2}{2} & \alpha\neq 1/2\\ R\cdot 2^{2R}\cdot\ln 2-2^R+1-\frac{(2^R-1)^2}{2} & \alpha=1/2\end{cases} \tag{B.6}$$

is the integral of b (5.16) from 0 to 2^R-1. Now, using (B.2) and (B.3), we can express the two bracketed terms in (5.15) involving Ψ_1 and Ψ_2 as

$$\begin{aligned}&\left[1-\exp\left(\frac{1-2^{R/\alpha}}{\Gamma_{1,d}}\right)-\exp\left(\frac{1-2^{R/\alpha}}{\Gamma_{1,2}}\right)\cdot\Psi_1(\gamma_{1,d},\Gamma_{1,d},\Gamma_{2,d},R,\alpha)\right]= \\ &\qquad\frac{(2^{R/\alpha}-1)^2}{\Gamma_T^2\Gamma_{1,d}\Gamma_{1,2}}-\frac{\Lambda(R,\alpha)}{\Gamma_T^2\Gamma_{1,d}\Gamma_{2,d}}+O\left(\frac{1}{\Gamma_T^3}\right)\end{aligned} \tag{B.7}$$

$$\begin{aligned}&\left[1-\exp\left(\frac{1-2^{R}}{\Gamma_{1,d}}\right)-\exp\left(\frac{1-2^{R/\alpha}}{\Gamma_{1,2}}\right)\cdot\Psi_2(\gamma_{1,d},\Gamma_{1,d},\Gamma_{2,d},R,\alpha)\right]= \\ &\qquad\frac{(2^{R}-1)(2^{R/\alpha}-1)}{\Gamma_T^2\Gamma_{1,d}\Gamma_{1,2}}-\frac{\Delta(R,\alpha)}{\Gamma_T^2\Gamma_{1,d}\Gamma_{2,d}}+O\left(\frac{1}{\Gamma_T^3}\right).\end{aligned} \tag{B.8}$$

Note that all the first-order terms have cancelled, leaving only second-order and higher-order terms. Finally, from (B.2) we see that

$$\exp\left(\frac{1-2^{R/\alpha}}{\Gamma_T\Gamma_{2,1}}\right)\cdot(\text{B.7}) = \frac{(2^{R/\alpha}-1)^2}{\Gamma_T^2\Gamma_{1,d}\Gamma_{1,2}}-\frac{\Lambda(R,\alpha)}{\Gamma_T^2\Gamma_{1,d}\Gamma_{2,d}}+O\left(\frac{1}{\Gamma_T^3}\right) \tag{B.9}$$

$$\left[1-\exp\left(\frac{1-2^{R/\alpha}}{\Gamma_T\Gamma_{2,1}}\right)\right]\cdot(\text{B.8}) = O\left(\frac{1}{\Gamma_T^3}\right), \tag{B.10}$$

which, when added, gives the result (5.20). The dependence on $\gamma_{2,1}$ occurs only in the terms of third-order and higher in (B.9). Note also that, as a result of (B.10),

$\Delta(R, \alpha)$ does not appear in the second-order terms of (5.20). Using (B.2) and (B.3) in a similar fashion results in (5.22). In addition, we can use the same techniques to obtain the asymptotic results for space-time cooperation (Section 5.1.3) and the selection decode-and-forward protocol of [40] (Appendix C).

APPENDIX C
SELECTION DECODE-AND-FORWARD

We can generalize the selection decode-and-forward scheme of [40] for independent inter-user channels, and obtain outage probability expressions as shown below. In this scenario the cooperation level α is 1/2 by definition. Again we have the same four cases, resulting from the first frame transmissions, as with coded cooperation. The corresponding outage events for User 1 become

$$\begin{aligned} C_{1,d}(\gamma_{1,d},\gamma_{2,d}|\Theta=1) &= \log_2(1+\gamma_{1,d}+\gamma_{2,d}) < 2R \\ C_{1,d}(\gamma_{1,d},\gamma_{2,d}|\Theta=2) &= \log_2(1+2\gamma_{1,d}) < 2R \\ C_{1,d}(\gamma_{1,d},\gamma_{2,d}|\Theta=3) &= \log_2(1+2\gamma_{1,d}+\gamma_{2,d}) < 2R \\ C_{1,d}(\gamma_{1,d},\gamma_{2,d}|\Theta=4) &= \log_2(1+\gamma_{1,d}) < 2R. \end{aligned} \tag{C.1}$$

For the case of independent inter-user channels, the outage probability for User 1 is

$$\begin{aligned} P_{out,1} &= \Pr\{\gamma_{1,2} > 2^{2R}-1\}\cdot\Pr\{\gamma_{2,1} > 2^{2R}-1\}\cdot\Pr\{\gamma_{1,d}+\gamma_{2,d} < 2^{2R}-1\} \\ &+ \Pr\{\gamma_{1,2} < 2^{2R}-1\}\cdot\Pr\{\gamma_{2,1} < 2^{2R}-1\}\cdot\Pr\left\{\gamma_{1,d} < \frac{2^{2R}-1}{2}\right\} \\ &+ \Pr\{\gamma_{1,2} > 2^{2R}-1\}\cdot\Pr\{\gamma_{2,1} < 2^{2R}-1\}\cdot\Pr\{2\gamma_{1,d}+\gamma_{2,d} < 2^{2R}-1\} \\ &+ \Pr\{\gamma_{1,2} < 2^{2R}-1\}\cdot\Pr\{\gamma_{2,1} > 2^{2R}-1\}\cdot\Pr\{\gamma_{1,d} < 2^{2R}-1\}. \end{aligned} \tag{C.2}$$

For Rayleigh fading, we have

$$\begin{aligned} P_{out,1} &= \exp\left(\frac{1-2^{2R}}{\Gamma_{1,2}}\right)\cdot\exp\left(\frac{1-2^{2R}}{\Gamma_{2,1}}\right)\cdot\iint_F \Phi(\gamma_{1,d},\gamma_{2,d},\Gamma_{1,d},\Gamma_{2,d})d\gamma_{1,d}d\gamma_{2,d} \\ &+ \left[1-\exp\left(\frac{1-2^{2R}}{\Gamma_{1,2}}\right)\right]\cdot\left[1-\exp\left(\frac{1-2^{2R}}{\Gamma_{2,1}}\right)\right]\cdot\left[1-\exp\left(\frac{1-2^{2R}}{2\Gamma_{1,d}}\right)\right] \\ &+ \exp\left(\frac{1-2^{2R}}{\Gamma_{1,2}}\right)\cdot\left[1-\exp\left(\frac{1-2^{2R}}{\Gamma_{2,1}}\right)\right] \\ &\quad\cdot\iint_G \Phi(\gamma_{1,d},\gamma_{2,d},\Gamma_{1,d},\Gamma_{2,d})d\gamma_{1,d}d\gamma_{2,d} \\ &+ \left[1-\exp\left(\frac{1-2^{2R}}{\Gamma_{1,2}}\right)\right]\cdot\exp\left(\frac{1-2^{2R}}{\Gamma_{2,1}}\right)\cdot\left[1-\exp\left(\frac{1-2^{2R}}{\Gamma_{1,d}}\right)\right], \end{aligned} \tag{C.3}$$

where

$$\begin{aligned} F &\equiv \{(\gamma_{1,d} + \gamma_{2,d}) < 2^{2R} - 1\} \\ G &\equiv \{(2\gamma_{1,d} + \gamma_{2,d}) < 2^{2R} - 1\} \end{aligned} \tag{C.4}$$

and $\Phi(\gamma_{1,d}, \gamma_{2,d}, \Gamma_{1,d}, \Gamma_{2,d})$ is the same as (5.14). Again, we can simplify (C.3) in a manner similar to that described in Appendix A for (5.13) to obtain

$$\begin{aligned} P_{out,1} = \exp\left(\frac{1-2^{2R}}{\Gamma_{2,1}}\right) & \\ \cdot \left[1 - \exp\left(\frac{1-2^{2R}}{\Gamma_{1,d}}\right) - \exp\left(\frac{1-2^{2R}}{\Gamma_{1,2}}\right) \cdot \Psi_3(\Gamma_{1,d}, \Gamma_{2,d}, R)\right] & \\ + \left[1 - \exp\left(\frac{1-2^{2R}}{\Gamma_{2,1}}\right)\right] & \\ \cdot \left[1 - \exp\left(\frac{1-2^{2R}}{2\Gamma_{1,d}}\right) - \exp\left(\frac{1-2^{2R}}{\Gamma_{1,2}}\right) \cdot \Psi_4(\Gamma_{1,d}, \Gamma_{2,d}, R)\right] & \end{aligned} \tag{C.5}$$

where

$$\begin{aligned} \Psi_3(\Gamma_{1,d}, \Gamma_{2,d}, R) &= \frac{1}{\Gamma_{1,d}} \exp\left(\frac{1-2^{2R}}{\Gamma_{2,d}}\right) \\ &\quad \cdot \int_0^{2^{2R}-1} \exp\left[-\gamma_{1,d}\left(\frac{1}{\Gamma_{1,d}} - \frac{1}{\Gamma_{2,d}}\right)\right] d\gamma_{1,d} \\ &= \begin{cases} \left(\frac{2^{2R}-1}{\Gamma_{1,d}}\right) \exp\left(\frac{1-2^{2R}}{\Gamma_{2,d}}\right) & \Gamma_{1,d} = \Gamma_{2,d} \\ \left(\frac{\Gamma_{2,d}}{\Gamma_{1,d}-\Gamma_{2,d}}\right)\left[\exp\left(\frac{1-2^{2R}}{\Gamma_{1,d}}\right) - \exp\left(\frac{1-2^{2R}}{\Gamma_{2,d}}\right)\right] & \Gamma_{1,d} \neq \Gamma_{2,d} \end{cases} \\ \Psi_4(\Gamma_{1,d}, \Gamma_{2,d}, R) &= \frac{1}{\Gamma_{1,d}} \exp\left(\frac{1-2^{2R}}{\Gamma_{2,d}}\right) \\ &\quad \cdot \int_0^{(2^{2R}-1)/2} \exp\left[-\gamma_{1,d}\left(\frac{1}{\Gamma_{1,d}} - \frac{2}{\Gamma_{2,d}}\right)\right] d\gamma_{1,d} \\ &= \begin{cases} \left(\frac{2^{2R}-1}{2\Gamma_{1,d}}\right) \exp\left(\frac{1-2^{2R}}{\Gamma_{2,d}}\right) & 2\Gamma_{1,d} = \Gamma_{2,d} \\ \left(\frac{\Gamma_{2,d}}{2\Gamma_{1,d}-\Gamma_{2,d}}\right)\left[\exp\left(\frac{1-2^{2R}}{2\Gamma_{1,d}}\right) - \exp\left(\frac{1-2^{2R}}{\Gamma_{2,d}}\right)\right] & 2\Gamma_{1,d} \neq \Gamma_{2,d} \end{cases}. \end{aligned} \tag{C.6}$$

For reciprocal inter-user channels, (C.2) simplifies to

$$\begin{aligned} P_{out,1} = \Pr\{\gamma_{1,2} > 2^{2R} - 1\} \cdot \Pr\{\gamma_{1,d} + \gamma_{2,d} < 2^{2R} - 1\} & \\ + \Pr\{\gamma_{1,2} < 2^{2R} - 1\} \cdot \Pr\left\{\gamma_{1,d} < \frac{2^{2R}-1}{2}\right\}. & \end{aligned} \tag{C.7}$$

Using the above results we can obtain for Rayleigh fading

$$P_{out,1} = \exp\left(\frac{1-2^{2R}}{\Gamma_{1,2}}\right)\left[1-\exp\left(\frac{1-2^{2R}}{\Gamma_{1,d}}\right)-\Psi_3(\Gamma_{1,d},\Gamma_{2,d},R)\right] + \left[1-\exp\left(\frac{1-2^{2R}}{\Gamma_{1,2}}\right)\right]\left[1-\exp\left(\frac{1-2^{2R}}{2\Gamma_{1,d}}\right)\right] \tag{C.8}$$

where $\Psi_3(\Gamma_{1,d},\Gamma_{2,d},R)$ is the same as in (C.6).

To determine the diversity achieved by selection decode-and-forward, we again re-parameterize $\Gamma_{i,j}$ and expand the exponential terms using Taylor's series as we did for coded cooperation (Section 5.1.2 and Appendix B). For the case of independent inter-user channels, we obtain

$$P_{out,1} = \frac{1}{\Gamma_T^2}\cdot\left[\frac{3(2^{2R}-1)^2}{2\Gamma_{1,d}}\left(\frac{\Gamma_{1,2}+\Gamma_{2,d}}{\Gamma_{1,2}\Gamma_{2,d}}\right)\right]+O\left(\frac{1}{\Gamma_T^3}\right), \tag{C.9}$$

and for the case of reciprocal inter-user channels we have

$$P_{out,1} = \frac{1}{\Gamma_T^2}\cdot\left[\frac{(2^{2R}-1)^2}{2\Gamma_{1,d}}\left(\frac{\Gamma_{1,2}+\Gamma_{2,d}}{\Gamma_{1,2}\Gamma_{2,d}}\right)\right]+O\left(\frac{1}{\Gamma_T^3}\right). \tag{C.10}$$

We see from (C.9) and (C.10) that selection decode-and-forward achieves full diversity order. We also note that, for reciprocal inter-user channels, (C.10) matches the asymptotic outage probability results given in [40].

REFERENCES

[1] 3rd Generation Partnership Project 3G TS 25.101, "UE radio transmission and reception (FDD)."

[2] S. M. Alamouti, "A simple transmit diversity technique for wireless communications," *IEEE Journal on Selected Areas in Communications*, vol. 16, no. 8, pp. 1451–1458, October 1998.

[3] M.-S. Alouini and A. J. Goldsmith, "Capacity of Rayleigh fading channels under different adaptive transmission and diversity-combining techniques," *IEEE Transactions on Vehicular Technology*, vol. 48, no. 4, pp. 1165–1181, July 1999.

[4] K. Azarian Yazdi, H. El Gamal, and P. Schniter, "On the design of cooperative transmission schemes," in *Proc. Allerton Conference on Communications, Control, and Computing*, Monticello, IL, October 2003.

[5] G. Bauch and J. Hagenauer, "Analytical evaluation of space-time transmit diversity with FEC-coding," in *Proc. IEEE GLOBECOM*, San Antonio, TX, November 2001, pp. 435–439.

[6] S. Benedetto, D. Divsalar, G. Montorsi, and F. Pollara, "A soft-input soft-ouput APP module for iterative decoding of concatenated codes," *IEEE Transactions on Communications*, vol. 1, no. 1, pp. 22–24, January 1997.

[7] ——, "Serial concatenation of interleaved codes: performance analysis, design, and iterative decoding," *IEEE Transactions on Information Theory*, vol. 44, no. 3, pp. 909–926, May 1998.

[8] S. Benedetto and G. Montorsi, "Unveiling turbo codes: Some results on parallel concatenated coding schemes," *IEEE Transactions on Information Theory*, vol. 42, no. 2, pp. 409–428, March 1996.

[9] ——, "A search for good convolutional codes to be used in the construction of turbo codes," *IEEE Transactions on Communications*, vol. 46, no. 9, pp. 1101–1105, September 1998.

[10] C. Berrou and A. Glavieux, "Near optimum error correcting coding and decoding: Turbo codes," *IEEE Transactions on Communications*, vol. 44, pp. 1261–1271, October 1996.

[11] W. H. Beyer, Ed., *CRC Standard Mathematical Tables*, 28th ed. Boca Raton, FL: CRC Press, 1987.

[12] E. Biglieri, J. Proakis, and S. Shamai (Shitz), "Fading channels: Information-theoretic and communications aspects," *IEEE Transactions on Information Theory*, vol. 44, no. 6, pp. 2619–2692, October 1998.

[13] G. Caire, G. Taricco, and E. Biglieri, "Optimum power control over fading channels," *IEEE Transactions on Information Theory*, vol. 45, no. 5, pp. 1468–1489, July 1999.

[14] J. K. Cavers, "Variable-rate transmission for Rayleigh fading channels," *IEEE Transactions on Communications*, vol. COM-20, pp. 15–22, February 1972.

[15] M. H. M. Costa, "On the Gaussian interference channel," *IEEE Transactions on Information Theory*, vol. 31, no. 5, pp. 607–615, May 1985.

[16] T. M. Cover and A. A. El Gamal, "Capacity theorems for the relay channel," *IEEE Transactions on Information Theory*, vol. 25, no. 5, pp. 572–584, September 1979.

[17] T. M. Cover and J. A. Thomas, *Elements of Information Theory*. New York: John Wiley and Sons, 1991.

[18] J. W. Craig, "A new, simple, and exact result for calculating the probability of error for two-dimensional signal constellations," in *Proc. IEEE MILCOM*, McLean, VA, October 1991, pp. 571–575.

[19] H. El Gamal and D. Aktas, "Distributed space-time filtering for cooperative wireless networks," in *Proc. IEEE GLOBECOM*, San Francisco, CA, December 2003.

[20] A. J. Goldsmith and S. G. Chua, "Variable-rate variable-power M-QAM for fading channels," *IEEE Transactions on Communications*, vol. 45, pp. 1218–1230, October 1997.

[21] A. J. Goldsmith and P. P. Varaiya, "Capacity of fading channels with channel side information," *IEEE Transactions on Information Theory*, vol. 43, no. 6, pp. 1986–1992, July 1997.

[22] I. S. Gradshteyn and I. M. Ryzhik, *Table of Integrals, Series, and Products*. San Diego, CA: Academic Press, 1994.

[23] M. Grossglauser and D. N. C. Tse, "Mobility increases the capacity of ad-hoc wireless networks," *IEEE/ACM Transactions on Networking*, vol. 10, no. 4, pp. 477–486, August 2002.

[24] P. Gupta and P. R. Kumar, "The capacity of wireless networks," *IEEE Transactions on Information Theory*, vol. 46, no. 2, pp. 388–404, March 2000.

[25] J. Hagenauer, "Rate-compatible punctured convolutional codes (RCPC codes) and their applications," *IEEE Transactions on Communications*, vol. 36, no. 4, pp. 389–400, April 1988.

[26] J. Hagenauer, E. Offer, and L. Papke, "Iterative decoding of binary block and convolutional codes," *IEEE Transactions on Information Theory*, vol. 42, pp. 429–445, March 1996.

[27] J. F. Hayes, "Adaptive feedback communications," *IEEE Transactions on Communication Technology*, vol. COM-16, pp. 29–34, February 1968.

[28] S. Haykin, *Adaptive Fiter Theory*, 3rd ed. Upper Saddle River, NJ: Prentice-Hall, 1996.

[29] V. O. Hentinen, "Error performance for adaptive transmission on fading channels," *IEEE Transactions on Communications*, vol. COM-22, pp. 1331–1337, September 1974.

[30] A. Høst-Madsen, "On the capacity of cooperative diversity in slow fading channels," in *Proc. Allerton Conference on Communications, Control, and Computing*, Monticello, IL, October 2002.

[31] ——, "On the capacity of wireless relaying," in *Proc. IEEE Vehicular Technology Conference (VTC)*, vol. 3, Vancouver, B. C., Canada, September 2002, pp. 1333–1337.

[32] T. E. Hunter and A. Nosratinia, "Coded cooperation under slow fading, fast fading, and power control," in *Proc. Asilomar Conference on Signals, Systems and Computers*, Pacific Grove, CA, November 2002.

[33] E. I. S.-. (IS-95), "Mobile station – base station compatibility standard for dual-mode wideband spread spectrum celluar system."

[34] J. D. Murray, *Asymptotic Analysis*. New York: Springer-Verlag, 1984.

[35] W. C. Jakes, Ed., *Microwave Mobile Communications*. New York: John Wiley and Sons, 1974.

[36] S. Kallel and C. Leung, "Efficient ARQ schemes with multiple copy decoding," *IEEE Transactions on Communications*, vol. 40, pp. 642–650, March 1992.

[37] R. Knopp and P. A. Humblet, "Information capacity and power control in single cell multiuser communications," in *Proc. IEEE International Conference on Communications (ICC)*, Seattle, WA, June 1995.

[38] ——, "On coding for block fading channels," *IEEE Transactions on Information Theory*, vol. 46, no. 1, pp. 189–205, January 2000.

[39] J. N. Laneman, "Cooperative diversity in wireless networks: Algorithms and architectures," Ph.D. dissertation, Massachusetts Institute of Technology, August 2002.

[40] J. N. Laneman, D. N. C. Tse, and G. W. Wornell, "Cooperative diversity in wireless networks: Efficient protocols and outage behavior," *IEEE Transactions on Information Theory*, accepted for publication. [Online]. Available: http://www.nd.edu/∼jnl/pubs/it2002.pdf

[41] J. N. Laneman and G. W. Wornell, "Energy-efficient antenna sharing and relaying for wireless networks," in *Proc. IEEE Wireless Communcations and Networking Conference (WCNC)*, Chicago, IL, September 2000, pp. 7–12.

[42] ——, "Distributed space-time-coded protocols for exploiting cooperative diversity in wireless networks," *IEEE Transactions on Information Theory*, vol. 49, no. 10, pp. 2415–2425, October 2003.

[43] J. N. Laneman, G. W. Wornell, and D. N. C. Tse, "An efficient protocol for realizing cooperative diversity in wireless networks," in *Proc. IEEE International Symposium on Information Theory (ISIT)*, Washington, D. C., June 2001, p. 294.

[44] E. Malkamäki and H. Leib, "Coded diversity on block-fading channels," *IEEE Transactions on Information Theory*, vol. 45, no. 2, pp. 771–781, March 1999.

[45] ——, "Evaluating the performance of convolutional codes over block fading channels," *IEEE Transactions on Information Theory*, vol. 45, no. 5, pp. 1643–1646, July 1999.

[46] L. H. Ozarow, S. Shamai (Shitz), and A. D. Wyner, "Information theoretic considerations for cellular mobile radio," *IEEE Transactions on Information Theory*, vol. 43, no. 2, pp. 359–378, May 1994.

[47] J. G. Proakis, *Digital Communications*, 3rd ed. New York: McGraw-Hill, 1995.

[48] T. S. Rappaport, *Wireless Communications: Principles and Practice*. Upper Saddle River, NJ: Prentice-Hall, 1996.

[49] D. N. Rowitch and L. B. Milstein, "On the performance of hybrid FEC/ARQ systems using rate compatible punctured turbo (RCPT) codes," *IEEE Transactions on Communications*, vol. 48, no. 6, pp. 948–959, June 2000.

[50] A. Sendonaris, "Advanced techniques for next-generation wireless systems," Ph.D. dissertation, Rice University, May 1999.

[51] A. Sendonaris, E. Erkip, and B. Aazhang, "Increasing uplink capacity via user cooperation diversity," in *Proc. IEEE International Symposium on Information Theory (ISIT)*, Cambridge, MA, August 1998, p. 156.

[52] ——, "User cooperation diversity–Part I: System description," *IEEE Transactions on Communications*, vol. 51, no. 11, pp. 1927–1938, November 2003.

[53] ——, "User cooperation diversity–Part II: Implementation aspects and performance analysis," *IEEE Transactions on Communications*, vol. 51, no. 11, pp. 1939–1948, November 2003.

[54] M. K. Simon and M.-S. Alouini, *Digital Communication over Fading Channels: A Unified Approach to Performance Analysis*. New York: John Wiley and Sons, 2000.

[55] H. Stark and J. W. Woods, *Probability, Random Processes, and Estimation Theory for Engineers*, 1st ed. Englewood Cliffs, NJ: Prentice Hall, 1986.

[56] R. Steele and L. Hanzo, Eds., *Mobile Radio Communications*, 2nd ed. West Sussex, UK: John Wiley and Sons, 1999.

[57] A. Stefanov and E. Erkip, "Cooperative space-time coding for wireless networks," in *Proc. IEEE Information Theory Workshop*, Paris, France, April 2003.

[58] G. L. Stüber, *Principles of Mobile Communication*, 2nd ed. Boston, MA: Kluwer Academic Publishers, 2001.

[59] V. Tarokh, H. Jafarkhani, and A. R. Calderbank, "Space-time block codes from orthogonal designs," *IEEE Transactions on Information Theory*, vol. 45, no. 5, pp. 1456–1467, July 1999.

[60] V. Tarokh, N. Seshadri, and A. R. Calderbank, "Space-time codes for high data rate wireless communication: Performance criteria and code construction," *IEEE Transactions on Information Theory*, vol. 44, no. 2, pp. 744–765, March 1998.

[61] F. A. Tobagi, "Modeling and performance analysis of multihop packet radio networks," *Proceedings of the IEEE*, vol. 75, no. 1, pp. 135–155, January 1987.

[62] S. Toumpis and A. J. Goldsmith, "Capacity regions for wireless ad hoc networks," *IEEE Transactions on Wireless Communications*, vol. 2, no. 4, pp. 736–748, July 2003.

[63] Y.-S. Tu and G. J. Pottie, "Coherent cooperative transmission from multiple adjacent antennas to a distant stationary antenna through AWGN channels," in *Proc. IEEE Vehicular Technology Conference (VTC)*, vol. 1, 2002, pp. 130–134.

[64] M. Valenti and B. Zhao, "Distributed turbo codes: Towards the capacity of the relay channel," in *Proc. IEEE Vehicular Technology Conference (VTC)*, Orlando, FL, October 2003.

[65] J.-J. van de Beek, P. O. Börjesson, M.-L. Boucheret, D. Landström, J. M. Arenas, P. Ödling, C. Östberg, M. Wahlqvist, and S. K. Wilson, "A time and frequency synchronization scheme for multiuser OFDM," *IEEE Journal on Selected Areas in Communications*, vol. 17, no. 11, pp. 1900–1914, November 1999.

[66] P. Viswanath, D. N. C. Tse, and R. Laroia, "Opportunistic beamforming using dumb antennas," *IEEE Transactions on Information Theory*, vol. 48, no. 6, pp. 1277–1294, June 2002.

[67] A. Viterbi and J. K. Omura, *Principles of Digital Communcation and Coding*. New York: McGraw-Hill, 1979.

[68] B. Vucetic, "An adaptive coding scheme for time-varying channels," *IEEE Transactions on Communications*, vol. 39, pp. 653–663, May 1991.

[69] W. T. Webb and R. Steele, "Variable rate QAM for mobile radio," *IEEE Transactions on Communications*, vol. 43, pp. 2223–2230, July 1995.

[70] S. B. Wicker, *Error Control Systems for Digital Communcation and Storage*. Englewood Cliffs, NJ: Prentice Hall, 1995.

[71] B. Zhao and M. Valenti, "Some new adaptive protocols for the wireless relay channel," in *Proc. Allerton Conference on Communications, Control, and Computing*, Monticello, IL, October 2003.

VITA

Todd Edward Hunter was born in Dallas, TX, U.S.A., in 1967, the son of Edward Todd Hunter and Diane Hunter. He received the degree of Bachelor of Science in Electrical Engineering from Texas A&M University, College Station, TX, in 1990, and the degree of Master of Science in Electrical Engineering from the University of Texas at Dallas, Richardson, TX, in 1996. In June 1999 he began working toward the Ph.D. degree in Electrical Engineering in the Multimedia Communications Laboratory at the University of Texas at Dallas.

From 1991 to 1997 he worked as a design support engineer with Texas Instruments, Defense Systems and Electronics Group, Lewisville, TX, and continued in the same position from 1997 to 1999 with Raytheon Systems Company after their acquisition of Texas Instruments' defense business. His primary responsibilities were to analyze electronics designs to verify that the requirements would be met and to recommend design changes to improve design reliability and robustness. During this time, he led an effort to develop a methodology for statistical performance analysis of analog and digital circuit designs, as part of Texas Instruments' Six Sigma program. He was certified as a Six Sigma Black Belt by Texas Instruments in 1995 as a result of these activities. During the summer of 2000 he was with the Wireless Communications Business Unit of Texas Instruments, Dallas, TX, as a systems engineer, working on the design and verification of a modem chip set compliant with the 3rd Generation Partnership Project (3GPP) standard for Wideband CDMA (WCDMA).

He currently lives in Lewisville, TX, with his beloved wife María Argeny.